Tracking Disaster Dynamics for Urban Resilience: Human-Mobility and Semantic Perspectives

Yan Wang

Dissertation submitted to the faculty of the Virginia Polytechnic Institute and State University in partial fulfillment of the requirements for the degree of

Doctor of Philosophy
In
Civil Engineering

John E. Taylor, Co-Chair
Michael J. Garvin, Co-Chair
Ignacio T. Moore
Earl W. Shealy
Qi Wang

April 12, 2018
Blacksburg, Virginia

Keywords: Big Data, Disaster Dynamics, Emergency Detection, Human Mobility, Sentiment, Twitter, Urban Resilience.

Tracking Disaster Dynamics for Urban Resilience: Human-Mobility and Semantic Perspectives

Yan Wang

ABSTRACT

Fostering urban resilience and creating agility to disaster response is an urgent task faced by cities worldwide in the context of climate change and increasing frequencies of natural disasters. Understanding and tracking the dynamic process of resilience to disasters is the first step to operationalize the concept of urban resilience. In this dissertation, I present four related but evolutionary perspectives to investigate the impact of natural disasters on interactive human-environment systems as well as the dynamic process of resilience, including human mobility, spatial networks, and coupled mobility and sentiment perspectives. In the first, human-mobility perspective, I examine the nuanced impact of a severe winter storm on human mobility patterns and the relationship between perturbed mobility during the storm and recurrent mobility under normal circumstances. In the second, where I adopt a spatial network perspective, I investigate the dynamic process of resilience over time by analyzing networked human-spatial systems using an ecology-inspired approach. The third perspective involves sentiment as an additional factor to human mobility to understand urban dynamics during an earthquake. In this perspective, I explore the relation between disaster magnitude and a population's collective sentiment, as well as temporal correlations between sentiment and mobility. Each of the three empirical studies employs a quantitative, empirical research methodology and uses voluntarily reported geo-referenced data collected through a Twitter Streaming API. After multiple investigations on diverse types of natural disaster (e.g. severe winter storm, flooding, hurricane, and earthquake), I develop a Detecting Urban Emergencies Technique (DUET), as the fourth part of my dissertation, for identifying and tracking general types of emergencies in a short period without prior definitions of emergent topics. Research findings from the three empirical studies and the proposed DUET detection technique introduce a new lens and approach for understanding population dynamics and achieving urban resilience. This dissertation contributes to a more complete understanding of urban resilience to disasters with crowdsourced data, and enables more effective urban informatics in the face of extreme events.

Tracking Disaster Dynamics for Urban Resilience: Human-Mobility and Semantic Perspectives

Yan Wang

GENERAL AUDIENCE ABSTRACT

Cities worldwide are facing the challenges of climate change and increasing frequencies of natural disasters. The first step of enhancing disaster responses in urban areas is to operationalize the concept of urban resilience by understanding the impact of disasters on urban systems at both spatial and temporal scales. In this dissertation, urban systems are characterized by individuals' movements, networks of spatial units, and population's sentiment, which also form three different but evolutionary perspectives to investigate the impact over time. In the first, human-movement perspective, I examine the nuanced impact of a severe winter storm on individuals' movement patterns and the relationship between individuals' most frequented locations (e.g. home or working places) under normal circumstances and their visited locations during the winter storm. In the second, where I adopt a spatial network perspective, I investigate the temporal process of resilience by analyzing networked human-spatial systems pre-, during, and post-disaster using an ecology-inspired approach. The third perspective involves sentiment, which is a measurement of people's emotion and attitude, as an additional factor to human movement to understand the impact of an earthquake on the urban system. In this perspective, I explore the relation between an earthquake's magnitude and a population's collective sentiment, as well as how sentiment and movement changed over time. These three empirical studies use a quantitative research methodology with geotagged tweets, which are collected from a Twitter Streaming API. After many investigations on different types of natural disaster, I develop a Detecting Urban Emergencies Technique (DUET) for identifying and tracking general types of emergencies in a short period. The empirical findings and the proposed DUET detection technique introduce a bottom-up perspective for understanding disasters' impact and enhancing urban resilience. This dissertation contributes to a more complete understanding of disaster resilience in urban areas with crowdsourced data, and enables more open and effective disaster communication.

Dedicated to Chen

ACKNOWLEDGEMENT

First and foremost, I would like to express my sincere gratitude to my advisor Prof. John Taylor for his motivation, encouragement as well as high standards and rigorous requirements. His effort and guidance help me to become a productive and effective researcher. He also teaches me to be a confident, creative and open-mined person. I will continue to learn from him as I carry the lessons he taught me.

I would also like to thank my co-chair Prof. Michael Garvin and all other members of my defense committee, Prof. Ignacio Moore, Prof. Tripp Shealy, Prof. Qi Wang for the time they have invested reviewing my dissertation, providing insightful feedback and, and leading me to the meaningful direction throughout my PhD adventure. In particular, I am grateful to Prof. Garvin for his continuous support of my PhD studies and conference trips, and Prof. Wang for opening up the human mobility research and giving a lot of time to provide me abundant help at the beginning of my academic journey.

My sincere thanks also goes to my mentors Dr. Neda Mohammad, Dr. Yilong Han, Dr. Jiayu Chen. I cherish their assistance through my PhD studies and their guidance for my professional development. I would also like to thank my fellow lab mates at the Network Dyanmic Lab at Georgia Tech, Abby Francisco, Susie Ha, and Chel Samuels as well as former mates at Virginia Tech for providing me valuable comments and feedback, and helping me improve. I was also fortunate to be surrounded by some extreme intelligent and supportive colleagues and friends, Wenyu, Armin, Sogand, Mo, Chen, Kaiwen etc. at Virginia Tech. I thank them for providing me academic and professional suggestions.

Most of all, I would like to thank my parents for their endless love, care and encouragement. They teach me to be a brave, persistent, and honest person. Also, my most profound appreciation goes to my fiancé Chen Wang for always standing for me, bringing me joy, helping me through frustration and making my life full. With his love, support, and patience, my PhD adventure has much more laughter.

Finally, I gratefully acknowledge the source of my funding, IGEP BioBuild Program at Virginia Tech, ICTAS, CEE department whose consistent and generous support throughout my PhD study has made this work possible.

Table of Contents

List of Figures

List of Tables

CHAPTER 1: INTRODUCTION

1.1 Disaster Resilience and Urban Challenges

Building disaster resilience has emerged as a critical agenda in both academic and policy discourse (Meerow et al. 2016) due to the increasing risk, frequency, and intensity of natural disasters caused by climate change. Specifically, urban systems have received increasing attention for the large and growing population, and extensive interconnected infrastructure system in urban areas (Cutter et al., 2014). According to a United Nations technical paper (Gu et al. 2015), in 2014, 944 out of 1,692 cities with at least three million inhabitants were at risk from at least one of six types of natural disaster (i.e. cyclones, floods, droughts, earthquakes, landslides and volcanic eruptions). Even worse, about 15 percent of coastal cities were at high risk of exposure of two or more types of natural disasters, and 27 cities faced three or more types of disaster (e.g. megacities Tokyo, Osaka, and Manila). Moreover, urban population occupied more than half of the world's population in 2014 (54 percent), and this percentage is projected to increase to 66 percent by 2050 (United Nations, 2015). The unequivocal evidence of climate change and rapid urbanization will put urban areas in a more susceptible position (Pachauri et al., 2014). Additionally, resource dependencies of cities on surrounding or other areas can incur a cascading impact on their dependent areas, and pre-existing urban stressors can multiply the effects of climate change (Cutter et al., 2014).

Currently, it is still impossible to precisely predict the climate extremes in terms of spatial distribution and temporal evolution (Linkov et al., 2014). These unknowns require redoubling our operational efforts in building resilience. Disaster management needs to have rigorous measurements to guide what is and how to measure success (Garmestani et al., 2013; Spears et al.,

2015). Although increased interest in managing urban resilience to disasters has stimulated efforts to develop an array of approaches for assessments and quantitative measures (Quinlan et al., 2015), scant attention has been paid on the dynamics of urban structure involving human activities during disasters. In addition, cities, as a complex system, do not lend themselves to easy measurement, and the multiplicity and vague definitions of resilience increase difficulties to measure. Moreover, it is normally difficult to access high-quality data to support quantification of resilience for disaster cases. We need to create new research perspectives to comprehend the dynamic process of perturbation and recovery in urban systems involving both spatial structure and population dynamics to build more resilient cities.

1.2 Big Data Opportunities

Newly available and massive sets of data have played an increasingly important role at different stages of crisis/disaster management (i.e. early warning, monitoring and evaluation), especially in forming bottom-up perspectives in understanding the evolving process of disasters (Ford et al., 2016). Currently, diverse sources of digital data have brought enormous opportunities in the research area of urban resilience. These sources mainly include cell phones (Lu et al., 2012), taxi trips (Peng et al,, 2012), bank notes (Brockmann et al., 2006), Wi-Fi signals (Sapiezynski et al., 2015), and a few social networking platforms (Wang & Taylor, 2017). Among them, Twitter is suitable for emergency environments in terms of its open design, wide usage, geo-enabled function and limited message length environments (Kryvasheyeu et al., 2016). Geo-referenced tweets can document geographical locations and collective reactions to crises unfolding in both spatial and temporal scales. Research involving sentiment analysis and human mobility have already taken advantage of the massive crowd-sourced data collected from Twitter. These two research topic areas help disaster managers make bottom-up decisions and play increasingly important roles in

disaster relief. Among a burgeoning stream of literature, characterization of human mobility patterns plays a critical role in developing models of urban planning (Horner & O'Kelly, 2001), traffic forecasting (Toole et al., 2015), spread of diseases (Wesolowski et al., 2015), social relationship predictions (Wang et al., 2011), and disaster resilience (Wang & Taylor, 2014, 2016). We can also take advantage of the large quantity of geolocations and use human mobility to understand and model the dynamic urban system. Additionally, sentiment analysis of short posts from social media has been shown to be an effective method to identify the dynamic polarity of sentiments over a disaster (Beigi et al., 2016), improve decision making regarding resource assistance, humanitarian efforts and disaster recovery, and obtain particular information (Nagy and Stamberger, 2012).

1.3 Defining Urban Resilience to Disasters

Definitions of resilience provide the basis to understand "what is resilience" and "what is a lack of resilience" in my studies. In this subsection, I will start with explaining the definitions of resilience in its pioneering research area, ecology. Then I will introduce how I define resilience in my studies.

1.3.1 Diverse Definitions of Resilience from Ecology

Resilience, though adopted in physics to describe the ability of something to return to its original shape after external shocks, gained its currency in the research area of ecology with a variety of definitions and measurements (Davoudi et al., 2012). A useful definition defines resilience as, "*the amount of disturbance that a system can withstand before it shifts into an alternative stable state* (Holling, 1973, p.14)". Holling (1973) also proposed two distinct concepts of resilience: engineering resilience and ecological resilience. The former denotes the ability of a system bouncing back to an equilibrium to respond to shocks and perturbations, while the latter underscores an adaption of a system to an alternative or multiple stable status instead of a single-

state equilibrium (Davoudi et al., 2012, Holling, 1986, Holling, 1996). Further, Carpenter et al. (2001) extended the definition of ecological resilience to social-ecological resilience to address the ability of system to stay in the domain of attraction, to self-organize, and to adapt.

1.3.2 Defining Resilience in the Dissertation

Although definitions of resilience vary among diverse applications in different backgrounds, these three definitions provide a shared theoretical foundation to quantify resilience. It is also worth noting that the particular context of resilience and a distinct way to define it will largely determine how it is quantified (Quinlan et al., 2015). It is important to properly define resilience before the quantification. Resilience in my studies is summarized in a schematic representation in Figure 1. In my research context, urban systems involving mobility and spatial structures are complex and intrinsically dynamic. As it is difficult to define the optimal state of urban systems and to measure the exact impact caused by disasters, it is inappropriate to assume that the system can bounce back to an equilibrium after external perturbations. Additionally, it is difficult to quantify the capability of a system in self-organization and adaptation to measure social-ecological resilience with current data. Therefore, we defined urban resilience to disasters to align with ecological resilience to incorporate the inherently dynamic nature of urban systems. It is worth noting that, in my study, resilience is a dynamic process of a system rather than a static measurement of ability of a system.

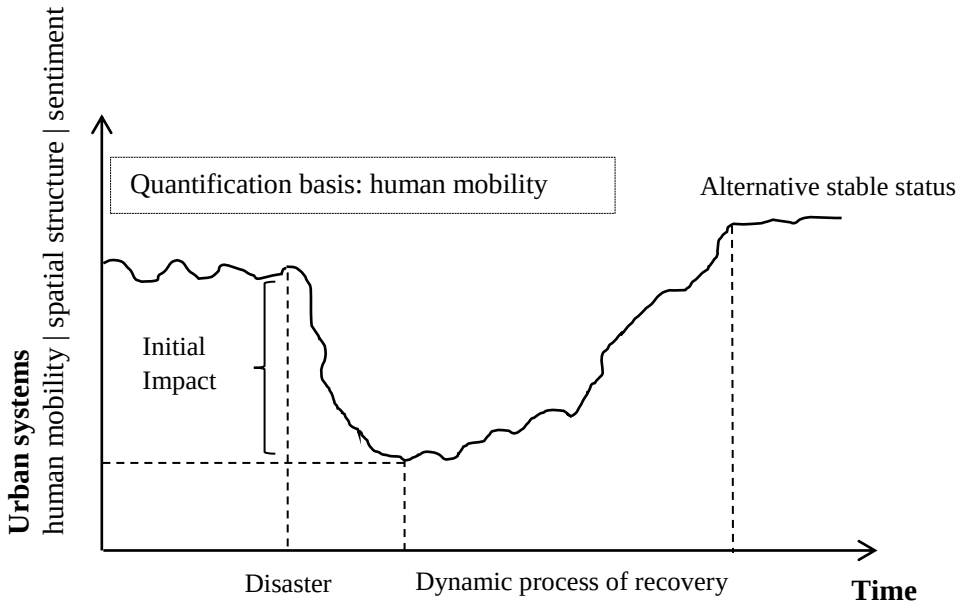

Figure 1: Schematic Representation of Urban Resilience to Disasters

1.4 Research Opportunity

Crowdsourced geographical and semantic data provide the possibility to measure and track the dynamics of urban resilience involving human movements, spatial structure and sentiment, as well as to develop an emergencies detection technique that leverages both geographic and semantic dimensions of disasters to achieve disaster agility. Specifically, research questions that need answers to quantitatively understand dynamic process of urban resilience to disasters and add agility in disaster response include:

- How do disasters affect human mobility patterns, and what is the relationship between recurrent mobility under normal circumstances and perturbed mobility during disasters?
- How do disasters influence networked human-environment systems characterized by human movement and the underlying spatial structure?

- How does a population's sentiment distribute in spatial scale over the course of a disaster and what is the temporal relation between sentiment and human mobility pre-, during-, and post-disasters?
- How can we detect disasters and emergencies of general types in urban environments based on an understanding of human dynamics (i.e. geographic and semantic characteristics)?

1.5 Research Methodology and Dissertation Structure

To investigate urban resilience to disasters quantitatively, I conducted *four interrelated studies*. The first three studies employ a quantitative, empirical research methodology, and the fourth study develops a new technique in methodology. The data used in the empirical studies and the validation part of the technique were collected through a Twitter Streaming API in the Network Dynamics Lab. Geolocation is used as the only filter to stream real-time Tweets with Python codes. As 1.24% of Tweets are geotagged (Pavalanathan & Eisenstein, 2015) and the streaming API can collect 1% of Tweets, the Twitter database is representative in terms of geotagged Tweets. The Twitter geotags are based on GPS Standard Positioning Service, which offers a worst-case pseudo-range accuracy of 7.8 meters with 95 percent confidence, and the positional accuracy is affected by weather and device factors (Swier, et al., 2015).

The four studies composing my dissertation are cumulative in nature in terms of research goals, quantifications base, and research results. Figure 2 generally describes the relationships among these four studies. The first three studies follow the process of exploring resilience. Study 1 attempts to quantify the aggregated impact of a natural disaster on human mobility patterns. Study 2 not only measures the impact of disasters but also investigates the dynamic process of perturbation and recovery. It directly examines the dynamics of the quantified system. Built upon

Study 1 and 2, Study 3 adds another important factor into analysis: sentiment. It explores how coupled sentiment and mobility together contribute to the dynamic process of resilience. After understanding the dynamic nature of disaster resilience in terms of mobility and sentiment, Study 4 aims to build a rapid detection system for urban crises to enable more intelligent crisis informatics and agile pre-, during- and post-crisis management, and to contribute to building more resilient communities in the context of urban crises and natural disasters.

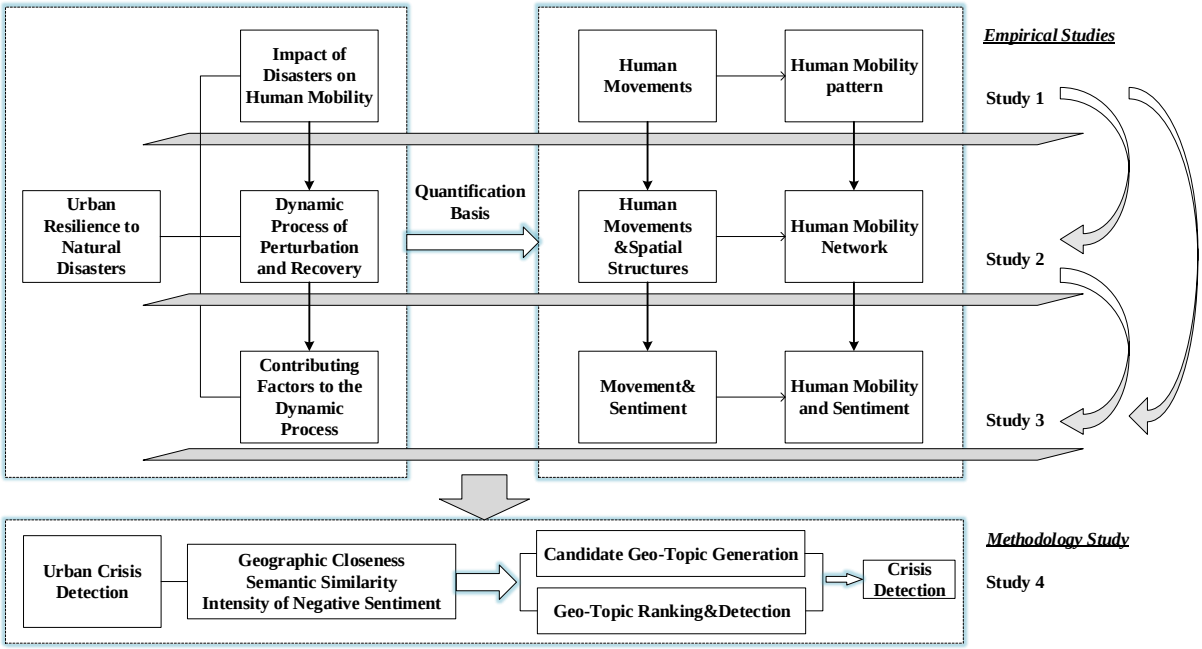

Figure 2: Cumulative Nature of Study 1, 2, 3, and 4

The dissertation is presented in seven chapters with several appendices.

Chapter 2 – Aggregated Responses of Human Mobility to Severe Winter Storms quantitatively analyzes the impact of a severe winter storm on human mobility patterns. This study specifically focuses on a major winter storm in the northeastern United States in 2015. This article was co-authored with Professor Qi Wang and Professor John E. Taylor and was published in the peer-reviewed journal *PlosONE* (Wang, et al. 2017).

Chapter 3 – Tracking Urban Resilience to Disasters: A Spatial Network Perspective proposed a quantitative framework, combining network analysis and Fisher information, to measure urban resilience to disasters. This study focuses on a major flooding case following Hurricane Harvey in the majority of the Greater Houston area, Texas in 2017. The preliminary work of this research has been presented at the 14th International Conference on Information Systems for Crisis Response and Management (ISCRAM 2017) in Albi, France, and was co-authored with Professor John E. Taylor (Wang & Taylor 2017). An expanded version of this manuscript is in the process of being developed with co-authors Professor John E. Taylor and Professor Michael Garvin. It will be submitted to an interdisciplinary journal which includes topics of natural disasters, ecology, landscape and urban planning, such as *Landscape and Urban Planning*.

Chapter 4 – Coupling Sentiment and Human Mobility in Natural Disasters proposes a new lens to evaluate population dynamics during disasters by coupling sentiment and mobility. This study specifically investigates a severe earthquake, the 6.0 magnitude (M6.0) South Napa, California Earthquake in 2014. The study uncovers the spatial characteristics of sentiment in an earthquake, and the temporal relationship between human mobility and sentiment level over time. This article, which I co-authored with Professor John E. Taylor, is a published research article at the disaster-focused peer-reviewed journal *Natural Hazards* (Wang and Taylor 2018).

Chapter 5- Detecting Urban Emergencies Technique (DUET): A Data-Driven Approach Based on Latent Dirichlet Allocation (LDA) Topic Modeling introduces a spatial and data-driven technique for natural hazards, manmade disasters and other emergencies. The detection technique addresses both geographic and semantic dimensions of events and is designed for streaming geo-referenced tweets. The completed manuscript was co-authored with Professor John E. Taylor and

has been submitted to an academic journal that addresses computing methodology in the area of civil engineering.

Chapter 6 - Contribution discusses the theoretical contributions of examining a disaster's impact and population dynamics from the three perspectives (i.e. human mobility, spatial network, and coupled mobility and sentiment perspectives), as well as developing the Detecting Urban Emergencies Technique. The section also presents the practical contributions of the studies to current practices of disaster management systems and approaches.

Chapter 7 - Suggested Avenues of Future Study describes the remaining initiatives for understanding urban resilience and creating agility in disaster management system. This section also outlines what future research avenues my research has enabled in terms of constructing connected, resilient and smart cities. References and supplementary materials referred to in this dissertation can be found at the end of the dissertation.

CHAPTER 2: AGGREGATED RESPONSES OF HUMAN MOBILITY TO SEVERE WINTER STORM[1]

2.1 Abstract

Increasing frequency of extreme winter storms has resulted in costly damages and a disruptive impact on the northeastern United States. It is important to understand human mobility patterns during such storms for disaster preparation and relief operations. We investigated the effects of severe winter storms on human mobility during a 2015 blizzard using 2.69 million Twitter geolocations. We found that displacements of different trip distances and radii of gyration of individuals' mobility were perturbed significantly. We further explored the characteristics of perturbed mobility during the storm, and demonstrated that individuals' recurrent mobility does not have a higher degree of similarity with their perturbed mobility, when comparing with its similarity to non-perturbed mobility. These empirical findings on human mobility impacted by severe winter storms have potential long-term implications on emergency response planning and the development of strategies to improve resilience in severe winter storms.

Keywords: disaster resilience, human mobility, severe winter storm, Twitter.

2.2 Introduction

Recent developments in information technology have provided an unprecedented amount of crowdsourced spatial-temporal data to study human mobility (Brockmann et al., 2006; Gonzalez et al., 2008; Peng et al., 2012; Sapiezynski et al., 2015; Wang & Taylor, 2014). Findings about

[1] This article was co-authored with Professor Qi Wang and Professor John E. Taylor and was published in the peer-reviewed journal *PlosONE*.
Wang Y, Wang Q, Taylor JE (2017) Aggregated responses of human mobility to severe winter storms: An empirical study. *PLoS ONE* 12(12): e0188734. https://doi.org/10.1371/journal.pone.0188734

daily patterned human movements have fundamentally changed our understanding of human mobility at varying spatial scales. However, human mobility patterns under perturbed states, such as in natural disasters, also require a deeper understanding in order to prepare for unfamiliar conditions in the future (Bagrow et al., 2011). Scholars in the disaster research area have identified scaling laws and evaluated the predictability of human mobility during and after extreme events using mobility patterns from non-perturbed states. Lu et al. (2012) used approximately one year of mobile phone data from 1.9 million users, and found that population movements following the Haiti earthquake had a high level of predictability, and destinations were correlated with normal-day mobility patterns and social support structure. Similar results have been found in the research of Song et al. (2014) on human mobility following the Great East Japan Earthquake and Fukushima nuclear accident. A study by Wang and Taylor (2014) showed that human mobility was significantly perturbed during Hurricane Sandy but also exhibited high levels of resilience. A more recent study on multiple types of natural disasters revealed a more universal pattern of human mobility, as well as the limitations of urban human mobility resilience, under the influence of multiple types of natural disasters (Wang & Taylor, 2016). This study also uncovered that resilience could be significantly impacted by more powerful disasters, which could force urban residents to adopt entirely different travel patterns from their norms. Other scholars have conducted longitudinal studies on the relationship between large-scale natural disasters and long-term population mobility. For example, Gray and Mueller (2012) investigated the effects of flooding and crop failures on local population mobility and long-distance migration over 15 years in rural Bangladesh. Their results revealed that natural disasters had significant effects on long-term population mobility but mobility did not universally serve as a post-disaster coping strategy.

Unlike other acute disasters (e.g., earthquakes, hurricanes, and floods), severe winter storms may not force residents to evacuate from their homes to safer places on a large scale, which may result in different perturbation patterns. Yet, relatively few studies have examined the relationship between winter hazards and human mobility in great detail. Over the past century, severe winter storms continue to occur with greater frequency in the eastern two-thirds of the contiguous United States (NOAA, 2016). The increased damages from these storms has resulted in costly and disruptive effects on people's daily lives. Large accumulations of snowfall and ice can incur catastrophic effects on infrastructure systems (Kunkel et al., 2013), specifically, electrical system emergencies and disturbances, and transportation delays and closures (OCIA, 2014), and further lead to communications breakdowns and public health issues. Studies in the transportation research area have examined impacts of snowstorms on traffic based on limited traffic modes at small scales. For example, snowstorms have been found to impact different dimensions of traffic, e.g. traffic demand, traffic safety, traffic operations and flow (Maze et al., 2006). The impact varies by trip purposes (Cools et al., 2010; Koetse & Rietveld, 2009) and distances (Maze et al., 2006), types of vehicles, different areas (Call, 2011), and time (Datla & Sharma, 2008). In terms of trip purposes, results from a survey (Cools et al., 2010) indicate that snow and stormy weather have the least impact on commuting (work, school) behavior: the work and location were the least frequently changed and the main change in commuting behavior was in timing of the trips; while for shopping trips and leisure tips, more than half of the responds chose to cancel the trip and even more changed route and location. However, it is still unclear what the quantitative relationship between peoples' recurrent mobility (characterized by their frequent visited places) and perturbed mobility during the winter storm is. In addition to traffic, heavy snow has been shown to have a negative impact on foot travel frequencies (de Montigny et al., 2011). However, these empirical

studies based on a single transportation mode at a small scale do not represent the population well, and, in turn, are unlikely to reveal the overarching impact of large-scale storms. The severity of the damages from winter storms calls for innovative research, particularly a fundamental understanding of human behaviors and activity patterns with aggregated data to achieve more effective snowstorm preparation and to build more resilient cities.

Based on the findings of studies on human mobility in disasters and the impact of snowstorms on traffic, in this paper, we tested four hypotheses: Hypothesis 1: Individuals' displacements of different lengths can be significantly perturbed by a severe winter storm and the perturbation varies among different ranges of distances and distinct days of a week; Hypothesis 2: Human mobility patterns can be affected by a severe winter storm, as measured by radii of gyration and the shifting distance of center of mass; Hypothesis 3: Individuals' frequently visited locations can better quantify their mobility patterns during a severe winter storm than non-perturbed patterns during normal days.

2.3 Methods

We selected the January 2015 severe winter storm in the northeastern United States for the seasonality and high frequency of this type of damage in this area and its large-scale impact. This severe storm caused a snow emergency to be declared by the Federal Emergency Management Agency (FEMA, 2015) during January 27 to 29 in six states, including New Hampshire, Massachusetts, Connecticut, Rhode Island, Maine and New Jersey. This winter hazard brought heavy snow to southern New England with blizzard conditions to much of Rhode Island and Massachusetts, beginning during the day on January 26 and lasting into the early morning hours of January 27. We narrowed the area within the spatial bounding box coordinates of Massachusetts due to the population distribution, and the statewide impact (latitude: 41.187 to 42.887, and

longitude: -73.508 to -69.859). The storm duration was from January 26 to 28 in this area. Much of this affected area received two to three feet of snow and experienced severe winds with gusts over 70 mph (NOAA, 2015b). The Category of Regional Snowfall Index (RSI, which estimates societal impacts of snowstorms within a region's borders) (Squires et al., 2014)for this storm has an Index value of 6.158 (NOAA, 2015a), which indicates a major snowstorm. A statewide driving ban was issued and MBTA public transportation service was suspended, thousands of flights were cancelled, and schools and activities observed weather-related cancellations for one or more days (NOAA, 2015b).

The raw data for this study is comprised of geotagged Tweets collected from a Twitter Streaming API (Wang & Taylor, 2015). We use geotagging as the only filter to collect real-time Tweets. As 1.24% of Tweets are geotagged (Pavalanathan & Eisenstein, 2015) and the streaming API can collect 1% of Tweets, the database of this study is representative in terms of geotagged Tweets. The Twitter geotags are based on GPS Standard Positioning Service which offers a worst-case pseudo-range accuracy of 7.8 meters with 95 percent confidence, and the positional accuracy are affected by weather and device factors (Swier et al., 2015). The studied time period includes four pre-storm weeks, a during-storm week, and a post-storm week – from December 29, 2014 to February 8, 2015. The data volume for each day can be found in Table A1. In total, 2,691,346 Tweets were collected over the 42 days and the average daily data volume was about 64,080 Tweets.

2.4 Results

2.4.1 Daily Displacements

To explore if severe winter storms can perturb people's daily trajectories, displacements of each distinct user during thirty-five 24-hour periods over January 5 to February 8, 2015 (Eastern Time)

were calculated and studied. Displacement in our studies is defined as the Haversine distance between two consecutive geolocations of an individual within a day. To avoid the inaccuracy of GPS services (Swier et al., 2015), we exclusively focused on displacements which are longer than *eight* meters. Six groups of distances were set, including 8-100 meters (r_1), 100-500 meters (r_2), 500-1,000 meters (r_3), 1-5km (r_4), 5-10km (r_5), and 10km and more (r_6). Data volume of displacements per day varied from 12,576 to 70,565 (see Table A2). Percentages of the number of displacements within the six sets during pre-storm weeks and the storm week were then computed and plotted for comparison. In Figure 3 (a-f) Points in each line represent percentages of a trip on distinct days in a week. The star points in blue lines refer to percentages during the severe winter storm week (Week 4), when the Monday, Tuesday and Wednesday were the exact three-day duration of the storm. Weeks 1-3 are the weeks before the storm and Week 5 is the week after the storm. Counts of displacements in all ranges can be found in Table A2.

The storm week (Week 4) exhibits a clear perturbation pattern for each group of distances. The four plots for normal weeks (Week 1, 2, 3, 5) exhibiting regularity are comparable within each group of distances. For example, during the normal weeks, the average percentages of short trips (r_1) decreases from Monday (72.92%) to Friday (60.81%), and increases from Friday to Sunday (74.38%). However, during the storm week, heavy snow incurs more short trips and the percentage of r_1 achieves the peak at 85.23% on Tuesday (the storm day) and decreases sharply to 60.20% on that Friday. It finally returns to a normal level (76.86%) on Sunday. In contrast, the long trips (r_6) experience a decreasing trend to its lowest percentage on Tuesday (2.18%) compared with the increasing trend from Monday to Friday under normal circumstances. It rebounds to its highest

value of 7.91% on Friday. Trips of other distance ranges also experienced substantial perturbation during the storm.

To quantitatively examine the observations from Figure 3, we adopted *binary logistic regression* to check if the severe winter storm statistically affected trips of different ranges. We set storm and non-storm statuses as binary explanatory variables (1 and 0 respectively), and percentages of trips of a distinct category as response variable. The coefficient and significance values can be found in Table A3. We found that percentages of longer trips (i.e. r_4, r_5, and r_6) and the shortest trip (r_1) were statistically significantly influenced by the winter storm (p-value<0.05). However, percentages of r_2 and r_3, although obviously decreased from the Monday to Tuesday during the storm week, were not statistically significantly changed by the snow storm over the three day period.

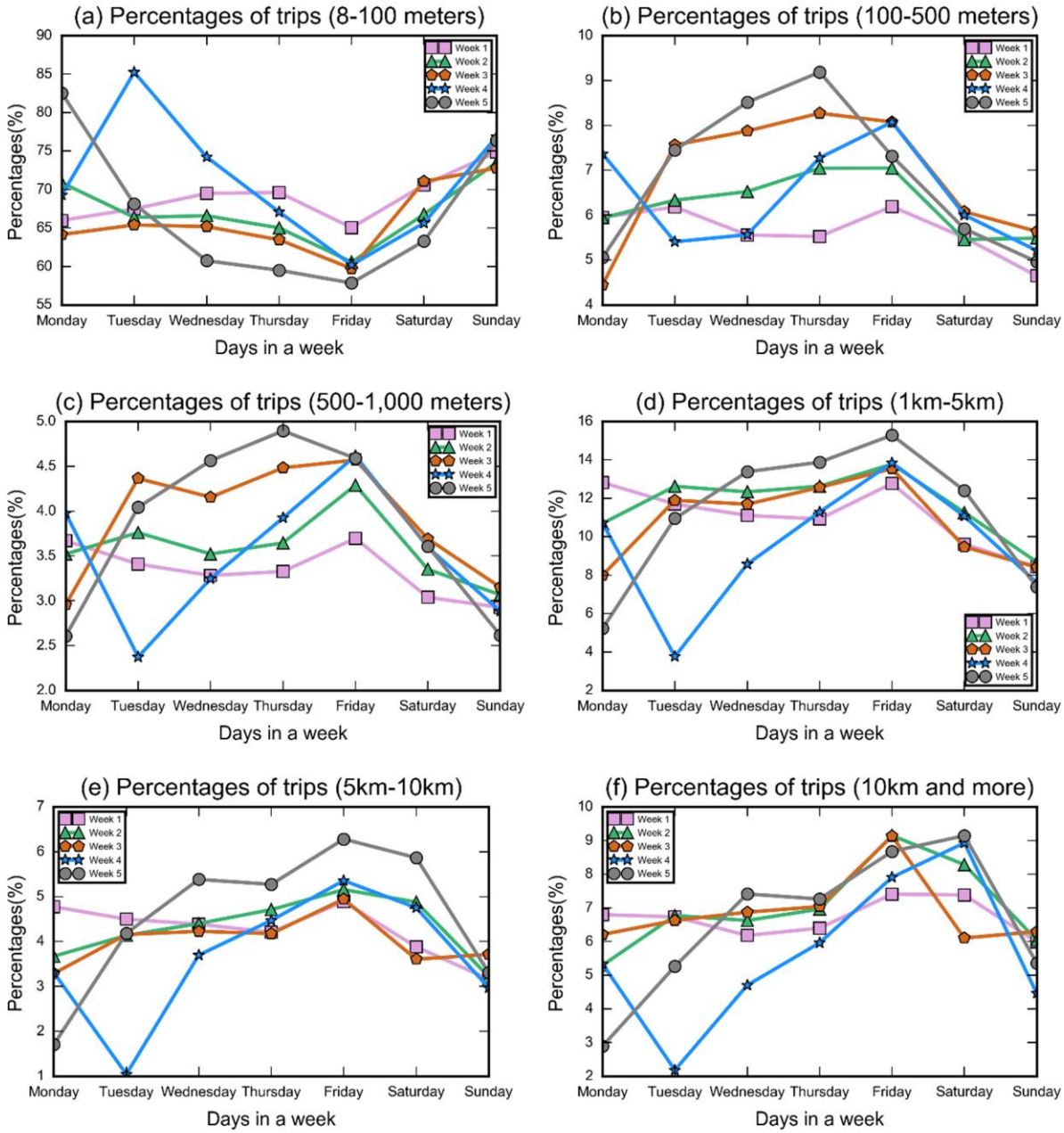

Figure 3: Impact of the Severe Winter Storm on Percentages of Trips in Different Distance Ranges

To arrive at a detailed understanding of the daily displacements, we further fitted daily displacements from January 5 to February 8 into distributions including lognormal, exponential, and power law, using the Python package Powerlaw (Alstott et al., 2014). *Lognormal distribution*

(Eq. 1) best characterized their distributions based on the loglikelihood ratio and the corresponding p value. We plotted the complementary cumulative distribution of displacements for empirical data and log-normal fitted data according to different days in a week in

Figure **4**. In Figure 4 (a-g) Graphs show the distributions of displacements from Mondays to Sundays during the studied weeks. The dashed lines in each graph represents the CCDF for empirical data, while the solid lines refer to the CCDF for log-normal fitted data. Blue lines represent the days in the storm-affected week, and other grey lines refer to days during normal weeks. The daily displacement distribution is well fitted with lognormal distribution.

$$P(x) \sim \frac{1}{x\sigma\sqrt{2\pi}} e^{-\frac{(Inx-\mu)^2}{2\sigma^2}} \tag{1}$$

The results of fitting and comparisons with other distributions are all included in Table A4. For the fitted parameters, the values of mean (μ) in all fittings are in the range 7.452±0.560 while January 27 has the smallest mean value of 4.627. However, all the snowstorm days and the following days have relatively smaller mean values than normal days. The values of standard deviation (σ) in all fittings are in the range of 2.077±0.239 except for the most severe day of the storm, January 27, with the highest value of 3.232 and the following Monday (February 2) with a value of 2.566, which indicates more differences among frequencies of different-length displacements. The displacements decay faster on that Monday perhaps because fewer people tended to travel longer distances due to the severe snow storm.

Both the results of the logistic regression and the scaling parameters from fitting log-normal distribution show that the severe winter storm has significantly impacted displacements, and the perturbation varies among distinct days of a week. Therefore, we find support for Hypothesis 1.

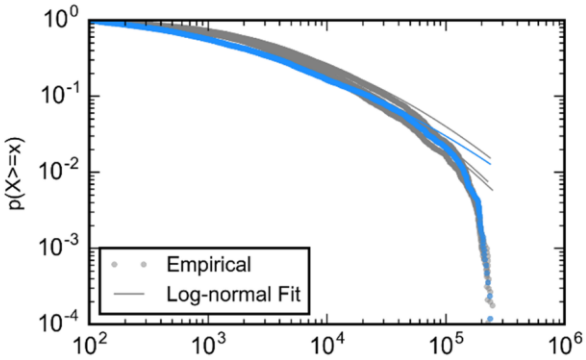

(a) Monday Displacement Frequency

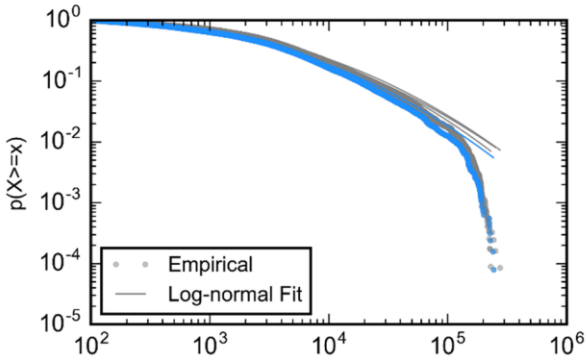

(b) Tuesday Displacement Frequency

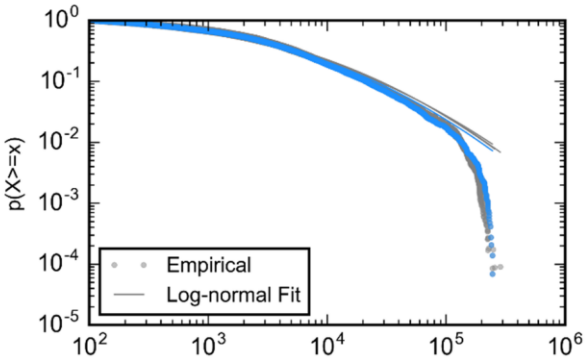

(c) Wednesday Displacement Frequency

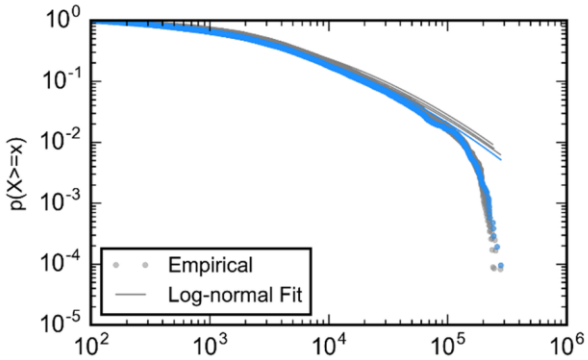

(d) Thursday Displacement Frequency

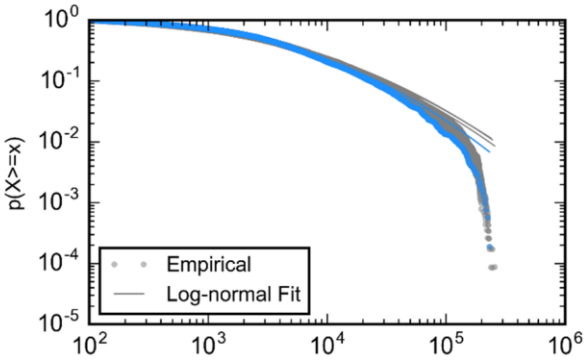

(e) Friday Displacement Frequency

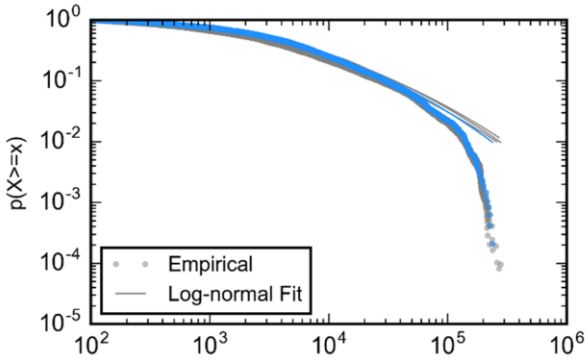

(f) Saturday Displacement Frequency

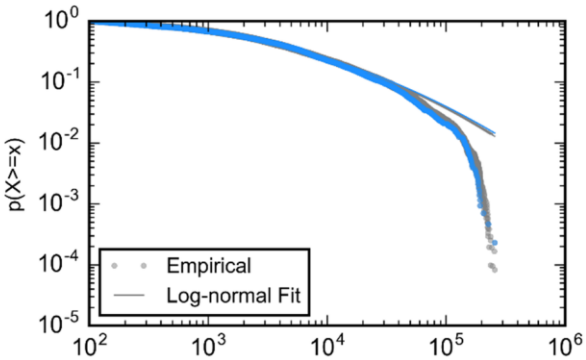

(g) Sunday Displacement Frequency

Figure 4: Complementary Cumulative Distribution Function of Displacements for Empirical Data and Log-normal Fitted Data

2.4.2 Radii of Gyration

Radii of gyration (r_g), a measurement of object movement from physics, has been widely used to quantify the size of trajectory of individuals since the study of Gonzalez et al. (2008). To achieve a more nuanced understanding of the perturbation of human mobility patterns, we computed the daily r_g of each distinct user from January 12 to February 8 to identify the change of daily radii of gyration over time. We adopted the formula in Eq. 2 (Wang & Taylor, 2016) to calculate the r_g of each distinct individual in the data set.

$$r_g = \sqrt{\frac{1}{n}\sum_{k=1}^{n}\left[2r \times \sin^{-1}\left(\sqrt{\sin^2(\frac{\phi_k - \phi_c}{2}) + \cos\phi_k \phi_c \sin^2(\frac{\varphi_k - \varphi_c}{2})}\right)\right]} \quad (2)$$

where n is the total frequency of visited locations of one individual, k is each visited location by the individual during a 24 hour period, c is the center location of the individual's trajectories, ϕ is the latitude, and φ is the longitude.

To minimize the variance among distinct days in a week and to better reflect the influence of the severe winter storm, We computed r_g based on a Monday, Tuesday and Wednesday (MTW-based r_g) which were the three days (January 26 to 28) experiencing the most substantial effects of the winter storm. We also computed four sets of r_g for four MTWs in consecutive weeks from December 29, 2014 to January 25, 2015, before the storm. We filtered users to make sure each distinct user had at least two geolocations during each three-day period. This resulted in 3,743 distinct users with at least ten entries over the 15 days, and 95.18 average geotags per person. The

total entries transmitted by the 3,743 users were 356,164, including 75,179 storm-day locations and 280,985 normal-day locations. We used Quantile-Quantile plots (also called Q-Q plots) to compare the distributions of MTW-based r_g among four pre-storm normal weeks and the storm week (Figure 5). In Figure 5(a-e), these plots show a plot of the quantiles of the five data sets of MTW-based radii of gyration against the quantiles of the theoretical data set distributed as standard normal. The referenced straight lines pass through the first and third quartiles. MTW5 refers to the storm affected days. Its curved line and reference line show an obvious deviation from lines of other sets. The deviations between different pairs of MTW were quantified with a two-sample Kolmogorov-Smirnov test. The statistics and p-values can be found in Table A5. The empirical distribution of MTW-based r_g during the snow storm week and during normal weeks has the largest value of deviation comparing with deviations between other pairs of distributions.

We further computed the daily r_g of each distinct user from January 12 to February 8 to identify the change of daily radii of gyration for the week before, during and after the winter hazard. We fitted the daily r_g to different distributions and found that *truncated power law* provides a better approximation of daily r_g than exponential and log-normal distributions. All the fits pass the Kolmogorov-Smirnov test for goodness of fit. The results can be found in Table A6.

We used the *scaling parameter* (α) to evaluate the human mobility pattern as well as the perturbation duration. For the whole six weeks, $\alpha = 1.62 \pm 0.17$ (mean $\pm$ standard deviation), which is not far from the values of the scaling parameter identified in former studies (Brockmann et al., 2006; Gonzalez et al., 2008; Wang & Taylor, 2014). For the four pre-storm weeks without any snow, $\alpha = 1.63 \pm 0.05$ (mean $\pm$ standard deviation), which demonstrates a steady mobility pattern. The stable pattern also lasts until the beginning two days of the snow (January 26 and 27), however,

α experiences its first peak at 1.78 on January 28, indicating more spread-out frequencies of all displacements. The values return back to a normal range in the next two days, but drop to the lowest points (1.00 and 1.41) in the weekends after the storm, which indicates a substantially changed mobility pattern. This may be caused by the increasing needs of individuals to take longer-distance trips to undertake activities that would have normally occurred in the weekdays when the heavy snow caused inconvenience for travel. Moreover, the relatively higher values of scaling parameters starting from the Thursday in the post-storm week may have been caused by the accumulation of snow on non-consecutive days (February 2, 3, 6, and 8) in some of the studied geographical area following the severe storm. Due to the severe winter storm, the snow depth examined in most areas included in this study exceeded ten inches (NOAA, 2015b). The accumulated snow may have been the cause of the perturbed mobility patterns. Based on these results, we find support for Hypothesis 2.

a. QQ plot of log(MTW1-based Radii of Gyration)

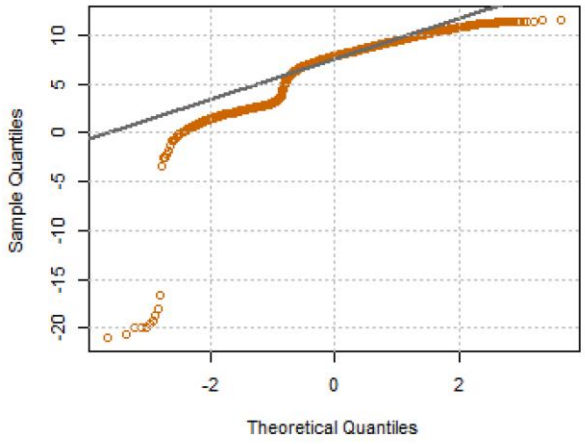

b. QQ plot of log(MTW2-based Radii of Gyration)

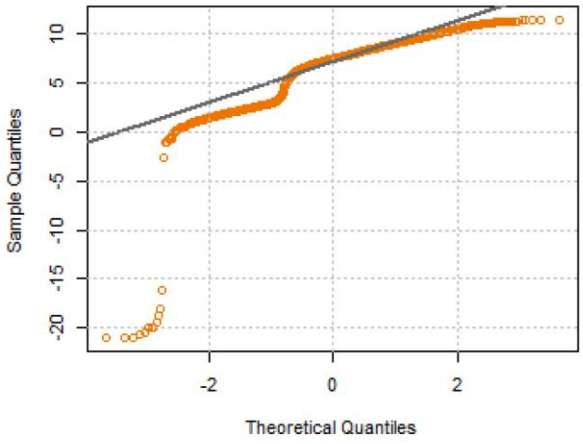

c. QQ plot of log(MTW3-based Radii of Gyration)

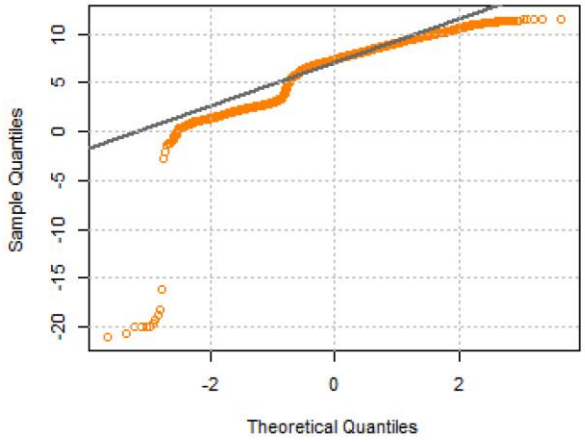

d. QQ plot of log(MTW4-based Radii of Gyration)

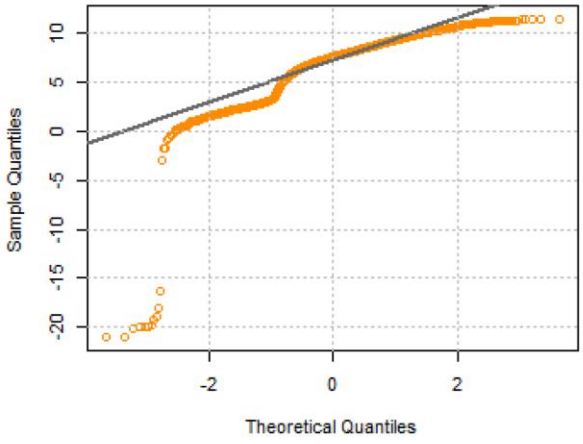

e. QQ plot of log(MTW5-based Radii of Gyration)

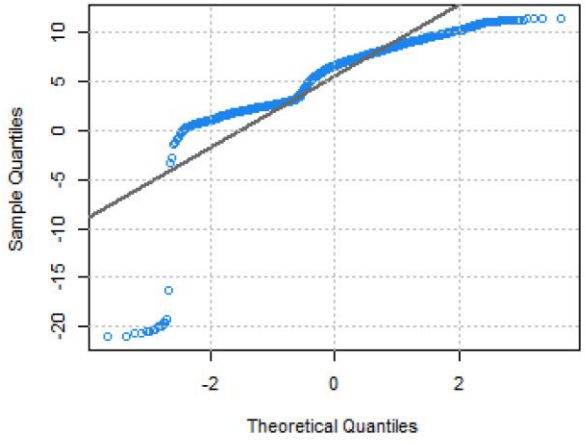

Figure 5: Comparison of Empirical Distributions of MTW-based r_g between Normal Status and Disaster Status based on Quantile-Quantile Plot

2.4.3 Shifting Distance of Center of Mass

We computed the shifting distance of the center of mass (Δd_{CM}) to quantify the change of mobility pattern. The average center of mass of distinct individuals under four normal statuses and one in the snowstorm period were calculated separately. The Δd_{CM} was the shifting distance of the average center of mass from the normal state to the perturbed snowstorm state. Eq. 3 was employed to calculate the shifting.

$$\Delta d_{CM} = \left| \vec{r}_{CM}^{S} - \vec{r}_{CM}^{N} \right| \tag{3}$$

Where $\vec{r}_{CM}^{S}$ is the average center of mass of a movement trajectory during the storm days, and $\vec{r}_{CM}^{N}$ is the average center of mass during the first four sets of Monday, Tuesday and Wednesday.

The *truncated power law* distribution was found to be the best distribution of Δd_{CM} compared to lognormal and exponential distributions (Eq. 4). The parameters were obtained using the KS fit method. Fitting and comparison results can be found in Table 1.

$$P(\Delta d_{CM}) \propto \Delta d_{CM}{}^{-1.3735} e^{-0.7396 \Delta d_{CM}} \tag{4}$$

Table 1: Truncated Power Law Fitting and Comparison Results of ΔdCM

β Value	λ Value	κ Value (m)	*KS*-test	Lognormal Comparison	p-value	Exponential Comparison	p-value
1.373	0.740	0.027	0.013	47.807	1.452e-30	1441.284	3.504e-55

2.4.4 Relationship Between Perturbed Mobility and Recurrent Mobility

The mobility patterns of individuals are dominated by their recurrent movement between a few primary locations (De Montjoye et al., 2013; C. Song, Koren, et al., 2010) and have a high predictability (Lu et al., 2012; Lu et al., 2013; C. Song, Qu, et al., 2010). These most frequently visited locations include home, work, and school, along with several less active subsidiary locations (Bagrow & Lin, 2012; Pappalardo et al., 2015). To examine if most frequented locations (MFLs) can quantify human mobility patterns under the severe winter storm as well, we compared the radii of gyration of MFLs (r_g^{MFLs}) with both r_g^n (normal status) and r_g^s (storm status) of each distinct individual. We defined the MFLs as the centroids of different clusters. Only users with at least two MFLs (two clusters) during normal days and at least two geolocations in a day under storm status were studied. MFLs of each distinct user were extracted from their four-week trajectories before the blizzard utilizing the DBSCAN algorithm. We set the required two input parameters for the clustering as follows: the maximum search radii was set as 20 meters, and the minimum number of points to form a cluster was set as two. The initial settings are based on the accuracy of the Twitter geotags, and the sensitivity analysis results on distance parameters of DBSCAN for Twitter data as identified in the study (Swier et al., 2015). The MFLs of distinct individuals were then ranked according to their visitation frequencies, and MFLs with the same visitation frequencies have different but consecutive rankings.

To quantify the human mobility pattern characterized by MFLs, we adopted the definition of the k-radii of gyration $r_g^{(k)}$ (Pappalardo et al., 2015), which is the radii of gyration of k-th MFLs of an individual. The comparisons between $r_g^{(k)}$ and r_g^s allows us to quantify the correlations between k-th MFLs and mobility pattern during the winter storm. We plotted the scatter graphs to observe the correlations with the point density which is colored from blue to red (

Figure **6**). We used Pearson correlation coefficient to quantify the strength of the correlation between $r_g^{(k)}$ and r_g^s. The value of Pearson correlation coefficient r and its corresponding p value are shown in Table 2. The p value is less than 0.01 for all comparisons, which indicates strong statistical significance. r is positive for each case. It ranges from 0.760 to 0.923 for the comparisons between r_g^n and $r_g^{(k)}$, and 0.161 to 0.404 for the comparisons between r_g^s and $r_g^{(k)}$ (k =2,…,8). With the increasing value of k, the radii of gyration of MFLs presents a stronger correlation with both r_g^n and r_g^s. However, by comparing the correlation coefficient r for both comparisons (r_g^n and $r_g^{(k)}$, and r_g^s and $r_g^{(k)}$) with the same k value, we found that the MFLs cannot characterize human mobility patterns during the severe winter storm better comparing with the higher similarity degree between recurrent mobility and mobility during the normal days. Therefore, Hypothesis 3 is rejected.

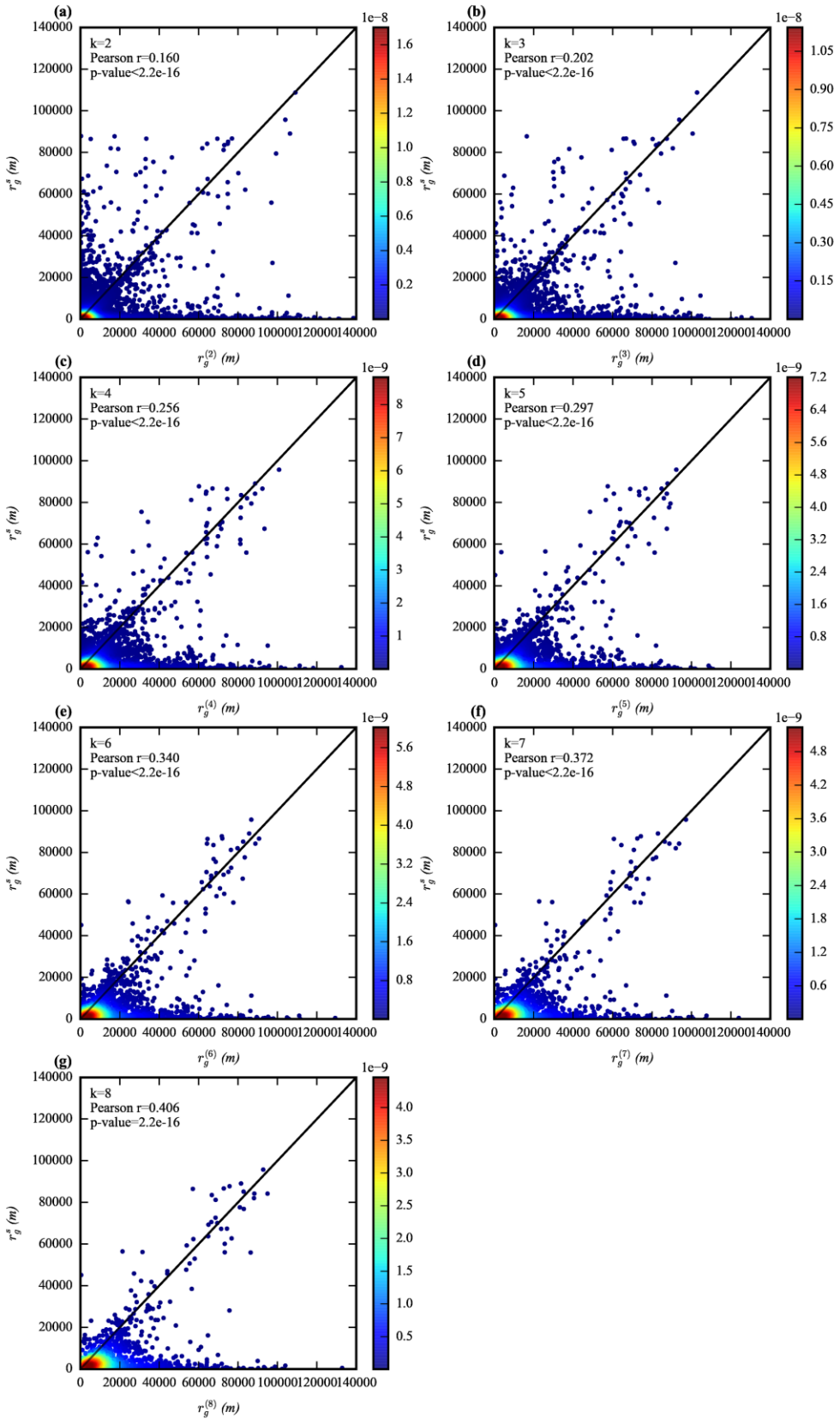
(a)
k=2
Pearson r=0.160
p-value<2.2e-16
(b)
k=3
Pearson r=0.202
p-value<2.2e-16
(c)
k=4
Pearson r=0.256
p-value<2.2e-16
(d)
k=5
Pearson r=0.297
p-value<2.2e-16
(e)
k=6
Pearson r=0.340
p-value<2.2e-16
(f)
k=7
Pearson r=0.372
p-value<2.2e-16
(g)
k=8
Pearson r=0.406
p-value=2.2e-16
1e−8
1e−9
r_g^s (m)
$r_g^{(2)}$ (m)
$r_g^{(3)}$ (m)
$r_g^{(4)}$ (m)
$r_g^{(5)}$ (m)
$r_g^{(6)}$ (m)
$r_g^{(7)}$ (m)
$r_g^{(8)}$ (m)

Figure 6: Comparisons between r_g^s and $r_g^{(k)}$.

Table 2: Pearson's Correlation Analysis between r_g^n and $r_g^{(k)}$ and, between r_g^s and $r_g^{(k)}$

k	2	3	4	5	6	7	8
correlation coefficient (r_g^n, $r_g^{(k)}$)	0.7599454	0.8558787	0.8860109	0.8953719	0.9071972	0.9147848	0.9228992
$p-value$	<2.2e-16	<2.2e-16	<2.2e-16	<2.2e-16	<2.2e-16	<2.2e-16	<2.2e-16
correlation coefficient (r_g^s, $r_g^{(k)}$)	0.1604997	0.2023405	0.2562723	0.2973382	0.3395652	0.3723097	0.4060454
$p-value$	< 2.2e-16	2.2e-16	< 2.2e-16	< 2.2e-16	< 2.2e-16	< 2.2e-16	2.2e-16
df	11619	8025	5598	4004	2956	2237	1695

2.5 Discussion

Previous research has found that natural disasters, e.g. hurricanes, floods and earthquakes, can cause significant impact on human mobility patterns (Bagrow et al., 2011; Gray & Mueller, 2012; Lu et al., 2012; X. Song et al., 2014; Wang & Taylor, 2014, 2016). We extend this research to severe winter storms showing that human mobility patterns are impacted in this different context. The results show that the severe winter storm caused significant perturbation on displacements in various ranges including short trips and long trips, which provide support to Hypothesis 1. The numbers of the shortest trips increased significantly while other longer trips decreased significantly. Similar findings have been found in single-mode transportation studies (Call, 2011; Datla & Sharma, 2008; de Montigny et al., 2011; Maze et al., 2006). This research builds upon these studies by examining large-scale empirical geo-temporal data, which may provide a more general perspective on human mobility. The high-accuracy geographical data also help to reveal

specific impacts of a winter storm on displacements of different length. By investigating distribution of daily displacements over nearly one month, we found that daily displacements can be best approximated with the lognormal distribution under both normal and perturbed states. This result is consistent with the findings of Zhao et al. (2015) and Alessandretti et al. (2017), which focused on a normal, steady state mobility pattern. Parameters of the fitted lognormal distribution further help to examine the first hypothesis and the changed values over phases can signal the effect of the natural disaster.

The prediction of Hypothesis 2 that human mobility patterns would be affected is also supported: To minimize the variance between weekdays and weekends, we investigated distributions of radii of gyration on a Monday-Tuesday-Wednesday basis and distributions of daily radii of gyration. Distributions of both types of radii of gyration reflect the perturbation on mobility patterns caused by the severe storm. For Monday-Tuesday-Wednesday based radii of gyration, two-sample Kolmogorov-Smirnov tests uncovered the largest deviations between distribution during the storm week and distributions during the normal weeks. In terms of the daily radii of gyration, we found that this measurement can be best approximated by truncated power law during the severe winter storm and the truncated power law was found to be the dominant scaling law of mobility patterns in previous research (Wang & Taylor, 2014, 2016). Scaling parameters of the fitted distributions help to detect the impact of the storm on the mobility pattern as well. To investigate the extent of the change of mobility pattern, we also measured the distance between center of mass of normal mobility and center of mass of perturbed mobility. The shifting distances fit a truncated power law distribution. We further investigated the degree of similarity between recurrent mobility and mobility under normal and perturbed circumstances separately (Hypothesis 3). Although previous studies showed that individuals' trajectories show a high degree of spatial regularity characterized

by a few highly frequented locations (De Montjoye et al., 2013; Gonzalez et al., 2008; C. Song, Koren, et al., 2010; C. Song, Qu, et al., 2010), the regularity does not remain during the severe winter storm. By comparing correlation between individuals' recurrent mobility and perturbed mobility with correlation between recurrent mobility and normal mobility, we found that, contrary to Hypothesis 3, most frequented locations cannot better characterize individuals' mobility pattern during the severe winter storm than during the normal circumstances. We also noticed that, for individuals with more recurrent locations, there is a higher correlation between recurrent mobility and perturbed mobility.

There are several limitations in this study deserving further research effort in the future. First, apart from the geotagged tweets used for this study, the self-reported locations in the text of tweets during disasters may also be included in future research data collection to achieve a broader sample. Only 1% of Twitter users geotag their tweets, but we still were able to evaluate 64,080 geotagged tweets per day, which is adequate for this analysis. Additionally, future analysis should examine the specific impact on human mobility of climate elements, such as snowfall and wind speed, and by expanding to multiple cases. This study narrowly examined the aggregated responses to the storm in a single case. Future research should examine how different geographical scales may influence the results. Regarding the relationship between recurrent mobility and normal and perturbed mobility, future research may examine and compare the specific semantic content of locations under different circumstances.

2.6 Conclusion

This work contributes to a growing body of literature aimed at enhancing disaster resilience and risk management by understanding and predicting human mobility using crowd-sourced data. The results evaluate overall and nuanced aspects of perturbation on mobility patterns, and how different

profiles of population mobility are affected following a large-scale and severe winter storm. The quantitative approaches adopted in this study form a framework to examine the impact of natural disasters on human mobility patterns using geolocation data from social media. This framework can be used to assess both spatial and temporal aspects of urban mobility during disasters, to supplement evaluations of evacuation performance, and to track urban resilience to natural disasters. The findings of this study form an important step toward understanding human mobility during disasters. The investigated mobility patterns in this paper could be combined with detailed transportation and weather data and semantic content from geo-social networking platforms to inform governments and policymakers regarding specific disaster responses and relief strategies, for example, through improved resource allocation, emergency information diffusion, disease prevention, and evacuation in disasters.

CHAPTER 3. TRACKING URBAN RESILIENCE TO DISASTERS: A MOBILITY-NETWORK-BASED APPROACH[2]

3.1 Abstract

Disaster resilience is gaining increasing attention from both industry and academia, but difficulties in operationalizing the concept remain, especially in the urban context. Currently, there is scant literature on measuring both spatial and temporal aspects of resilience empirically. We propose a bio-inspired quantitative framework to track urban resilience to disasters. This framework was built upon a daily human mobility network, which was generated by geolocations from a Twitter Streaming API. System-wide metrics were computed over time (i.e. pre-, during and post-disasters). Fisher information was further adopted to detect the perturbation and dynamics in the system. Specifically, we applied the proposed approach in a flood case in the metropolis of São Paulo. The proposed approach is efficient in uncovering the dynamics in human movements and the underlying spatial structure. It adds to our understanding of the resilience process in urban disasters.

Keywords: crowd-sourced data; disaster management; fisher information; network analysis; urban resilience.

[2] This paper has been presented at the 14th International Conference on Information Systems for Crisis Response and Management (ISCRAM 2017) in Albi, France, and was co-authored with Professor John E. Taylor. An expanded version of this manuscript is in the process of being developed with co-authors Professor John E. Taylor and Professor Michael Garvin.
Wang, Y. & Taylor, J.E., (2017). Tracking urban resilience to disasters: a mobility network-based approach. *Proceedings of the 14th International Conference on Information Systems for Crisis Response and Management* (ISCRAM 2017) (pp. 97–109). Albi, France.

3.2. Introduction

Due to the increasing risk, frequency, and intensity of natural disasters caused by climate change, disaster resilience has gained momentum in both academic and policy discourse (Meerow, Newell, and Stults, 2016). Building urban resilience emerges as a critical agenda due to rapid urbanization, and extensive interconnected infrastructure systems in urban areas (Cutter et al., 2014). Resource dependencies of cities on surrounding or other areas can incur cascading impact on their dependent areas, and pre-existing urban stressors can aggravate the effects of climate change (Cutter et al., 2014). We lack a unified definition of disaster resilience. However, one that contains many characteristics of disaster resilience is from the National Academy of Sciences (NAS): "*the ability to prepare and plan for, absorb, recover from, and more successfully adapt to adverse events*" (Cutter et al., 2012). Resilience in the disasters research field, though overlapped with concepts of vulnerability and robustness, has a different emphasis on the dynamic process of adapting or recovering from natural disasters or extreme events (Hufschmidt, 2011; Zhou et al., 2010). Tailored to the urban context, disaster resilience should highlight both temporal and spatial scales. These scales can be used to describe its capability of maintaining or returning to desired functions, adapting to change, and transforming systems after perturbations (Meerow et al., 2016) to address the complexity and dynamics of cities.

Currently, it is still impossible to precisely predict the climate extremes in terms of spatial distribution and temporal evolution, regardless of their increased intensity or frequency (Linkov et al., 2014). These unknowns require redoubling operational efforts in building resilience. We need rigorous measurements to guide what and how to measure success (Garmestani et al., 2013; Spears et al., 2015). This is important because operationalizing the concept of urban resilience to disasters has been difficult to apply and manage; moreover, inappropriate usage of the term can

bring significant negative impacts when guiding responses to natural disasters of urban systems (Angeler and Allen, 2016). However, the multiplicity and vague definitions of resilience increase difficulties to measure resilience. Cities, as complex systems, do not lend themselves easily to measurement. It is also difficult to access high-quality data during disasters to support quantification.

Fortunately, an array of approaches for assessments and quantitative measures of disaster resilience have been developed (Quinlan et al., 2015). Some conceptual frameworks have been proposed to quantify disaster resilience in a deterministic way for decision making in different scenarios, e.g., Zobel (2011), Zobel (2014), Zobel and Khansa (2014), and MacKenzie and Zobel (2015). Most of them were based on the relationship between an initial impact of a disaster event and subsequent time to recovery. Some focused on empirical quantifications (Cimellaro et al., 2010; Pant et al., 2014; Cutter et al., 2014; Lam et al., 2015) from a specific perspective such as facility, economy, social, policy etc. Some of these studies have examined the dynamic nature of resilience over time, especially for the recovery process (e.g. Pant et al., 2014; Zobel, 2014;). Few scholars have recognized the importance of spatial and temporal attributes of resilience. For example, Frazier et al. (2013) built a set of place-specific indicators to estimate baseline resilience at a community level. However, these studies cannot capture spatio-temporal dynamics of resilience over the course of a disaster in terms of urban structure involving human activities. We need to study the dynamics from this new perspective to understand the whole process of perturbation and recovery of both urban spatial structure and human movements.

To address the methodological challenges, we investigated bio-inspired approaches in the research area of ecology, which is the original study field of resilience. As resilience has emerged as a unifying concept across various disciplines including ecology and disaster management (Quinlan

et al., 2015), approaches of quantifying resilience in ecology can provide diverse and fundamental insights in tracking urban resilience to disasters. We identified two effective tools in assessing and measuring resilience in this field: *network analysis* and *Fisher information*.

Network analysis has been proven to be a useful quantitative tool for exploring social-ecology resilience and tracking changes in vulnerability (Moore et al., 2014; Moore et al., 2015). It represents the complex ecology system as an aggregation of vertices and edges and makes it possible to be analyzed in standard mathematical approaches. Moreover, network analysis can also describe the connectivity among fragmented landscapes (Estrada and Bodin, 2008), characterize the spatially structured population in these landscapes (Bodin and Norberg, 2007), and disentangle the complexity within the spatio-temporal interactions between individuals and their environment (Jacoby and Freeman, 2016). These advantages show its potential in capturing the dynamic process of urban systems involving both human movements and spatial structure during natural disasters.

Fisher information (FI) was developed by Ronald Fisher (1922) as a measure of the amount of information of a parameter from observable data. It has been effectively used in measuring resilience in ecological systems by assessing changes in variables that charaterize the condition of the system (Eason and Cabezas, 2012; Eason et al., 2016; Karunanithi et al., 2008; Spanbauer et al., 2014). This information theory-based approach is beneficial in detecting both swift and subtle changes in system dynamics (Eason et al., 2016). Cities affected by disasters, involving fragmented spatial structure and perturbed human movements, are characterized by complexity. The complementary perspectives of networks and information processing are effective in describing complex systems. Therefore, we propose to combine the two tools to track the process of disaster resilience in cities.

Recent developments in information technology have provided an unprecedented amount of spatio-temporal data from diverse sources to study urban issues, such as human mobility patterns (Yan et al., 2014), human diffusion and city influence (Lenormand et al., 2015), land use and mobility (Lee and Holme, 2015), congested travels (Çolak et al., 2016), spreading of infectious disease (Brockmann et al., 2009), dynamic urban spatial structure (Louail et al., 2015; Noulas et al., 2015), and disaster resilience (Wang and Taylor, 2014, 2016). We also take advantage of these large-scale geolocations to bridge the data gaps in measuring disaster resilience. To begin, we used the human mobility network to describe the dynamic urban system. The movement network is reliant on the underlying urban spatial structures and social environment; it can help to reveal the impact of extreme events on human movement, usage of urban space, and spatial structure. The network is formed from aggregated geolocations at a daily basis in a disaster-affected city. Then we adopt FI in evaluating changes in network metrics over time. This helps clarify the dynamic process of resilience from a temporal aspect. Our study uniquely combined the two tools to evaluate both spatial and temporal aspects of urban resilience in the research field of disaster management.

3.3 Methods: A Bio-inspired Approach

3.3.1 Defining Urban Resilience to Disasters for Measurement

Resilience, though adopted in physics to describe the ability of something to return to its original shape after external shocks, gained its currency in the research area of ecology with a variety of definitions and measurements (Davoudi et al., 2012). A useful definition defines resilience as “a measure of the persistence of systems and of their ability to absorb change and disturbance” Holling (1973, p.14) also proposed two distinct concepts of resilience: engineering resilience and ecological resilience. The former denotes the ability of a system bouncing back to an *equilibrium*

to respond to shocks and perturbations, while the latter underscores an adaption of a system to an *alternative* or multiple stable status instead of a single-state equilibrium (Davoudi et al., 2012; Holling, 1986; Holling, 1996). Further, Carpenter et al. (2001) extended the definition of ecological resilience to social-ecological resilience to address the ability of system to stay in the domain of attraction, to self-organize, and to adapt.

Although definitions of resilience vary among diverse applications in different backgrounds, these three definitions provide a shared theoretical foundation to quantify resilience. It also worth noting that the particular context of resilience and a distinct way to define it will largely determine how it is quantified (Quinlan et al., 2015). Therefore, it is important for us to properly define resilience before the quantification. In our research context, urban systems involving mobility and spatial structure are complex and intrinsically dynamic. As it is difficult to define the optimal state of urban systems and to measure the exact impact caused by disasters, it is inappropriate to assume that the system can bounce back to an equilibrium after external perturbations. Additionally, it is also difficult to quantify the capability of a system in self-organization and adaptation to measure social-ecological resilience with current data. Therefore, we defined urban resilience to disasters to align with *ecological resilience* to incorporate the inherently dynamic nature of urban systems. We defined it as an adaption of urban system to an alternative or multiple stable status after a perturbation caused by disasters.

3.3.2 Construction of Human Mobility Network from Geo-Enabled Tweets

The raw data for our building human mobility network is comprised of geotagged Tweets collected from Twitter Streaming API (Wang and Taylor, 2015). We used geotagging as the only filter to collect real-time Tweets. As 1.24% of Tweets are geotagged (Pavalanathan and Eisenstein, 2015) and the streaming API can collect 1% of Tweets, our database is representative in terms of geo-

enabled Tweets. The Twitter geotags are based on GPS Standard Positioning Service which offers a worst-case pseudo-range accuracy of 7.8 meters with 95 percent confidence, and the positional accuracy is affected by weather and device factors (Swier et al., 2015). The data process map can be found in Figure 7. We filtered geolocations into a disaster-affected city, and aggregated the filtered data into a human mobility network on a daily basis. This choice of temporal scale for forming a network can measure changes in network metrics and detect nuanced changes of the daily mobility network over time. The human mobility network formed in this study is a *weighted undirected* network, where nodes are distinct geographical locations, edges are displacements between two locations, and the number of displacements between the same pair of locations is the weight of the edge regardless of the direction.

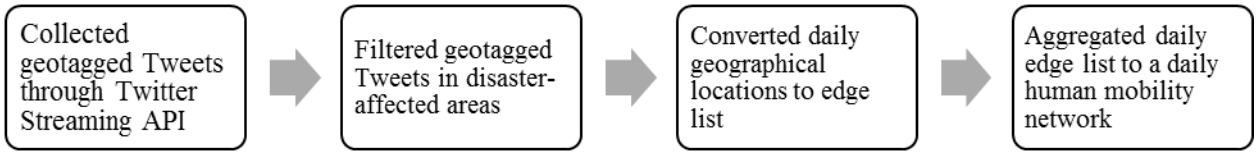

Figure 7: Process map of Building Human Mobility Network

3.3.3 Network Metrics for Measuring Topological Dynamics

We considered a variety of network metrics to achieve a comprehensive description of a human mobility network (HMN) and the underlying urban spatial structure. One set of network metrics focus on *system-wide* properties, including number of vertices, number of edges, density, diameter, average path length, size of giant component, and global and local transitivity.

Specifically, *density* measures the proportion of displacements in HMN of all possible displacements in the same network. It can characterize the network-wide frequency of interactions between locations. *Diameter* of a mobility network is the maximal geodesic distance between any pair of locations, which reflects the ability of two locations to connect with each other. *Average*

path length is the mean geodesic distance (ℓ) between two distinct locations in a network. *Giant component* describes all connected locations that a daily mobility network encompasses. *Transitivity* measures the probability that the adjacent locations of a trip are connected. We computed both *global transitivity* and *local average transitivity*. Global transitivity measures the fraction of triples that have their third edge filled in to complete the triangle. It is represented by the overall clustering coefficient $CI(g)$ CIg :

$$CI(g) = \frac{3 \times number\ of\ triangles\ in\ the\ network}{number\ of\ connected\ triples\ of\ nodes} \qquad \text{(eqn. 5)}$$

where the connected triple refers to a node with edges to an unordered pair of nodes. While local transitivity is defined on an individual node basis:

$$CI_i(g) = \frac{number\ of\ triangles\ connected\ to\ location\ i}{number\ of\ triples\ centered\ at\ i} \qquad \text{(eqn. 6)}$$

$$CI^{Avg}(g) = \frac{1}{n}\sum_i CI_i(g) \qquad \text{(eqn. 7)}$$

Assortativity coefficient describes the level of homophily of a network (Newman, 2003). In HMN, this measurement quantifies the tendency of locations to be connected with other locations with similar connected displacements. We adopted the Pearson correlation coefficient with degree of adjacent vertices (Newman, 2002) (see eqn. 4 for the normalized correlation function).

$$r = \frac{1}{\sigma_q^2}\sum_{jk} jk\left(e_{jk} - q_j q_k\right) \qquad \text{(eqn. 8)}$$

where q_k is the normalized distribution of remaining degree. σ_q^2 is the variance of q_k . e_{jk} is defined to be the joint probability distribution of the remaining degrees of the two vertices at either end of a randomly chosen edge. The coefficient lies between -1 to 1. Positive correlation indicates

assortative mixing between locations of similar degree, while negative correlation is for disassortative mixing.

3.3.4 Fisher Information

We adopted FI to assess the process of perturbation and resilience in HMN. The form of FI in these studies are shown in equation eqn. 6 (Mayer et al., 2007).

$$FI = \int \frac{ds}{p(s)} [(dp(s)) / ds]^2 \qquad \text{(eqn. 9)}$$

Here, the urban mobility system is defined as a function of network variables which charaterize normal condition and perturbed conditions due to extreme events. $p(s)$ refers to the probability of an observed network metric (s) of the urban system. The equation shows that FI is proportional to the change in the probability of observing an urban mobility state ($dp(s)$) versus the change in state (ds). In order to minimize the calculation errors, let $q^2(s) \equiv p(s)$,

$$FI = 4\int \left[\frac{dq}{ds}\right]^2 ds \qquad \text{(eqn. 10)}$$

With discretization, $dq = q_i - q_{i+1}$ dq=qi-qi+1and $ds = s_i - s_{i+1}$. Additionally, as the the state of the urban mobility system is denoted as ordinal number, $s_i - s_{i+1} = 1$. Therefore, the final equation for computing FI is:

$$FI = 4\int [q_i - q_{(i+1)}]^2 \qquad \text{(eqn. 11)}$$

We interpreted the FI based on the *expanded Sustainable Regimes Hypothesis* (Karunanithi et al., 2008): (a) regimes are identified as periods with a stable and nonzero time-averaged FI; (b) a declining FI indicates a shift in a system with decreasing dynamic order; (c) an increasing FI signifies that the patterns are moving towards more stable patterns with increasing dynamic order;

and (d) a regime shift is charaterized by a steep drop in FI. Therefore, in this research, we assumed that the change of FI is consistent with dynamics of urban systems involving human movements and underlying spatial structures.

3.4 Results

3.4.1 Overview of the Dataset

The metropolitan region of São Paulo, Brazil experienced a severe inland river flood during March 10 to 17, 2016 caused by extreme rainfall. São Paulo was selected as our studied area due to the high frequency of flooding in this area and its large urban population in South America (around 16 million inhabitants). This flood resulted in 24 casualties and 24 injured. The heavy rain began to fall on March 10, and ended the morning of March 11. 87.2 mm of rain was recorded in 24 hours in Mirante de Santana, north of São Paulo. We filtered collected geotagged Tweets into a *spatial bounding box* of the city of São Paulo with longitude from -47.3394 to -45.8134 and latitude from -24.1513 to -23.1762. The geographical box helps to include the largest size of flooding-affected area and population into our study. Five weeks of Tweets ranging from February 22 to March 27, 2016 are included in this study. This period consisted of two pre-flood and two post-flood weeks.

3.4.2 Pre-, During and Post-Flood Comparisons of Network-Wide Metrics

Over the five weeks, there are 2,449 daily average vertices (locations) and 2,194 daily average edges (displacements) included in a daily HMN. The dynamics of system-wide network metrics over weeks can be found in Figure 8. In this figure, each point represents a value of a network metric on a specific day. Each dashed line links the points to show the trend over time. Solid lines represent the Locally Weighted Scatterplot Smoothing of the scatter points. The two orange vertical lines define the duration of the flood event from March 10 to 17. The number of edges, number of vertices, and average degree (Figure 8 (a-c)) follow a similar trend over time: all witness

their peak values during the beginning four days of the flood event, and the values decrease with fluctuations after the peaks. The increased values at the beginning of the flood are likely to have been produced by the massive evacuation.

The values of edge density are very small (0.00068), which indicates that the daily aggregated mobility network is a sparse graph, and frequency of a displacement relative to another one is quite low in this network. The trend of this metric is quite steady and the impact of the flood is not obvious from visual inspection of the figure (Figure 8d).

Values of average path and network diameter also have similar trends over the weeks (Figure 8 (e-f)). The mean geodesic distance between distinct pairs of locations achieves its highest value at 13.19 on March 10 when the flood began, then it drops to the lowest value of 5.83 on March 13. Similarly, on March 10, the diameter of the mobility network increases to 119. But four days later, HMN has the lowest diameter at 22. Both metrics keep increasing with fluctuations post-flood. These changes may have resulted from fragmentations in spatial structure and perturbations in the population's movements. The flooding led to a fragmented landscape, which further increased the geodesic distance between different locations; besides, due to the heavy rains and accumulation of water, the fragmentation increased, and most connections have been affected. Therefore, geodesic distances between locations decreased remarkably after its peak value during the flood event.

The more fragmented landscape and perturbed mobility can also decrease the transitivity of HMN (Figure 8 (g-h)). Under the normal circumstances pre-flood, the daily average value of global transitivity was 0.65. This means that there is a high probability of two locations connected with each other when they are in adjacent trajectory. However, this average value decreases to 0.31

during the flood, and it is even lower (0.27) post-flood. Local average transitivity behaves similarly with average values of 0.36 (pre-flood), 0.16 (in-flood), and 0.20 (post-flood), respectively.

Interestingly, the relative size of the giant component (daily average 13.85%) during the disaster is larger than the size during normal days (daily average 8.41%) (Figure 8j). The number of vertices contributing to the giant component is different under the two circumstances: 360.38 under perturbed circumstances versus 205.18 under normal circumstances (Figure 8i). This can be caused by the reduction of displacements between affected areas and an increase of travels from affected areas to unaffected areas in the city.

The assortativity coefficient is very responsive to the flood compared to other system-wide metrics (Figure 8k). The coefficients are negative pre- and post-flood, indicating a disassortative mixing of HMN: locations are not connected to locations with similar degree. However, during the most severe flooding period (from March 11 to 14), the coefficient becomes positive but small, which suggests that HMN exhibits a low degree of assortative mixing patterns: locations become more connected to locations with similar degree. This transition can also result from fragmented landscape and the evacuation, which make less affected area more connected with each other by people's movements, while more affected areas appear to have almost lost connections with other places.

To further examine if the flood has statistically impacted the network-wide metrics, we conducted adjacent-categories logistic regression analysis to investigate the relationship between three states (i.e. pre-, during- and post-disaster) and each distinct network metric. Adjacent category regressions are a specific form of generalized logistic regression for multinomial outcomes (O'Connell, 2006). This approach compares response outcomes of adjacent categories. Before the

regression analysis, we performed the runs test (Bradley, 1968) for detecting the randomness in values of each network metric Table 3. *p-values* of all data sets are larger than 0.05, which indicates that values of each network metric are random, and adjacent-categories logistic regression is appropriate to be used. We then set the three states as ordinal response variables (specifically, 0 for the pre-flood state, 1 for the state during the flood, 2 for the post-flood state), and set a network metric as an explanatory variable in each logit model. The outcomes and *p-values* can be found in Table 3.

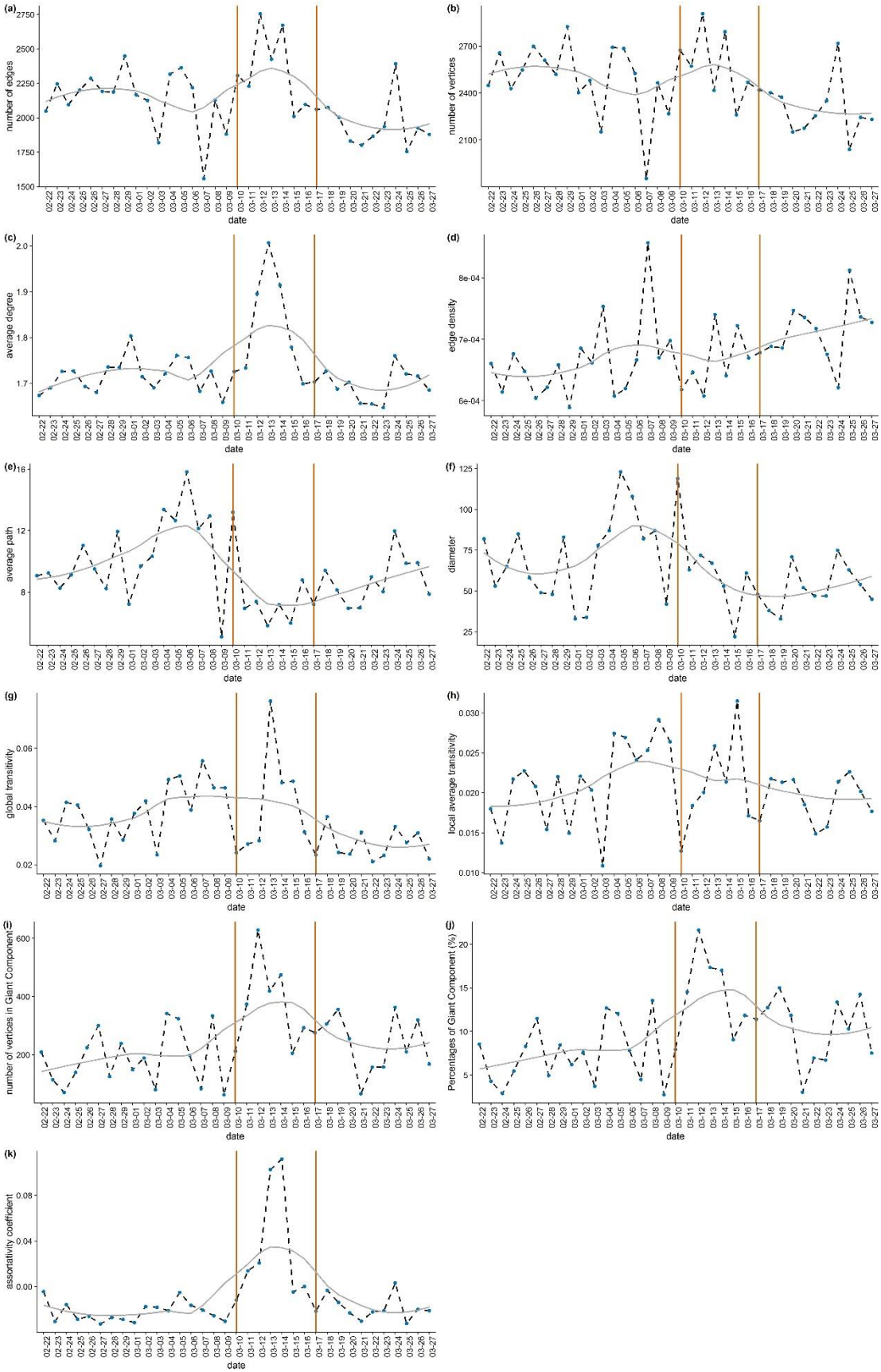
(a)
number of edges
date
(b)
number of vertices
date
(c)
average degree
date
(d)
edge density
date
(e)
average path
date
(f)
diameter
date
(g)
global transitivity
date
(h)
local average transitivity
date
(i)
number of vertices in Giant Component
date
(j)
Percentages of Giant Component (%)
date
(k)
assortativity coefficient
date

Figure 8: Dynamics of Network-Wide Metrics over Five Weeks

For the comparisons between pre- and during-flood states, the significance tests of the logistic regression reveal that assortativity coefficient, average path, and size of giant component are three metrics that have been significantly impacted by the flood event ($p < 0.05$). In comparison, number of edges, vertices, average degree, and global transitivity only exhibit statistically significant differences post-flood. They are relatively resistant to the flood at the beginning. Notably, assortativity coefficient is the only metric that responds to each state change, but metrics such as edge density, diameter, and local transitivity are stable over the course of three adjacent periods.

Table 3: Randomness of Values of Network Metrics and Outcomes of Adjacent-Categories Logistic Regression and Significance Tests

	Standardized Runs Statistic	***p-value***	**pre vs. during**	***p-value***	**during vs. post**	***p-value***
number of edges	-1.884	0.05957	-0.003744	0.08848	0.008310	0.00573 **
number of vertices	0.34832	0.7276	-0.00192	0.3817	0.006196	0.0243 *
average degree	-1.1971	0.2313	-18.230	0.0514	35.072	0.0189 *
assortativity coefficient	- 0.85368	0.3933	-150.5485	0.00836 **	106.5233	0.04288 *
edge density	-0.85368	0.3933	-488.201	0.955	- 14705.559	0.118
average path	-1.0449	0.296	0.5772	0.0305 *	-0.2863	0.2894
diameter	-1.5405	0.1234	0.01345	0.481	0.02629	0.282
global transitivity	-0.85368	0.3933	-0.7187	0.9836	137.7141	0.0337 *
local transitivity	-1.1971	0.2313	39.60258	0.670	41.15769	0.692
giant component (#)	-0.5103	0.6099	-0.0149	0.00875 **	0.00977	0.07024
giant component (%)	-2.0899	0.03663	-0.4375	0.0051 **	0.234	0.09743

Significance: '***' p<0.001; '**' p<0.01; '*' p<0.05.

3.4.3 Analysis of Resilience Based on Fisher Information (FI) of Network-Wide Metrics

We further computed the FI of all the network-wide metrics using a set of Python codes (Ahmad *et al.*, 2015). Each day was taken as a time step. Given the 35 days of data, eight time steps were set as a window size (Eason and Cabezas, 2012) to ensure that one point in the window does not improperly affect the general computaion. The window increment was one time step. Herein, FI was integrated over an eight-day window that is moved forward in one-day increments. Values of a network metric in each time window were binned into discrete states. The probability density was then computed in each time window, and provided the basis for calculating FI. Figure 9(a-k) are plots of FI for the 11 network-wide metrics over 28 days in the study. Metric values of the beginning eight days were used to calculate the initial value of FI. The orange bars highlight the flooding period and vertical grey lines define weeks.

According to the *expanded Sustainable Regimes Hypothesis* (Karunanithi et al., 2008), changes in values of FI can imply changes in regimes for the dynamic urban system. Except for FI of diameter, declining FI trends during the flooding period are found for almost all network metrics, indicating that the dynamic order decreases and the system becomes less stable. For network metrics—i.e. edge number (Figure 9a), vertice number (Figure 9b), average path (Figure 9f), and global transitivity (Figure 9h) —a local FI minimum occurs in the middle of the flooding period; for network metrics—i.e. average degree (Figure 9c), assortativity coefficient (Figure 9d), local transitivity (Figure 9i), and size of Giant Component (Figure 9k-j) —a local FI minimum occurs at the end of the flooding period. For all of these network metrics, their FI gradually increases after the lowest value, signalling the system gains dynamic order and becomes more stable. Post-flood values of FI may be lower or higher than the pre-flood values, which indicates an alternative stable status rather than an equal stable status. For the overall system, results of the FI assessment of

network-wide metrics indicate that the examined urban system exhibited no “regime shift” due to the flooding because there is no shifted FI value over the studied period. Additionally, the system exhibits resilience over the studied period: it lost dynamic order and became less stable during the flood, but gradually bounced back to an alternative stable status after the perturbation.

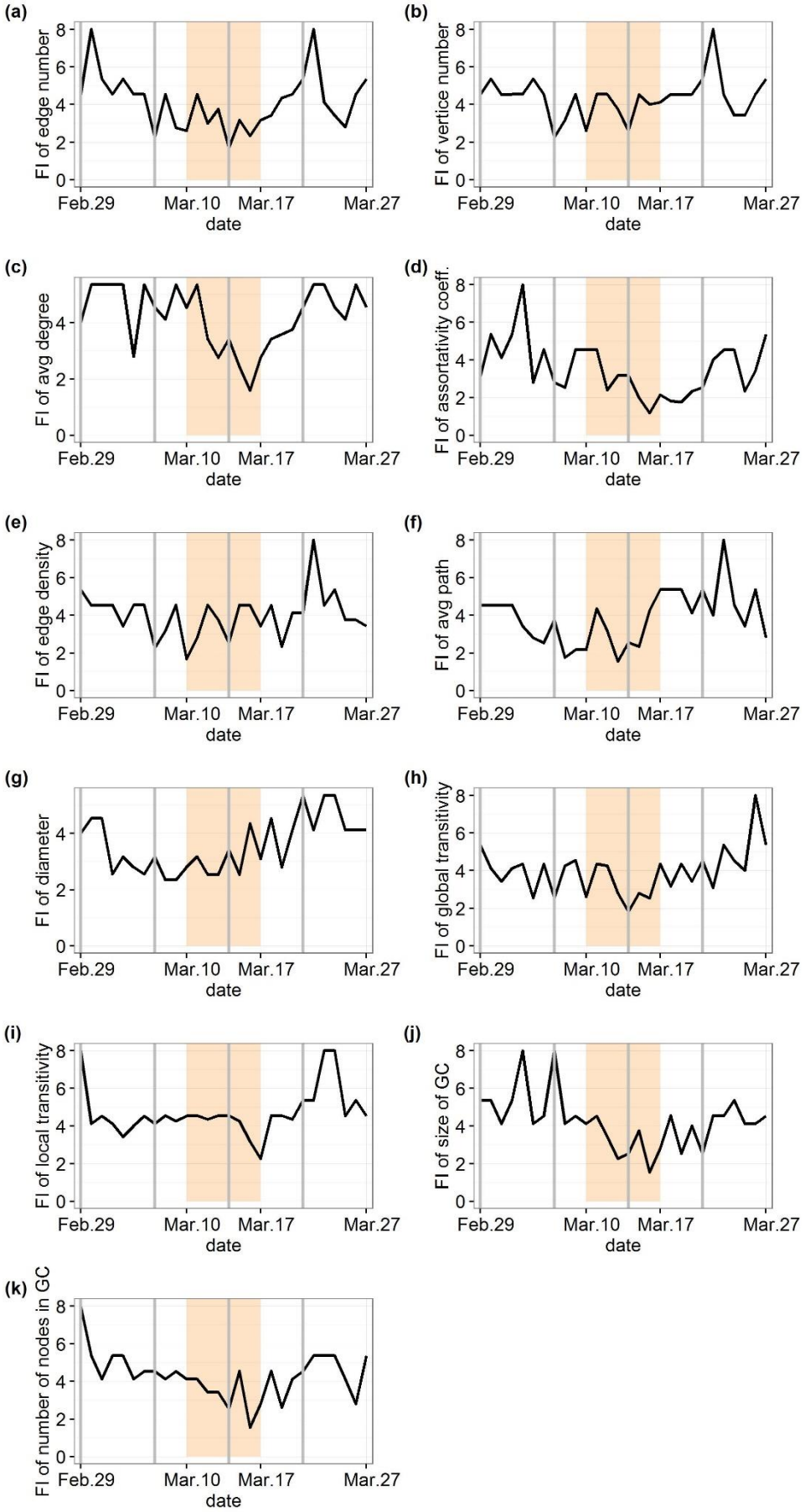
(a)
FI of edge number
(b)
FI of vertice number
(c)
FI of avg degree
(d)
FI of assortativity coeff.
(e)
FI of edge density
(f)
FI of avg path
(g)
FI of diameter
(h)
FI of global transitivity
(i)
FI of local transitivity
(j)
FI of size of GC
(k)
FI of number of nodes in GC
0
2
4
6
8
Feb.29
Mar.10
Mar.17
Mar.27
date

Figure 9: Trend of FI of Network-Wide Metrics over Time

3.5 Discussion

Previous work on measuring disaster resilience tends to be conceptual rather than quantitative (Cimellaro et al., 2010; Zobel, 2011; Zobel and Khansa, 2014). These resilience assessment frameworks have been applied to management systems and for building capacity in communities. Despite the fact that different dimensions of resilience have been addressed in different contexts and systems (Cutter et al., 2014; Cutter and Finch, 2008; Frazier et al., 2013; Lam et al., 2015), it is still difficult to quantify resilience in ways that are flexible and appropriate across a range of urban systems. Besides, although resilience has been identified as a dynamic process, few current assessments include the dynamics of how urban systems respond to disasters from both spatial and temporal aspects. Simultaneously, in spite of the shared theoretical foundations of resilience across different scientific disciplines, little cross-fertilization progress has been made, save for a handful of examples (Barrett and Constas, 2014; Quinlan et al., 2015). Our studies were inspired by definitions and approaches in measuring resilience in the pioneering field of resilience research: ecology. We applied network analysis in characterizing an urban system and used FI to detect dynamics in the resilience process.

Our constructed human mobility network can describe the dynamics of urban mobility and the underlying spatial structure. It is more representative of a general mobility network compared with networks formed from a single type of transportation mode. It is worth mentioning that our study is different from previous studies on modeling/simulating network resilience of infrastructure networks (e.g. freight transportation network, metro network, railway network, etc. (Miller-Hooks et al., 2012; Bhatia et al., 2015; Chopra et al., 2016; Gao et al., 2015; Wang, 2015)). Our research is focused on empirical data and used network metrics to describe the system. Our results show

that most network metrics can capture the change of the urban mobility network and its underlying spatial structure. The *adjacent-categories logistic regression* further examined the statistically significant impacts of the flood. For distinct network metrics, the impact can be either at the beginning or at the end of the event. However, some network-wide metrics are less responsive to the perturbation of the flood. This indicates the intrinsic resilience of urban systems.

One limitation of our research is the sample size. Clearly 2,449 daily average vertices in HMN are not enough to make generalizations about the network of all locations in a megacity. However, from the results, it can show the impact caused by the flood. With more geo-temporal data with higher resolution, a directed and weighted mobility network can be built to explore these concepts further. Additionally, a smaller time window (e.g. half day, hourly) and higher accuracy of geolocations can be used to form a network to achieve a more nuanced spatial temporal analysis. Our proposed approach has only been applied in one type of natural disaster. With increasing availability of geographical and disaster data, this bio-inspired method can also be used in assessing urban resilience to other types of disasters such as hurricanes and earthquakes. And we can also compare resilience of the same type of disaster among distinct cities. In this way, we can explore the baseline of resilience and impact factors on the resilience, such as the scale of the study area, magnitude of disasters, etc. In terms of the research assumption, we used *ecological resilience* as the basis for quantification. With deeper understanding of urban systems, we may also assume urban resilience as socio-ecological resilience to explore and measure the capability of adaption and self-organization of systems.

3.6 Conclusions

Defining and measuring resilience is an important step to address challenges caused by natural disasters. It is of critical importance to help complex urban systems quickly recover and adapt when extreme events occur. Our study contributes to knowledge in the following ways. First, it adds to the paucity of empirical literature on measuring urban resilience to disasters. We provide a quantitative framework for describing and tracking the dynamic process of resilience in terms of human mobility and underlying spatial structure at both spatial and temporal scales. Second, our method is repeatable with large-scale crowed sourced spatiotemporal data from diverse resources such as mobile phone records, social media, GPS devices, etc. Upon further validation, it can be utilized at different scales (e.g. city, area, country and larger scales), and provide convenience for spatial comparisons. Third, it paves the way for further research on quantifying resilience of a larger complex system involving urban spatial structure and human movements; moreover, this study devotes effort in measuring resilience as a unifying concept across disciplines through a bio-inspired endeavor. In practice, combining with more detailed meteorological and geographical data, our framework can help disaster managers to trace and evaluate the process of perturbation and recovery more easily. This can further facilitate effective strategic decision making regarding when and where to arrange resources during and after disasters.

CHAPTER 4: COUPLING SENTIMENT AND HUMAN MOBILITY IN NATURAL DISASTERS[3]

4.1 Abstract

Understanding population dynamics during natural disasters is important to build urban resilience in preparation for extreme events. Social media has emerged as an important source for disaster managers to identify dynamic polarity of sentiments over the course of disasters, to understand human mobility patterns, and to enhance decision making and disaster recovery efforts. Although there is a growing body of literature on sentiment and human mobility in disaster contexts, the spatiotemporal characteristics of sentiment and the relationship between sentiment and mobility over time have not been investigated in detail. This study therefore addresses this research gap and proposes a new lens to evaluate population dynamics during disasters by coupling sentiment and mobility. We collected 3.74 million geotagged tweets over eight weeks to examine individuals' sentiment and mobility before, during and after the M6.0 South Napa, California Earthquake in 2014. Our research results reveal that the average sentiment level decreases with the increasing intensity of the earthquake. We found that similar levels of sentiment tended to cluster in geographical space, and this spatial autocorrelation is significant over areas of different earthquake intensities. Moreover, we investigated the relationship between temporal dynamics of sentiment and mobility. We examined the trend and seasonality of the time series and found cointegration between the series. We included effects of the earthquake and built a segmented regression model to describe the time series finding that day-to-day changes in sentiment can either

[3] This article was co-authored with Professor John E. Taylor. It was published at *Natural Hazards*.
Wang, Y. & Taylor, J.E. (2018) Coupling sentiment and human mobility in natural disasters: A Twitter-based study of the 2014 South Napa Earthquake. *Natural Hazards*. https://doi.org/10.1007/s11069-018-3231-1.

lead or lag daily changed mobility patterns. This study contributes a new lens to assess the dynamic process of disaster resilience unfolding over large spatial scales.

Keywords: disaster informatics, earthquake, human mobility, sentiment, social media, Twitter.

4.2 Introduction

Natural disasters adversely affect human beings and the built environment. According to the latest report from Munich RE (2017), over the past seven years from 2010 to 2016, natural loss events (with at least one fatality and/or produced normalized losses larger than US$ 100 thousand, 300 thousand, 1 million, or 3 million depending on the assigned World Bank income group of the affected country) caused yearly average insurance losses of 55 billion U.S. dollars and overall losses of 174 billion U.S. dollars. During the same time period, there were in total 188 catastrophic natural events, and each of them caused more than 1,000 fatalities and/or more than 100 million U.S. dollars normalized losses (Munich RE 2017). Urban areas, due to their large and concentrated population and complex networked infrastructure systems, are highly susceptible to natural hazards, e.g. flooding, drought, storms, earthquake, tsunamis and landslides (Godschalk 2003). It is crucial to improve urban resilience to natural hazards. Among the tasks of disaster risk reduction, benchmarks for strengthening urban resilience and adaptation is urgent because it is difficult to manage something that is not measured (UNISDR 2017).

Big data offers the potential to revolutionize our understanding of managing disaster risks in terms of vulnerability assessment, early warning, monitoring and evaluation (Ford et al. 2016). Taking advantage of the increasing use of social media platforms, e.g. Facebook and Twitter (Pew Research Center 2017), researchers have extended our understanding of disaster dynamics from diverse perspectives (Guan and Chen 2014; Tang et al. 2015; Wang and Zhuang ; Wang et al. 2016). These platforms can document geographical locations and collective reactions to extreme

events in both virtual and physical worlds at a broad scale, which facilitates the development of research and practices in various branches of disaster management.

Twitter, among the most popular social media platforms, provides plentiful opportunities for detecting, tracking, and documenting extreme events. Its open design, wide usage, geo-enabled functionality and limited message lengths are well suited for emergency environments (Kryvasheyeu et al. 2016). Research involving sentiment analysis and human mobility have already taken advantage of the massive crowd-sourced data collected from Twitter. These two research topic areas help disaster managers make bottom-up decisions and play increasingly important roles in disaster relief. Specifically, sentiment analysis of short posts from social media has been shown to be an effective method to identify the dynamic polarity of sentiments over a disaster (Beigi et al. 2016), improve decision making regarding resource assistance, humanitarian efforts and disaster recovery, and obtain particular information (Nagy and Stamberger 2012). Additionally, human mobility, defined as the quantification of an individuals' movement trajectory, provides a basis to understand the perturbed movement patterns during and after disasters and to predict displacements (Wang and Taylor 2014).

We developed the approach outlined in this study to enable a data-driven understanding of disaster dynamics in urban areas. To examine the spatiotemporal dynamics of urban areas during natural disasters, we: (a) examined the correlation between disaster intensity and collective sentiment, and the spatial association of sentiment in different disaster intensity zones; (b) investigated the temporal characteristics of sentiment and human mobility using an interrupted time series model; and (c) explored the relationship between individuals' sentiment and mobility over time over the course of a disaster.

4.3 Related work

4.3.1 Sentiment Analysis and Natural Disasters

Sentiment analysis is method of evaluating and characterizing people's attitude and feeling toward a situation or event. Sentiment analysis of short posts from social media plays an increasingly important role in disaster relief and urban resilience. It is an effective method to help disaster managers to identify the dynamic polarity of sentiments over the course of a disaster (Beigi et al. 2016), improve decision making regarding resource assistance and requests, humanitarian efforts and disaster recovery, and obtain particular information (Nagy and Stamberger 2012). Vo and Collier (2013) classified and tracked the emotions of affected people using tweets during earthquakes in Japan. Eight types of emotion were selected to annotate tweets, including unconcerned, concerned, calm, unpleasantness, sadness, anxiety, fear and relief. The results revealed that fear and anxiety were the main emotions after an earthquake occurred, while calm and unpleasantness were only detected during severe earthquakes. Cody et al. (2015) explored the collective sentiment of tweets containing the word "climate", and found the connection between climate-change-related topics and a change of happiness. Bai and Yu (2016) proposed an incident monitoring framework in a post-disaster situation based on crowd negative sentiment of Chinese short blogs from Weibo. The framework was applied in the Ya'an earthquake and discovered aftershocks and potential public crises effectively. Although a few critical efforts have been made to classify sentiment during and after disasters, few studies have worked on examining both spatial and temporal dynamics of sentiment over the course of a disaster. A study by Neppalli et al. (2017) found unique spatial tweeting patterns of positive and negative sentiment following Hurricane Sandy: both positive and negative sentiment generally showed increasing clustering tendency to the point of Hurricane Sandy's maximum impact and then dispersed on the following days, while

negative sentiment consistently clustered in closer proximity to Hurricane Sandy. It remains unclear what role disaster intensity plays in influencing sentiment, and what spatial patterns of sentiment may be during other types of disasters.

4.3.2 Human Mobility during Natural Disasters

Human mobility, as a critical quantification basis of human dynamics, has triggered interest from diverse research areas, such as urban planning, traffic congestion, disease diffusion, and natural disasters. Different sources of crowd sourced geo-referenced data have been utilized including Twitter, mobile phone records, billing records, etc. The analysis of these data has ushered a new era to quantitatively understand urban population dynamics. Recently, human mobility patterns during natural disasters have received considerable research attention. Scholars in the disaster research area have identified scaling laws and evaluated the predictability of human mobility during and after extreme events using mobility patterns from non-perturbed states. Lu et al. (2012) used approximately one year of mobile phone data of 1.9 million users, and found that population movements following the Haiti earthquake had a high level of predictability, and destinations were correlated with normal-day mobility patterns and social support structure. A study by Wang and Taylor (2014) showed that human mobility was significantly perturbed during Hurricane Sandy but also exhibited high levels of resilience. A more recent study on multiple types of natural disasters revealed a more universal pattern of human mobility, as well as the limitations of urban human mobility resilience under the influence of multiple types of natural disasters (Wang and Taylor 2016). A recent study by Wang et al. (2017) also revealed that human mobility was perturbed by severe winter storms. These studies quantitatively improve our understanding of human mobility dynamics during events, however the change of mobility pattern associated with sentiment levels over time before, during and after a natural disaster has yet been investigated.

4.3.3 Hypothesis Development

Although few disaster-oriented studies examine the spatial and temporal characteristics of sentiment and its relationship with mobility over time, these topics have drawn interest of researchers from other fields (e.g. urban studies and computer science). For instance, Bertrand et al. (2013) visualized sentiment in New York City based on 603,954 geotagged Tweets over two weeks. They identified that the level of sentiment is connected with location, e.g., it progressively improved with proximity to Times Squares. They also found periodic patterns of sentiment at both daily and weekly scales: tweets on weekends tend to be more positive than on weekdays; midnight tweets are the most positive while 9:00 am and noon have the lowest-level-of-sentiment tweets. Lin (2014) examined sentiment segregation in urban communities with three-month geotagged tweets in Pittsburg. He explored the sentiment stability of neighborhoods and correlations between their sentiment orientations and the neighborhoods' demographic attributes. The results indicated a significant sentiment segregation effect. Mitchell et al. (2013) investigated the relationship between sentiment and geographic, emotional, demographic and health characteristics with 80 million geotagged tweets in 2011. Frank et al. (2013) characterized sentiment as a function of human mobility using a collection of 37 million geo-located tweets from 180,000 individuals. Research results of the two studies revealed that expressed happiness increased logarithmically with distance from an individuals' center of mass; it also increased logarithmically with the radius of gyration when binning individuals into ten equally sized groups by the radius of gyration.

These studies and our motivation to examine urban population dynamics during disasters inspired us to extend the spatiotemporal analysis of sentiment and mobility over time to the disaster context. We therefore propose two sets of hypotheses below:

Category 1. Spatial characteristics of sentiment

Hypothesis 1a: Sentiment level is correlated with earthquake intensity: the higher intensity of disaster polygons that tweets/individuals are in, the lower sentiment levels tweets/individuals have.

Hypothesis 1b: Sentiment level is clustered in space: tweets/individuals of similar sentiment levels tend to cluster together.

Category 2. Disasters can disrupt the temporal relationship between sentiment and mobility

Hypothesis 2a: There is a significant interrupted time series of sentiment and mobility.

Hypothesis 2b: There is a cointegrated time series of sentiment and mobility.

Hypothesis 2c: Change in sentiment (Δsentiment) and change in mobility (Δmobility) are cross correlated over time, and Δsentiment is a predictor of Δmobility.

4.4 Data and Methods

4.4.1 South Napa, California Earthquake

We elected to design our study of sentiment and mobility in natural disasters to focus on a severe earthquake. Geophysical disasters, such as earthquakes, are among the most severe natural disasters in terms of fatalities and damage and the least predictable. The 6.0 magnitude (M6.0) South Napa, California Earthquake was the strongest earthquake in 25 years in the Northern California Bay Area of the United States. The earthquake occurred at 10:20:44 UTC (03:20:44 PDT) on August 24, 2014 north of San Francisco. It reached the Modified Mercalli Intensity (MMI) Scale of VIII (severe) and on the moment magnitude scale a 6.0. MMI is a qualitative measure of the strength of ground shaking at a particular site and the United States employs the MMI scale, which ranges from I (not felt) to X (extreme) (USGS 2017). According to the Earthquake Engineering Research Institute (EERI 2014), the earthquake caused approximately 200

injuries and one fatality, and the total amount of federal aid was 30.8 million USD. Perceived shaking, potential damage and selected cities exposure under different estimated MMI can be found in Table 4 (USGS 2017).

Table 4: Affected Areas and Population in Different Intensity Zones

Intensity	II-III	IV	V	VI	VII	VIII	IX	X+
Perceived Shaking	Weak	Light	Moderate	Strong	Very Strong	Severe	Violent	Extreme
Potential Damage	None	None	Very light	Light	Moderate	Mod/ Heavy	Heavy	Very Heavy
Selected City	Sacramento Fremont Stockton	Oakland San Francisco	--	EI Verano Sonoma Temelec	American Canyon Yountville	Napa	--	--
Exposed Population	466K, 214K, 292K	391K, 805K	--	4K, 11K, 1K	19K, 3K	77K	--	--

4.4.2 Data Description

The raw data for this study is comprised of geotagged tweets collected from Twitter Streaming API (Wang and Taylor 2015). We use geotagging as the only filter to collect real-time tweets. As 1.24% of tweets are geotagged (Pavalanathan and Eisenstein 2015) and the streaming API can collect 1% of tweets, our database is representative in terms of geotagged tweets. Additionally, the Twitter geotags are based on GPS Standard Positioning Service, which offers a worst-case pseudo-range accuracy of 7.8 meters with 95 percent confidence (Swier et al. 2015).

We used a spatial bounding box of intensity 2.5 contour to filter geotagged tweets (latitude from 37.382170 to 39.048830, longitude from -123.561700 to -121.061700), because intensity 2.5 contour represents the lowest level of perceived shaking for this disaster case. The study period was set from August 3 to September 27, 2014. Specifically, we consider 3am (PDT) as the starting time of day to aggregate 24-hour tweets for further daily-based analysis due to the time the earthquake occurred (3:20 PDT). In total, we collected 3,737,325 geotagged tweets. As we focused

exclusively on tweets in English, the data volume reduced to 3,310,323 tweets. The daily average percentage of English tweets is 88.58% during the study period, which indicates that these tweets are generally representative for the population in the studied area.

Additionally, for detailed analysis, five different intensity polygons were generated based on the contours of macroseismic intensity including 7.0, 6.0, 5.0, 4.0, and 3.0 intensity polygons. For instance, the 7.0 polygon refer to the polygon surrounded by 6.5 intensity line, and 6.0 polygon refers to the polygon surrounded by 5.5 to 6.5 intensity polylines. The GIS files in this study were obtained from USGS (2014). Allocations of the Twitter geolocations in the different intensity polygons on August 24, 2014 is illustrated in Figure 10. Data volumes of English geotagged tweets in distinct intensity polygons are: 3,008 (Intensity 7.0 polygon), 2,280 (Intensity 6.0 polygon), 2,655 (Intensity 5.0 polygon), 34,336 (Intensity 4.0 polygon), 40,173 (Intensity 3.0 polygon), and 1,282 (Intensity 2.5 polygon).

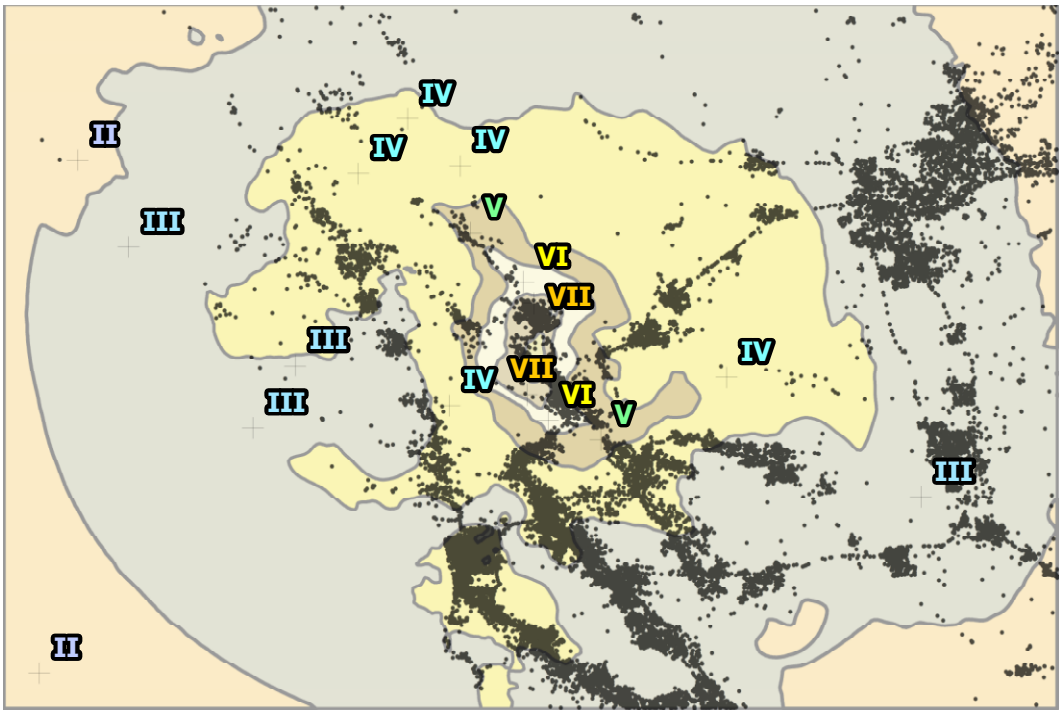

Figure 10: Twitter Geolocations in Different Intensity Polygons on August 24, 2014

4.4.3 Sentiment Analysis

Twitter allows its users to share short 140-character messages. The texts can include words, URLs, mentions, emotions, abbreviations, etc. We cleaned the text by removing URL links and user mentions (@). We did not delete negations and kept as much context as possible for more accurate sentiment analysis. We adopted an unsupervised lexicon-based method to measure the sentiment. The method is based on an affective word list AFINN to assign sentiment scores to words in tweets (Nielsen 2011). The latest version of the word list includes 2,477 words. The valence of a word ranges from -5 (very negative) to +5 (very positive) as an integer. The sum of valence without normalization of words represents the combined sentiment strength for a tweet. A Python Package "afinn" was used to compute the sentiment scores.

Comparing with methods that classify tweets to nominal categories (e.g. "negative, neutral, and positive"), numerical scores for sentiment contain more information about levels of sentiment and is more suitable for statistical analysis in this study. Additionally, the AFINN is a Twitter based sentiment lexicon including Internet slangs and obscene words. It has been tested in different types of tweets corpora and performs at a consistently satisfactory level of accuracy for both two classes (positive and negative) and three classes (positive, negative and neutral), compared with other unsupervised methods for sentence-level sentiment analysis (Ribeiro et al. 2015). Moreover, the AFINN word list has shown its advantages in analyzing tweets for disaster and crises sentiment detection (e.g., Nagy and Stamberger (2012) and Walther and Kaisser (2013)). We therefore selected the AFINN lexicon to evaluate the sentiment polarity of our collected tweets.

4.4.4 Radii of Gyration

Radii of gyration (r_g), a measurement of object movement from physics, has been widely used to quantify the size of trajectory of individuals since the study of Gonzalez et al. (2008). To achieve a more nuanced understanding of the perturbation of human mobility patterns, we computed the daily r_g of each distinct Twitter user over eight weeks to identify the change of daily radii of gyration over time. The authors adopted the formula in Eq.1 (Wang and Taylor 2016) to calculate the r_g of each distinct individual in the data set.

$$r_g = \sqrt{\frac{1}{n}\sum_{k=1}^{n}\left[2r \times \sin^{-1}\left(\sqrt{\sin^2(\frac{\phi_k - \phi_c}{2}) + \cos\phi_k\phi_c \sin^2(\frac{\varphi_k - \varphi_c}{2})}\right)\right]} \tag{12}$$

where n is the total frequency of visited locations of a Twitter user, k is each visited location by the user during a 24 hour period, c is the center location of the user's trajectories, ϕ is the latitude, and φ is the longitude.

4.4.5 Spatial Autocorrelation

We employed Moran's I (Moran 1950) and Geary's C (Geary 1954) to measure the spatial autocorrelation of sentiment in earthquake affected areas. As Moran's I is a more global measurement and sensitive to extreme values, and Geary's C is more sensitive to differences in small neighborhoods, we adopted both statistics for a validation purpose.

Moran's I (Moran 1950) can measure how sentiment level of a location is similar to others surrounding it. Its value ranges from -1 (perfect clustering of dissimilar values) to 1 (perfect clustering of similar values), and 0 indicates no autocorrelation (perfect randomness).

$$I = \frac{n}{(\sum_{i=1}^{n}\sum_{j=1}^{n} w_{ij})} \frac{\sum_i \sum_j w_{ij}(x_i - \bar{x})(x_j - \bar{x})}{\sum_i (x_i - \bar{x})^2} \tag{13}$$

where $\bar{x}$ is the mean of the x variable, w_{ij} are the elements of the weight matrix.

Geary's C statistic (Geary 1954) is based on the deviations in responses of each observation with one another. It ranges from 0 (perfect positive autocorrelation) to a positive value (high negative autocorrelation). If the value is less than 1, it indicates positive spatial autocorrelation.

$$C = \frac{n-1}{2(\sum_{i=1}^{n}\sum_{j=1}^{n} w_{ij})} \frac{\sum_i \sum_j w_{ij}(x_i - x_j)^2}{\sum_i (x_i - \bar{x})^2} \tag{14}$$

4.4.6 Time Series Analysis

4.4.6.1 Interrupted time series

We employed a segmented regression model (Wagner et al. 2002) to describe the interrupted time series of sentiment and mobility before, during and after the earthquake. This regression model is powerful in assessing the intervention effects in interrupted time series over time. We regarded the earthquake as a change point to divide the time series into two portions. Two parameters were used to define each segment of the time series: level and trend. The level refers to the value of the series at the start of a certain interval, while the trend is the rate of change during a portion.

The segmented regression model for sentiment (Eq. 4) and mobility (Eq. 5) are listed below:

$$S_t = \beta_0 + \beta_1 \times time_t + \beta_2 \times disaster_t + \beta_3 \times time\_after\_disaster_t + e_t \tag{15}$$

$$M_t = \beta_0 + \beta_1 \times time_t + \beta_2 \times disaster_t + \beta_3 \times time\_after\_disaster_t + e_t \tag{16}$$

S_t and M_t : daily average value of individual's adjusted sentiment and radius of gyration respectively (removed seasonality); $time_t$: a continuous variable indicating time in days at time *t* from the start of the observation period; $disaster_t$: an indicator for time *t* occurring pre-earthquake ($disaster_t$ = 0) or post-earthquake ($disaster_t$ = 1), which was implemented at day 22 in the series; $time\_after\_disaster_t$:a continuous variable counting the number of days after the disaster at time t; β_0 estimates the baseline level of the outcome, mean value of adjusted sentiment per individual per day, at time zero; β_1 estimates the change in the mean value of adjusted sentiment that compute with each day before the disaster occurs (i.e. the baseline trend); β_2 estimates the level change immediately after the disaster, that is, from the end of the preceding segment; β_3 estimates the change in the trend after the earthquake, compared with the daily trend before the disaster; the sum of β_1 and β_3 is the post-disaster slope.

4.4.6.2 Cointegration of time series

The relationship of cointegration reveals the *co-movement* of two time series in the long term. It can be illustrated by the simplest possible regression equation (Granger 1981) in our research scenario (Eq. 6):

$$M_t = \alpha + \beta S_t + \varepsilon_t \tag{17}$$

where M_t is the dependent variable, S_t the single exogenous regressor, and $\{\varepsilon_t\}$ a white-noise, mean-zero sequence. The definition of cointegration can be illustrated as "two non-stationary time series are cointegrated if some linear combination of them is a stationary series" (Metcalfe and Cowpertwait, 2009, pp 217).

4.4.6.3 Cross-correlation of time series

We also employed cross correlation analysis (see Eq.7) to identify lags of the daily changed sentiment that might be useful predictors of daily changed mobility.

$$M_{t+h} = b + a\sum_{j=0}^{k-1} S_{t-j} + \varepsilon_t \tag{18}$$

where M_t is the time series of radius of gyration, S_t is the time series of sentiment. ε_t is the Gaussian noise, and h is the lag hyperparameter. A negative value for h is a correlation between sentiment at a time before t and the mobility at t, which means S_t leads M_t; while positive h means S_t lags M_t.

4.5 Results

4.5.1 Earthquake Intensity and Sentiment

We focused our analysis on the first 24 hours after the earthquake. We specifically classified the collected tweets into six intensity polygons, and conducted both tweet-based analysis and individual-based analysis. Firstly, we grouped the tweets into six bins of distinct intensities. The average *sentiment of tweets* in each bin is taken as the sentiment strength of the bin. The relationship between sentiment of tweets and intensity is shown in Figure 11 (A). Sentiment decreases linearly with the intensity level. We also placed individuals into six intensity groups based on their center of mass (average location). For individuals who tweeted more than once during the 24 hours, we calculated sum of sentiment of their tweets.Sentiment score of each group is the statistic of individuals' sentiment. The significant correlation between sum of individual's sentiment and earthquake intensity were are plotted in Figure 11 (B).

According to the results of linear regressions, earthquake intensity can linearly explain the sum sentiment of individual's tweets better than other statistics ($R^2 = 0.944$). The average sentiment of tweets also has a significant correlation with the intensity. However, extreme sentiment of individual's daily tweets (i.e. max and min) cannot be explained by the earthquake intensity very well ($p > 0.1$).

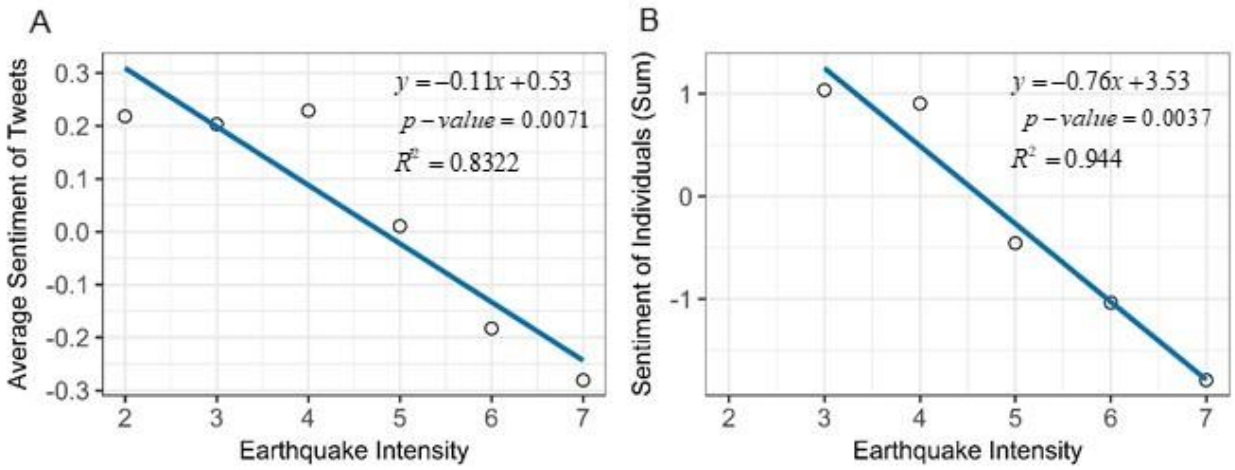

Figure 11: Sentiment of Tweets and Individuals and Earthquake Intensity

4.5.2 Spatial Association of Sentiment

We performed spatial correlation analysis of sentiment scores across six disaster zones of distinct intensity and the whole area with Geary's C and Moran's I. The results of Geary's C and Moran's I are statistically significant with all *p*-value less than 0.001. Moran's I at different spatial scales is positive and values of Geary's C are less than 1, which indicates spatial dependencies for similar levels of sentiment in all earthquake-affected areas of different intensities. Note, however, that the values of Moran's I for the whole area and all the intensity zones are small, suggesting a weak but significant tendency of similar levels of sentiment to cluster in different areas. The autocorrelation analysis results can be found in Table 5.

Table 5: Spatial Autocorrelation of Sentiment during 24 Hours After the Earthquake.

	Moran's I			Geary's C		
	Statistics	*p*-value	Std.	Statistics	*p*-value	Std.
Whole Area	0.0692	*< 2.2e-16*	30.98	0.9258	*< 2.2e-16*	15.637
7 Intensity Zone	0.0653	1.311e-08	5.565	0.9425	0.0007042	3.1929
6 Intensity Zone	0.0623	1.819e-06	4.6311	0.9521	0.002832	2.7666
5 Intensity Zone	0.0651	9.001e-08	5.2189	0.9236	6.299e-05	3.8342
4 Intensity Zone	0.0668	< 2.2e-16	19.19	0.9291	< 2.2e-16	9.0739
3 Intensity Zone	0.0689	< 2.2e-16	21.389	0.9239	< 2.2e-16	10.812
2 Intensity Zone	0.0573	0.0007405	3.1784	0.9356	0.004594	2.605

4.5.3 Temporal Analysis of Sentiment and Mobility

4.5.3.1 Decomposition of time series

We normalized daily sentiment and radius of gyration by dividing by the number of individuals (Eq. 8 and Eq. 9). Only individuals with at least two distinct locations in a single day were included into the analysis. By examining Twitter postings from at least two distinct locations removes static tweets from bots and organizations.

$$normalized\_sentiment = \frac{\sum daily\_average\_sentiment\_of\_individuals}{number\_of\_individuals} \tag{19}$$

$$normalized\_mobility = \frac{\sum radius\_of\_gyration}{number\_of\_individuals} \tag{20}$$

The changes of sentiment and mobility over the study period were plotted in Figure 12 and Figure 13, respectively. We decomposed the time series based on a moving average method to investigate the trends and seasonal effects (assumed weekly). The additive decomposition within each plot includes the observed time series, trend, seasonal effect, and random variables with mean zero

(irregular plot). The unit of time scale is a week. According to the trend plot in the decomposition plots, there is a decreasing trend before the earthquake occurred, and an increasing trend post disaster for both series.

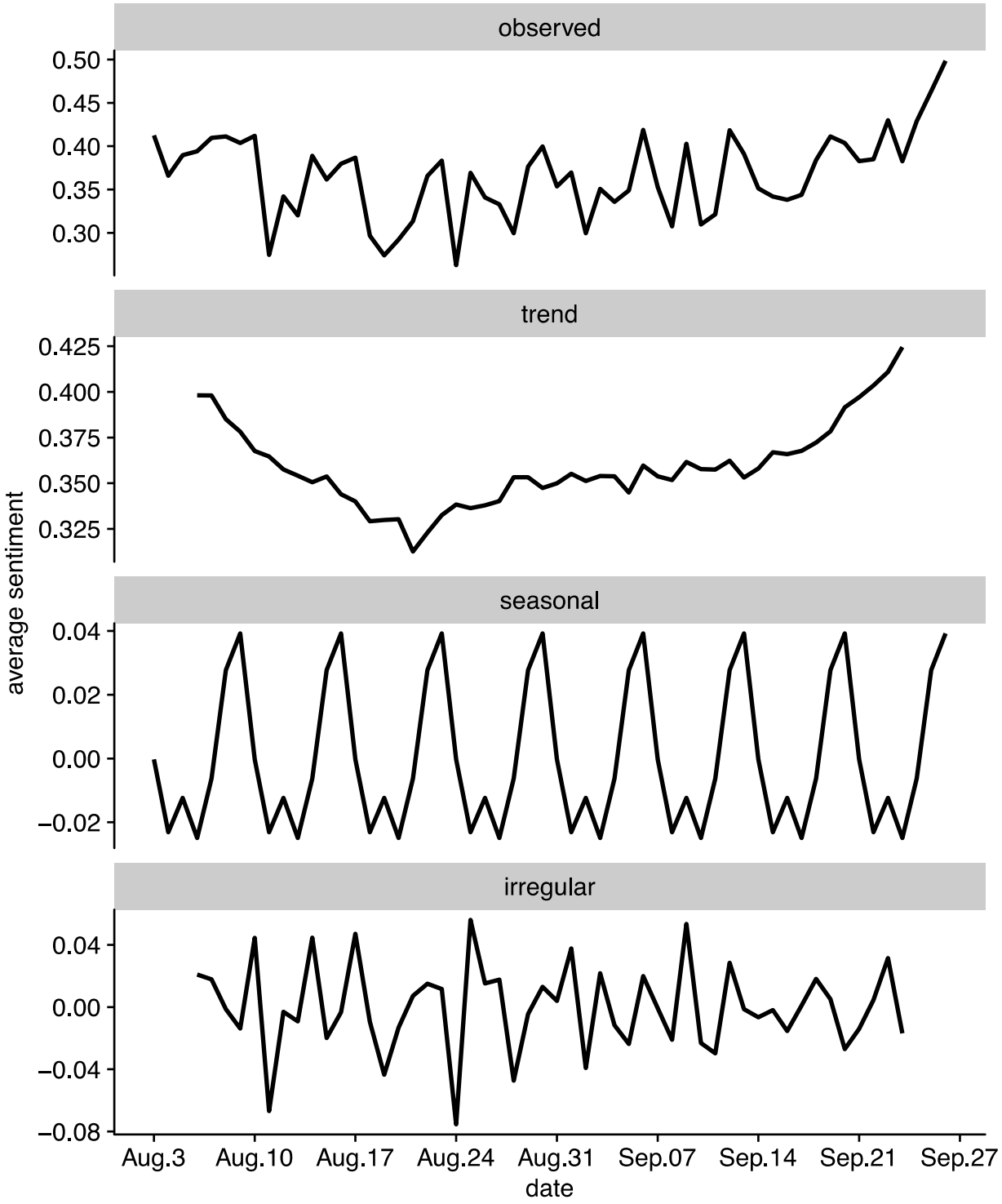

Figure 12. Additive Decomposition of Time Series of Average Sentiment

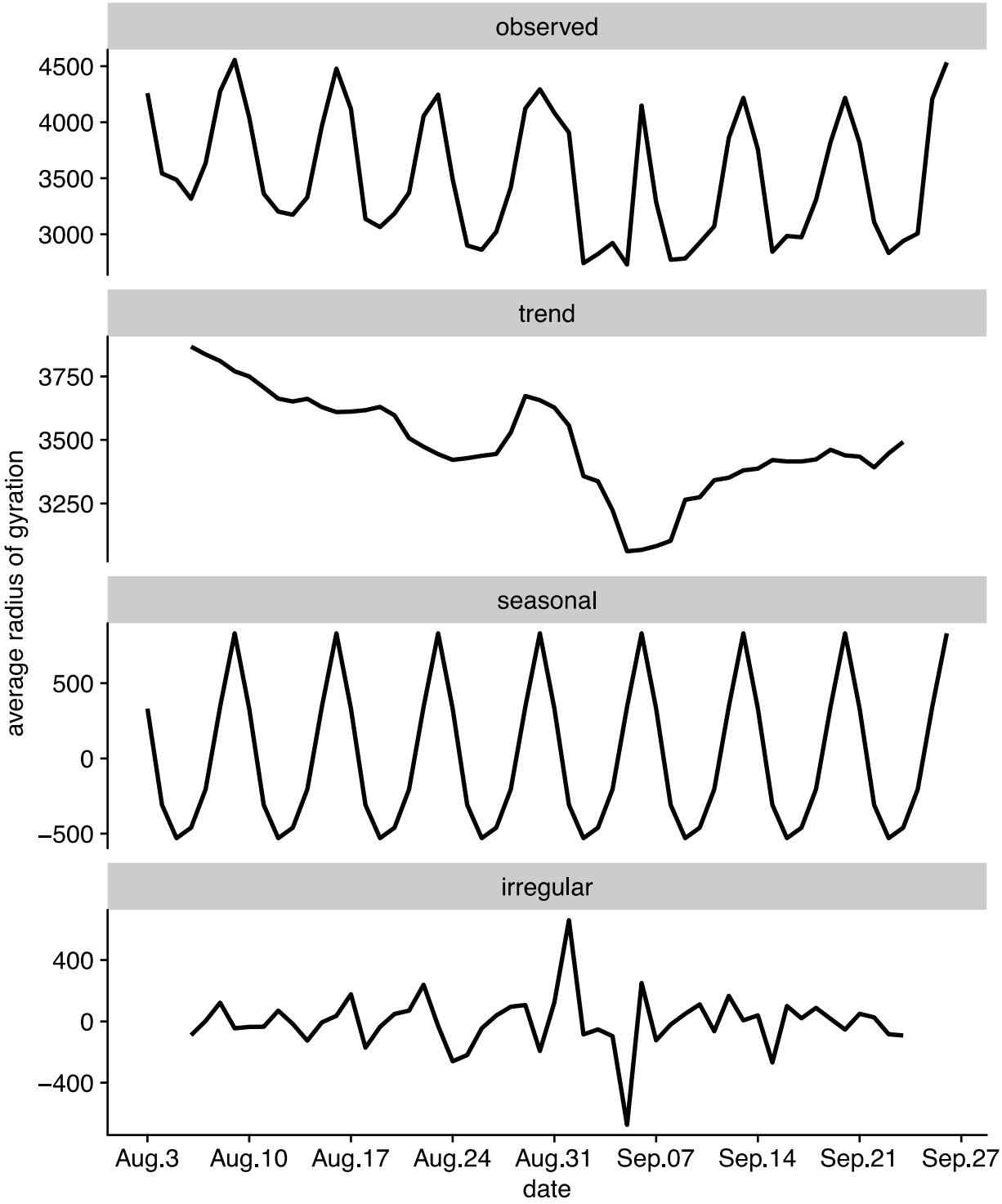

Figure 13: Additive Decomposition of Time Series of Average Radius of Gyration

4.5.3.2 Stationarity and cointegration.

We adjusted the time series by removing the seasonality prior to further analysis. This is necessary to avoid the impact of the intrinsic autocorrelation of the time series and avoid the false identification of a relationship between sentiment and mobility. We conducted the Augmented Dickey-Fuller (ADF) Test (Said and Dickey 1984) with the null hypothesis of a unit root is present in a time series sample, and alternative hypothesis of stationarity. We did not find support to reject the hypothesis in both time series of sentiment S_t (p-value= 0.8089, Dickey-Fuller= -1.4189) and time series of radius of gyration M_t (p-value< 0.1442, Dickey-Fuller= -3.0673). This means we did not find evidence to support the stationarity for both M_t and S_t. Therefore, there is no clear tendency for time series of mobility and sentiment to return to or fluctuate around a constant value or a linear trend.

We then tested if the two adjusted non-stationary time series are cointegrated with the Phillips-Ouliaris Cointegration Test (Phillips and Ouliaris 1990). We found support to reject the null hypothesis that the two series are not cointegrated (Phillips-Ouliaris demeaned = -32.458, p-value ≤ 0.01). This cointegration means that there exists a linear combination of the two variables that is stationary. In another words, sentiment and mobility share a trend together over time: specifically, a change in one will be permanent only if both change; an interruption to only one will be meaningless in the long run because it will be pulled back to the long-term path determined by the other one.

4.5.3.3 Interrupted time-series analysis

The parameter estimate from the linear segmented regression model of effects of earthquake on the mean sentiment of population can be found in Table 6. The fitted model is demonstrated by

Eq.10. The results indicate that just before the study period, the daily average sentiment in the study period was 0.413. Before the earthquake, there was a significant day-to-day change in the value (p-value for baseline trend = 6.65e-05). Just after the earthquake, the day-to-day change in sentiment increased by 0.006 statistically (p-value for trend change=2.60e-05), but there was no significant change in the sentiment level. We eliminated the non-significant term and the most parsimonious model includes only intercept, baseline trend and trend change in the daily average sentiment of individuals.

$$S_t = 0.413 - 0.005 \times time_t + 0.023 \times disaster_t + 0.006 \times time\_after\_disaster_t \quad (21)$$

The parameter estimate from the linear segmented regression model of effects of earthquake on the mean value of radius of gyration of individuals can be found in Table 7. The fitted regression models are expressed in Eq.11. The results indicate that just before the study period, the daily average radius of gyration in the study period was 3,920.155 meters. Before the earthquake, there was a significant day-to-day decreasing trend in the value (p-value for baseline trend = 0.0351). After the earthquake, the fitting results show that the day-to-day change in sentiment increases by 17.363 statistically and the level decreases by 110.076, but not significantly for both parameters. We eliminated the non-significant term and the most parsimonious model includes only intercept and the baseline trend.

$$M_t = 3920.155 - 19.549 \times time_t - 110.076 \times disaster_t + 17.363 \times time\_after\_disaster_t \quad (22)$$

Table 6: Segmented Regression Model for Interrupted Time Series of Sentiment

	Coefficient	Standard error	t-statistic	p-value
a. Full segmented regression model				
Intercept β_0	0.413039	0.013548	30.488	< 2e-16 ***

Baseline trend β_1	-0.004743	0.001079	-4.396	6.65e-05 ***
Level Change after EQ β_2	0.022834	0.017154	1.331	0.19
Trend Change after EQ β_3	0.006028	0.001286	4.686	2.60e-05 ***
Adjusted R-squared: 0.2958; p-value: 0.0002885				
b. Most parsimonious segmented regression model				
Intercept	0.4064146	0.0127058	31.987	< 2e-16 ***
Baseline trend	-0.0038399	0.0008458	-4.540	4.04e-05 ***
Trend Change after EQ	0.0056762	0.0012695	4.471	5.06e-05 ***
Adjusted R-squared: 0.284; p-value: 0.0001728				

Table 7: Segmented Regression Model for Interrupted Time Series of Mobility

	Coefficient	Standard error	t-statistic	p-value
a. Full segmented regression model				
Intercept β_0	3920.155	112.962	34.703	<2e-16***
Baseline trend β_1	-19.549	8.996	-2.173	0.0351*
Level Change after EQ β_2	-110.076	143.032	-0.770	0.4456
Trend Change after EQ β_3	17.363	10.726	1.619	0.1125
Adjusted R-squared: 0.3311, p-value: 9.459e-05				
b. Most parsimonious segmented regression model				
Intercept	3813.927	73.871	51.63	< 2e-16 ***
Baseline trend	-12.061	2.572	-4.69	2.38e-05 ***
Adjusted R-squared: 0.3043, p-value: 2.383e-05				

4.4.3.4 Cross-correlation

We further computed the first order difference of M_t (Eq. 12) and S_t (Eq. 13), ΔM_t and ΔS_t, which also denote the daily change in radius of gyration and sentiment. Both ΔM_t and ΔS_t are stationary after ADF test with $p-value < 0.01$.

$$\Delta M_t = M_t - M_{t-1} \tag{23}$$

$$\Delta S_t = S_t - S_{t-1} \tag{24}$$

To explore the relationship between ΔM_t and ΔS_t over the time, we employed cross correlation analysis to examine the relationship between the two time series. Cross-correlogram for ΔM_t and ΔS_t can be found in Figure 14.

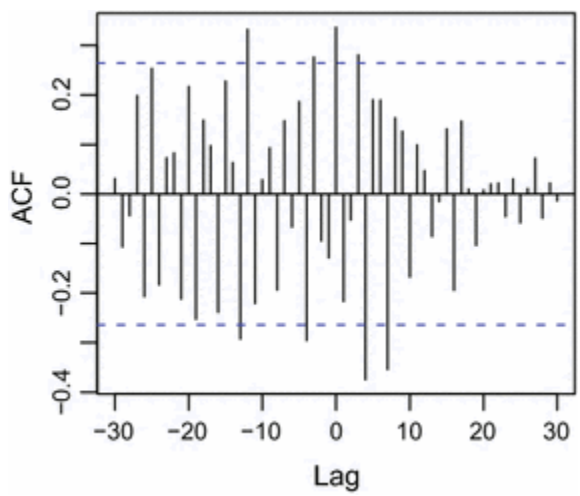

Figure 14: Cross-correlogram for ΔM_t and ΔS_t

Based on the cross correlation analysis, the most dominant correlation is -0.554, when lag (h) is -1 or 1. The negative value of lag indicates that ΔS_t leads ΔM_t, and ΔS_t is a predictor of ΔM_t, while positive value of lag mean that changed ΔS_t lags ΔM_t, and ΔM_t can be a predictor of ΔS_t. Therefore, we conclude that daily changed sentiment can either lead or lag daily changed mobility.

4.6 Discussion

Massive amounts of geocoded data on human-environment interactions have increased the potential for researchers to quantitatively assess dynamic processes over disaster-affected areas. Specifically, geo-referenced tweets allowed us to examine large-scale sentiment and human mobility patterns over the course of a severe earthquake and form "bottom-up" perspectives to understand urban population dynamics during an extreme event perturbation. Our study examined these dynamics before, during and after the earthquake by analyzing the spatial and temporal

characteristics, and the relationship between sentiment and mobility. The proposed framework couples collective sentiment and mobility to evaluate the diversity of human-environment interactions and to inform efforts to improve disaster resilience.

Prior research demonstrates some spatial characteristics of sentiment correlate with nominal types of sentiment, and this is used to characterize locations (Bertrand et al. 2013; Lin 2014). Although one study (Neppalli et al. 2017) has evaluated the clustering pattern of positive and negative sentiment during Hurricane Sandy, the spatial patterns of sentiment has not been explored fully in the disaster context in terms of disaster intensity/magnitude and its spatial scale, nor considered other types of natural disaster. Also, the spatial characteristics of sentiment level in a numerical form have yet been examined. Our linear regression analysis of sentiment and earthquake intensity quantitatively reveals the negative correlation between disaster emotion and severity: the higher the earthquake intensity is, the lower the level of the collective sentiment. Different statistics of individuals' daily sentiment have different correlations with intensity level, of which, the average values of mean and sum of individuals' sentiment during the 24 hour after earthquake show high correlation with the earthquake intensity. And these statistically significant results provide support to accept Hypothesis 1a. With more available earthquake datasets that include both geographical locations and semantic contents, we will strive to find the best fitting model to denote the relationship between sentiment level and earthquake intensity level, i.e. comparing results from the linear model and non-linear models, in order to achieve more general conclusions.

In addition, by employing Geary's C and Moran's I, we found evidence that sentiments of similar levels tend to cluster in geographic space, though the spatial autocorrelation is weak, and this spatial association has been found across disaster affected areas of distinct intensities (Hypothesis 1b). These findings extend the former studies that classified sentiment in earthquakes (Vo and

Collier 2013) by including the spatial factor, e.g. the scale of earthquake intensity and the clustering pattern.

Furthermore, employing the interrupted time series model, we descriptively demonstrate the temporal dynamics of human mobility and sentiment with the interruption of the earthquake. Results of statistical tests for the parameters in the model reveal that the earthquake interrupted the time series of sentiment significantly by changing the trend of the time series, while both level and trend of time series of mobility have not been perturbed significantly by the earthquake. As both fitted models for sentiment and mobility are statistically significant, we found evidence to support Hypothesis 2a regarding the interruption of the earthquake, although with deviations for level and trend changes for sentiment and mobility.

We further investigated the relationship between sentiment and mobility over time (Hypothesis 2b) and found that the time series are cointegrated, which indicates their co-evolution over time. Moreover, we expected that Δsentiment and Δmobility were cross-correlated over time, and Δsentiment was a predictor of Δmobility (Hypothesis 2c). Our analysis results found support for the hypothesis that Δsentiment can lead the change of Δmobility; however, we also found that Δ sentiment can lag the change of Δmobility. This first effort to examine disaster dynamics over time by coupling sentiment and mobility contributes a new, expanded and quantitative understanding of these dynamics. These findings also extend former studies (Frank et al. 2013) regarding the relationship between mobility pattern and sentiment to the disaster context.

However, there exist some limitations in this study in terms of data characteristics, geographical scales, and sentiment methods. We exclusively analyzed English tweets due to the unequal development of methods for analyzing sentiment in other languages and the dominant role of

English language in studied area. The research results should be generalized to the diverse-language-speaking population with caution because the demographical structure of users posting the English tweets is unknown. Fortunately, as the English tweets occupy nearly 90% of collected geo-referenced daily tweets, the results are able by and large to reveal the urban population dynamics in the disaster affected area.

Our studied area is the spatial bounding box of a 2.5 intensity line and includes uneven distribution of urban areas in different intensity polygons. Diverse geographical scales of earthquakes and other natural disasters may lead to dissimilar effects on sentiment levels and human mobility patterns. We plan to address these differences among multiple types of disasters and disasters of distinct geographical scales in future studies to achieve a more nuanced understanding of the spatiotemporal dynamics of resilience in areas of distinct scales. As this paper focuses more about the collective influence of disaster at a large scale, our analysis is adequate in terms of examining the proposed hypotheses.

Additionally, with the development of methods for sentiment analysis in specific domain, especially in the context of natural disasters and extreme events, further studies can reveal more practical information in terms of contents and sentiment levels for targeted disaster topics. We collectively analyze the sentiment of geotagged tweets in disaster affected area to achieve a broad understanding of the influence of earthquake in different intensity zones. Our next efforts will also focus on developing disaster-specific lexicon generated from social media to classify tweets to more specific emotion types based on disaster psychology.

4.7 Conclusion

This study expands our understanding of disaster resilience and urban dynamics with crowd-sourced data from the platform of social media. It examined hypotheses of spatial characteristics of sentiment before, during and after a severe earthquake. The results uncovered a significant negative correlation between sentiment levels and earthquake intensity levels, and demonstrated that sentiment tends to cluster in space in distinct earthquake intensity zones. Moreover, the study investigated the temporal relationship of sentiment and human mobility, including the dynamic effects of the earthquake over time. The time series of radius of gyration and sentiment exhibited co-movement over time, and Δsentiment can either lead or lag the change of Δmobility in the disaster context. We hope to extend the proposed research framework on other types of disasters to generalize findings of the relationship between disaster magnitude and sentiment levels and correlation between sentiment and mobility, and utilize the framework to evaluate the dynamic process of disaster resilience at different spatial scales. With more specific "small data", e.g. government strategies and disaster characteristics, the research findings based on "big data" can provide "bottom-up" knowledge to facilitate disaster informatics and management in terms of monitoring and evaluation in the built environment.

CHAPTER 5. DETECTING URBAN EMERGENCIES TECHNIQUE (DUET): A DATA-DRIVEN APPROACH BASED ON LATENT DIRICHLET ALLOCATION (LDA) TOPIC MODELING[4]

5.1 Abstract

Social networking platforms have been widely employed to detect and track physical events in population-dense urban areas. They can be effective tools to understand when, where, and what happens either retrospectively or in real time. Correspondingly, a variety of approaches have been proposed for detecting either targeted or general events. However, neither type of event detection technique has been developed to detect urban emergencies that happen in specific geographic locations and with unpredictable characteristics. Therefore, we propose a spatial and data-driven Detecting Urban Emergencies Technique (DUET) (e.g. for natural hazards, manmade disasters and other emergencies). The method addresses both geographic and semantic dimensions of events using a geo-topic detection module and evaluates their crisis levels based on the intensity of negative sentiment through a ranking module. DUET was designed specifically for geo-referenced tweets from a Twitter streaming API. To validate the technique, we conducted multiple experiments with geotagged tweets in different urban environments over a period of four to six consecutive hours. Our urban emergency detection technique successfully identified emergencies of different types among all the candidate geo-topics. Our future work focuses on enabling online-mode detection with high scalability with large volumes of streaming data and providing interactive visualization through a GIS system. The proposed detecting urban emergencies technique can identify emergencies of general types and provide timely emergency reports to both

[4] This technical paper was co-authored with Professor John E. Taylor and has been submitted to an academic journal that addresses computing methodology in the area of civil engineering.

first responders and the public. The system contributes to building an efficient and open disaster information system through a crowdsourcing effort and adding agility to urban resilience regarding crisis detection, situation awareness, and information diffusion.

Keywords: Disaster Informatics; Emergency Detection; LDA Topic Modeling; Natural Language Processing; Sentiment Analysis; Social Media.

5.2 Introduction

Recent natural hazards and manmade disasters have had a devastating impact on human life and the environment. In 2017 alone, there were a series of hurricanes in the Atlantic coastal area (e.g. Hurricane Harvey, Irma, Maria, and Nate), destructive California wildfires, and severe infrastructure disasters such as the Grenfell Tower fire in London, England and the Interstate 85 collapse in Atlanta, Georgia. These extreme events have reminded disaster managers and the public of the importance of timely emergency communication and revealed the shortcomings in our ability to effectively detect crises, alert the population, and provide assistance (National Academies of Sciences 2017).

In the United States, current emergency reporting and warning mainly rely on the Integrated Public Alert and Warning System and the Wireless Emergency Alerts System, and calling 911 is the preferred approach for reporting emergencies. However, under some circumstances, people cannot make calls, the crisis is too time critical for a 911 call to be effective, or calls have been made, but the emergency responders are unable to assess the relative gravity of one crisis over another to deploy first responders efficiently. In a recent hurricane, Hurricane Harvey, when emergency telephone hot lines were jammed, victims turned to social media for help, even posting their full addresses in desperation (Seetharaman and Wells 2017). Thus, it is necessary to incorporate these new communication platforms into existing disaster and emergency information systems.

Additionally, a successful disaster management system should incorporate six capabilities: identification, prediction, mitigation, preparation, response, and recovery (Pradhan et al. 2007), but most current studies have mainly focused on the warning phase (Ghosh et al. 2013) and post-disaster phase (Peña-Mora et al. 2010; Peña-Mora et al. 2012). Few have addressed the identification phase of emergencies. We focus on new communication platforms and in this research develop a technique for detecting geographically constrained urban emergencies in order to supplement current disaster information systems in terms of openness, effectiveness, and efficiency.

Newly available and massive sets of data from geosocial platforms (e.g. Twitter, Facebook, Foursquare, and Instagram) have played an increasingly important role at different stages of disaster and emergency management (Ford et al. 2016). This crowdsourcing data has brought new opportunities in understanding human mobility patterns (Gonzalez et al. 2008), examining dynamic spatial networks (Wang and Taylor 2017), and tracking a population's sentiment (Kryvasheyeu et al. 2016; Wang and Taylor 2018) in the context of a disaster. These geosocial platforms have also played an increasingly critical role in early warning, monitoring, and evaluation of emergent events. It is especially crucial to enable early detection through social media because timely detection of emergencies can facilitate more immediate responses, may provide information to reduce potential casualties and damage, and may lead to more effective resource allocation (Li et al. 2017). Early detection also contributes to characterizing an event in terms of spatiotemporal scale, collective emotions, semantic topics, and the dynamic evolution of emergencies over time.

Among a variety of geosocial networking platforms, Twitter is especially suitable for emergency environments in terms of its open design, wide usage, geo-enabled function, and limited message length environment (Kryvasheyeu et al. 2016). Geo-referenced tweets can document geographical locations and collective reactions to crises unfolding in both spatial and temporal scales. A number of studies concerning event detection techniques in the context of Twitter have been published in recent years. Some studies focus on targeted events with supervised methods (Sakaki et al. 2010; Sun et al. 2016) while others intend to identify general events which rapidly escalate in contents, time and space (Maurya et al. 2016; Xie et al. 2016; Yu et al. 2017; Zhang et al. 2016). These proposed detection techniques can be built based on clustering, supervised classification, latent Dirichlet allocation (LDA), or by hybrid means. However, few have explored the context of urban disasters and emergencies (e.g. infrastructure failures, building fires, and natural hazards).

Compared to other events, urban disasters and emergencies can be regarded as more "targeted", but also unpredictable in types and forms. It is difficult to employ current supervised techniques designed for targeted events to identify an un-characterized emergency. Moreover, detection approaches for general events have not stressed the distinct characteristics of disasters and emergencies in terms of their geographical and thematic impact, as well as their high-intensity of negative sentiment. Therefore, to address this methodological gap, we propose a data-driven technique to detect urban emergencies with a focus on geotagged tweets from a Twitter Streaming API. We describe the system as the Detecting Urban Emergencies Technique—or, DUET—to highlight its specification in detecting emergency events that happen in the confined physical locations of cities, and to describe the symbiotic socio-technical relationship that can exist between first responders and the public during emergencies. The proposed detection system can inform resource-constrained disaster managers and first responders when and where a potential

emergency is, the emergency details, and the collective sentiment level. Such a system could enable more intelligent and integrated disaster informatics and agile pre-, during-, and post-disaster management, and contribute to building more resilient communities in the context of extreme events.

5.3 Background

Event detection using Twitter streams has witnessed a mounting number of publications in recent literature. We classified recent approaches based on their detection objectives into two types: targeted event detection and general event detection. Existing techniques for general event detection were either retrospective or real-time. We exclusively discuss the latter because most real-time methods were built based on retrospective methods, and our final goal is to enable real-time event detection.

5.3.1 Targeted Event Detection

Targeted event detection requires pre-defined keywords and mainly adopts supervised detection techniques. For example, Sakaki et al. (2010) proposed a targeted event detection system that monitored tweets and delivered prompt notifications. Their system was specifically applied in reporting earthquakes with tweets in Japan. They first devised classifiers to classify event-related tweets and unrelated tweets. Then the related tweets were used to develop a probabilistic spatiotemporal model for event detection and location/trajectory estimation. In other work, Sun et al. (2016) designed a novel method to detect and locate power outages from Twitter. The system was based on a heterogeneous information network, which included time, locations, and texts. Supervised LDA was then used to compute the probability of the topics of tweets that were related to a power outage. Gu et al. (2016) proposed a real-time traffic incident (TI) detection approach based on tweet texts. Each imported tweet was mapped into a binary vector of a dictionary and

classified as TI-related or not. The TI-related tweets were further geo-coded and classified into different incident categories.

Detection techniques for distinct targeted events are effective in identifying specific events with pre-envisioned and pre-defined characteristics. However, due to the diversity in terms of the types of urban disasters, event detection through pre-defined characteristics may require a large volume of keywords to describe different types of potential events, not to mention unexpected types of events. Therefore, without pre-defining its specific characteristics, it is impractical to employ a supervised approach to detect general and unknown disasters.

5.3.2 General Event Detection

5.3.2.1 Clustering-based approaches.

Clustering-based approaches include threshold-based online approaches, graph-based clustering algorithms, and other new approaches. For example, Yu et al. (2017) proposed a real-time emerging anomaly monitoring system over microblog text streams, named RING. The system was based on a graph stream model. It was able to detect events at an early stage, to conduct correlation analysis between emerging events, and to track evolution of events over time. Specifically, the graph regarded keywords as nodes, their co-occurrence in each tweet as edges, and an accumulated frequency as weights of edges. A k-clique percolation method was then employed to identify communities (events) in the built graph. SigniTrend is a scalable detection technique developed by Schubert et al. (2014), which measured significance of terms to detect trending words based on their co-occurrences, and used a hashing technique to track all the keyword pairs. The final stage of this approach was to cluster the detected keywords into larger topics. This method was used to detect emerging topics before they become “hot tags”. Some techniques included geolocation as a main dimension to capture real-world occurrences. EvenTweet (Abdelhaq, et al., 2013) identified

localized events using geotagged tweets. It extracted keywords based on the burstiness degree of words, and then computed the spatial density distribution (spatial signature) over a keyword in a spatial grid. The event keywords were further partitioned based on the cosine similarity of their spatial signatures. Finally, the clusters were scored to uncover the real-world local events. GeoBurst (Zhang et al. 2016) was also designed to extract local events from streams of geotagged tweets in real time. It identified candidate events based on both geographical and semantic impact between each pair of tweets, and ranked the candidates according to their spatial and temporal bustiness. However, most of the clustering based approaches used co-occurrences of keywords to measure the semantic relationship between documents and, as such, they cannot reveal the latent structure of topics underlying the text corpora.

5.3.2.2 LDA-topic-model-based methods.

Latent Dirichlet allocation (LDA) is a basic probabilistic topic model, which analyzes the words from a sample of text to reveal the underlying themes and their connections (Blei 2012). Recently, researchers have explored the advantages of LDA in allowing for the examination of multiple topics within a document and generating a probabilistic distribution of words under a topic. This has been employed using LDA as a basis to extract thematic content from social networks for event detection. For example, Semantic Scan (Maurya et al. 2016) was a contrastive topic modeling approach based on LDA to identify new topics in a text stream, it then used a statistical scan to find the spatially localized events. The technique has been tested on Yelp and Emergency Department datasets, and the moving window size was three days, which is long for detecting emergencies. Moreover, the method required a pre-defined number of topics for both background corpus and foreground topics. Topic Sketch (Xie et al. 2016) was designed to detect bursty topics from Twitter, with the assumption that each tweet is only related to one latent topic. Topics were

generated based on sketch-based topic modeling using Singular Value Decomposition of word pair frequency matrices or tensor decomposition of word triple frequency matrices. It also employed a hashing-based dimension reduction technique, and conducted an effective sketch maintenance based on acceleration of word postings.

These methods only included temporal and semantic dimensions in the detection process without considering the geographic dimension. However, in terms of urban disasters, the physical locations and spatial patterns of an event may be as important as text contents and time. Current LDA-based event detection methods have not been tailored to detect disasters, which are different from other events—such as celebrations, football games, and marathons—in terms of the intensity of negative emotions. Therefore, we propose a technique to specifically detect urban emergencies. The technique takes both geolocations and the text contents of social media micro-blog postings into consideration, and the semantic correlation is measured based on LDA. To separate urban crises from other events, we employ intensity of negative sentiment to filter the events.

5.4 Detecting Urban Emergencies Technique

We defined urban emergencies in our study as events with the following properties: (i) they are geographically proximal and semantically related; and (ii) they influence people's emotion and trigger a high intensity of negative sentiment over a certain time period. The properties also form the basic assumptions of the detection approach. The main modules included in our proposed technique are illustrated in Figure 15. The first module for collecting geo-referenced tweets from a Twitter Streaming API is a built system in our lab (Wang and Taylor 2015). On the basis of this collection module, we firstly built a "Data Pre-Processing" module to normalize texts in tweets, then we developed a "Geo-Topic Detection" module to identify distinct events (i.e. geo-topics). This geo-topic detection module combines both geographic closeness and LDA-based semantic

similarity to extract geo-topics. To further evaluate the "emergency level" of candidate geo-topics, we employed the intensity of negative sentiment to rank the events in a "Geo-Topic Ranking" module, where events with higher average intensity of negative sentiment over certain consecutive time windows are identified as candidate urban emergencies.

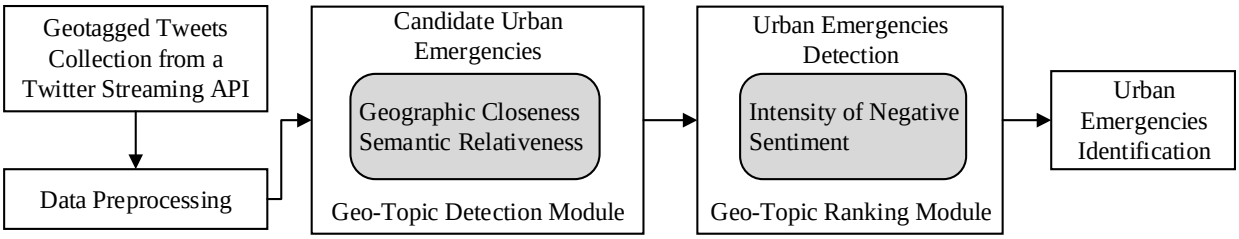

Figure 15: Detecting Urban Emergencies Technique (DUET)

5.4.1 Data Preprocessing Module

Twitter allows its users to share short 140-character messages (this length is in the process of expanding). The texts can include words, URLs, @mentions, hashtags, emoticons, abbreviations, etc. To analyze this data, we clean the texts by removing URL links and user mentions (@), which are not relevant to the core meaning of the text in a large amount of tweets. We also remove the special characters (i.e. '#$%^&*', punctuation marks, and independent numeric numbers) that are unnecessary for further analysis. We tokenize the tweets to unigrams based on regular expression patterns. Each tweet is segmented into their constituent words and converted to lowercase. We also remove the stop words that have no significance (e.g. *a*, *the*, and *me*) and words with less than two characters.

We further conduct parts of speech (POS) tagging and lemmatization. POS tagging is to classify and label POS tags for words in a sentence, and the main tags include noun, verb, adjective, and adverb. The Penn Treebank notation is used in this study for tagging, which is also the most-widely used POS tag set in various text analytics including tweets. Following the POS tagging, we convert

inflectional words to their base forms called lemma. This standardization process finds the base form or lemma for a given word based on the word and the POS by checking the WordNet corpus. It uses a recursive technique for removing affixes from the words until a match is found in WordNet; words remain unchanged if no match is found. Thus, the lemmatization is largely influenced by the POS.

Before saving the cleaned texts into a corpus for analysis, we also delete infrequently used words that appeared in fewer than 0.1% or 0.5% of tweets (depending on text frequencies in different cases as in Denny and Spirling (2017)), because the infrequently used terms do not contribute much information about text similarity. Discarding these terms can also greatly reduce the size of the vocabulary and speed up the text analysis. A Python Package *NLTK (Natural Language Tookit)* is employed to tokenize tweets, remove stop words, tag POS, and lemmatize words in tweets. Notably, the aforementioned procedures are conducted to generate a dictionary and corpus for LDA topic modeling. The text normalization steps for sentiment analysis have some differences: only URL links and user mentions (@) are removed from the original tweets, because we try to keep as much information as possible for sentiment analysis. Figure 16 demonstrates the process of normalizing tweets.

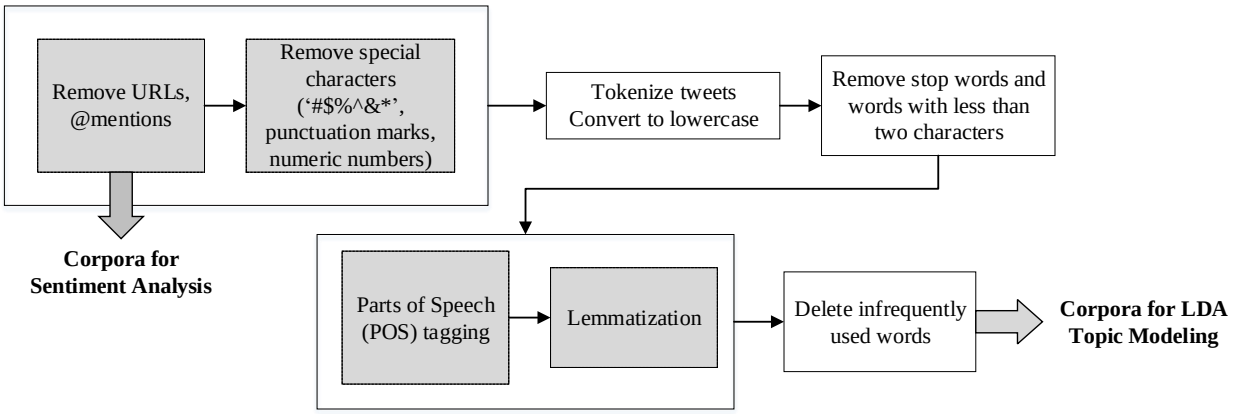

Figure 16: Data Preprocessing

5.4.2 Candidate Geo-Topics Generation

5.4.2.1 LDA-based topic modeling.

We employ latent Dirichlet allocation (LDA) (Blei et al. 2003) to identify latent topic information in the corpora of tweets. A tweet is treated as a "bag of words", disregarding the word order and grammar. The basic idea of this generative probabilistic model in our research context is that each tweet is represented as a probability distribution over a pre-defined number of topics, and each topic is represented as a probability distribution over words. We employed the graphical model (Blei 2012) to formally describe LDA (Figure 17).

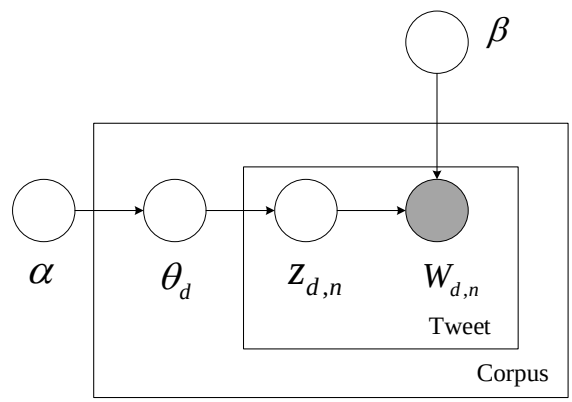

Figure 17: LDA Topic Modeling of Tweets Corpora (Blei 2012)

According to (Blei 2012; Blei et al. 2003), $\beta_{1:K}$ denotes topics, where β_K is a distribution over the vocabulary corpus. θ_d represents the topic proportions for the *d*th tweet, and $\theta_{d,k}$ is the topic proportion for topic k in tweet d. The topic assignments for the *d*th tweet are z_d, where z_d is the topic assignment for the *n*th word in tweet d. Lastly, the observed words for tweet d are w_d, where $w_{d,n}$ is from the fixed vocabulary and the *n*th word in tweet *d*. In the graphical model, only the shaded node ($w_{d,n}$) is observed, while other nodes (i.e. the topic proportions, assignments, the topics) are hidden nodes. LDA assumes that for each tweet in a corpus:

1. Choose. $tweet \sim Poisson\ (\xi)$.

2. Choose. $\theta \sim Dir(\alpha)$.

3. For each of the word $w_{d,n}$ in tweet d :

(a) Choose a topic $z_d \sim Multinomial(\theta)$.

(b) Choose a word $w_{d,n}$ from $p\,(w_n \mid z_d, \beta)$, a multinomial probability conditioned on the topic z_d.

5.4.2.2 LDA-based topic similarity.

Compared to other semantic measurements, results of LDA-based cosine similarity is much closer to human perception of document similarity (Towne et al. 2016). We then use cosine similarity of tweets' topics for our similarity measure (see Eq. 1).

$$C\left(t \to t'\right) = \cos\left(topic_t, topic_{t'}\right) \qquad (1)$$

t and t' are two distinct tweets. $topic_t$ represents a topic vector of a tweet, and the topic vector is a probability distribution over the pre-defined number of topics.

5.4.2.2 Geographical closeness.

We adopt Epanechnikov kernel to measure the geographical closeness of two tweets due to its high efficiency and simplicity (Zhang et al. 2016) (See Eq. 2).

$$K(t \to t') = 0.75 \times \left(1 - c(\left\| loc_t - loc_{t'} \right\|)^2\right) \qquad (2)$$

$\left\| loc_t - loc_{t'} \right\|$ is the Haversine distance between locations of two distinct tweets; c is the scaling function that transforms the distance to the range $(0, 1)$.

5.4.2.3 Geo-Topic clustering.

We build an undirected graph named "Tweet Geo-Topic Graph": $G = (V, E)$, where V is a set of tweets and E is a set of edges. The weight of an edge is the product of semantic similarity and geographical closeness. If the weight is less than the pre-defined threshold, the edge is not built. The node with the highest sum weight is regarded as a hub. Each hub with each of its connected neighbors is regarded as a candidate geo-topic.

5.4.3 Geo-topics ranking and crisis detection

The previous study of Kryvasheyeu et al. (2016) reveals that negative average sentiment can indicate an emergency situation based on their examination of sentiment change during Hurricane Sandy. Research by the authors has also identified a significant negative correlation between sentiment level and the intensity of an earthquake (Wang and Taylor 2018). We therefore rank the candidate geo-topics based on their intensity of negative sentiment: *Geo-topics with higher average intensity of negative sentiment over certain time windows have a higher rank*.

We adopt an unsupervised lexicon-based method to measure sentiment. The method is based on the affective word list AFINN to assign sentiment scores to words in tweets (Nielsen 2011). The AFINN word list includes 2,477 words. The valence of a word ranges from -5 (very negative) to +5 (very positive) as an integer. The sum of valence without normalization of words represents the combined sentiment strength for a tweet. A Python Package "afinn" was used to compute the sentiment scores. AFINN is a Twitter-based sentiment lexicon including Internet slangs and obscene words. It has been tested in different types of tweets corpora and performs consistently at a satisfactory level of accuracy for both two classes (positive and negative) and three classes (positive, negative and neutral), compared with other unsupervised methods for sentence-level sentiment analysis (Ribeiro et al. 2015). Moreover, the AFINN word list has shown its advantages in analyzing tweets for disaster and crisis sentiment detection, e.g. Nagy and Stamberger (2012)

and Walther and Kaisser (2013). We therefore selected the AFINN lexicon to evaluate the sentiment polarity of our collected tweets.

Intensity of negative sentiment. Since we are mainly concerned with negative tweets (in an emergency situation), we convert the numeric scores of sentiment to binary score. Specifically, we use "zero" to represent both positive and neutral sentiment, and "one" for negative sentiment. We employ intensity of negative sentiment under each candidate geo-topic to quantify their crisis level (see Eq. 3).

$$S_t = \frac{n_{tweet^{(-)}}}{n_{tweet}} \qquad (3)$$

$n_{tweet^{(-)}}$ is the number of tweets with negative sentiment in each cluster; and n_{tweet} is the total number of tweets in each cluster. To include the impact duration of each crisis, we calculate the average values of the intensity over consecutive time windows (see Eq. 4).

$$\overline{S} = (\sum_{1}^{i} S_t) \Big/ i \qquad (4)$$

i is the number of consecutive time windows and $i \geq 1$.

5.5 Validation

To assess and validate the functionality of the proposed detection technique, we implemented DUET to detect different types of emergencies in multiple scenarios, including the Interstate 85 Collapse in the City of Atlanta, Georgia, the Grenfell Tower fire in London, England, the Magnitude 5.8 earthquake in Oklahoma City, Oklahoma, and the Tubbs Wildfire in Northern California (see Table 1). The collected geo-referenced tweets were further filtered in the spatial bounding box of selected urban areas, which were characterized by different geographical scales. We specifically selected a short and hourly-based period as the detection period, during which the

targeted detection events were happening. Each studied period was sliced into several equal-length time windows in order to analyze the average of intensity of negative sentiment for geo-topics. Detailed geographic and time information is provided in Table 8. Table 8 also demonstrates the data volume of English tweets and the size of the *cleaned* vocabulary corpus. Notably, words with frequency lower than 0.1% or 0.5% of the total number of tweets were removed from the vocabulary corpus, and in each different case, distinct common words were deleted from the corpus. Our experiments were conducted with Python 2.7 in the Anacondor environment.

Table 8: Experimental Geotagged Tweets Corpora Specification

Targeted Cases	Detected Area (Bounding Box)	Period (UTC Time)	Number of Tweets (English)	Number of Vocabulary Words (Cleaned)
Interstate 85 Collapse	Atlanta, Georgia	23:00 March 30 to 4:00 March 31, 2017 (6 hours)	596	326
Grenfell Tower Fire	Greater London	5:57 to 9:56 on June 14, 2017 (4 hours)	1,309	1,274
Oklahoma Earthquake	Oklahoma City, Oklahoma	12:00 to 17:57 on September 3, 2017. (6 hours)	539	244
Tubbs Fire (wildfires)	Northern California Megaregion	12:00 to 16:00 on October 9, 2017 (4 hours)	1,035	241

5.5.1 Candidate Event Generations

To generate geo-topics based on both semantic similarity and geographical closeness, we set the threshold of semantic similarity as 0.7 and set geographical closeness as zero to generate neighbors of each tweet. The number of LDA topics was set differently because the diversity level of Twitter topics varies in these areas. Specifically, the number of LDA topics is place-specific and, as such,

it may be used consistently in a certain area, but there is a difference among distinct regions. We determined the number of topics by comparing the results from topic modeling with different numbers of topics (from 5 to 15) based on the highest topic coherence (Röder et al. 2015), which measures the semantic coherence of topics with respect to the correlation to human judgement. Finally, we obtained a different number of unique geo-topics for each dataset (see Table 9). We also calculated the geo-topics' average number of tweets in each case (Table 9). It is to be noted, however, that one tweet may belong to none or more than one geo-topic.

Table 9: Parameters Setting and Generation of Geo-Topics

	#LDA topic	topic coherence	threshold of semantic similarity	threshold of geographical closeness	#unique geo-topics	avg #tweets under each geo-topic
Interstate 85 Collapse	10	-15.96	0.7	0	36	89
Grenfell Tower Fire	15	-15.91	0.7	0	68	113
Oklahoma Earthquake	7	-11.66	0.7	0	20	136
Northern California Megaregion Wildfire	15	-12.76	0.7	0	72	82

5.5.2 Geo-Topic Ranking

We further ranked all candidate geo-topics based on the average intensity of negative sentiment over consecutive time windows for each case. Examples of the hub tweets related to the emergencies (tweet with highest sum of weights) and the average intensity of negative sentiment over time windows for top-ranked geo-topics are provided in Table 10. During the six hours encompassing the Interstate 85 bridge collapse in Atlanta, four of the top five geo-topics characterized by the highest intensity of negative sentiment were related to this event and traffic

situation. Similarly, for geo-topics in London, four of the top ten geo-topics mentioned the Grenfell Tower or the fire. In Northern California, our detection system identified several fire spots in the affected area of the Tubbs Wildfire. And, finally, in the Oklahoma City Magnitude 5.8 earthquake, the emergency was also detected by our system; the top five geo-topics were all related to the earthquake. The network structure of geo-topics in Atlanta, Georgia is demonstrated in Figure 18. The black squares refer to the hub tweet, and the grey circles are individual tweets. One tweet may belong to multiple geo-topics. The number close to the hub is the number of its corresponding tweet. For example, Tweet 398 is the hub tweet of the top-ranked geo-topic over the time period, which is also listed in Table 10.

Table 10: Hub Tweets and Sentiment for Top-Ranked Emergency-Related Geo-Topics

Targeted Emergency Events	Hub Tweet for Emergency-Related Geo-Topics	Avg Intensity of -Sentiment
Interstate 85 Collapse	(#1) I85 fire. Here's what was burning. But why? #i85 #i85collapse @mention <url>	0.368
Grenfell Tower Fire	(#2) #grenfell towerfire as seen from white city #iglondon #ig_london @mention	0.248
Oklahoma Earthquake	(#1) A M5.6 magnitude earthquake occurred in Oklahoma. Details: <url> Map: <url>	0.1724
Northern California Megaregion Wildfire	(#2) Huge wild fire in the north bay this morning!!! Saw it in the climb gnarly winds in the night.	0.352

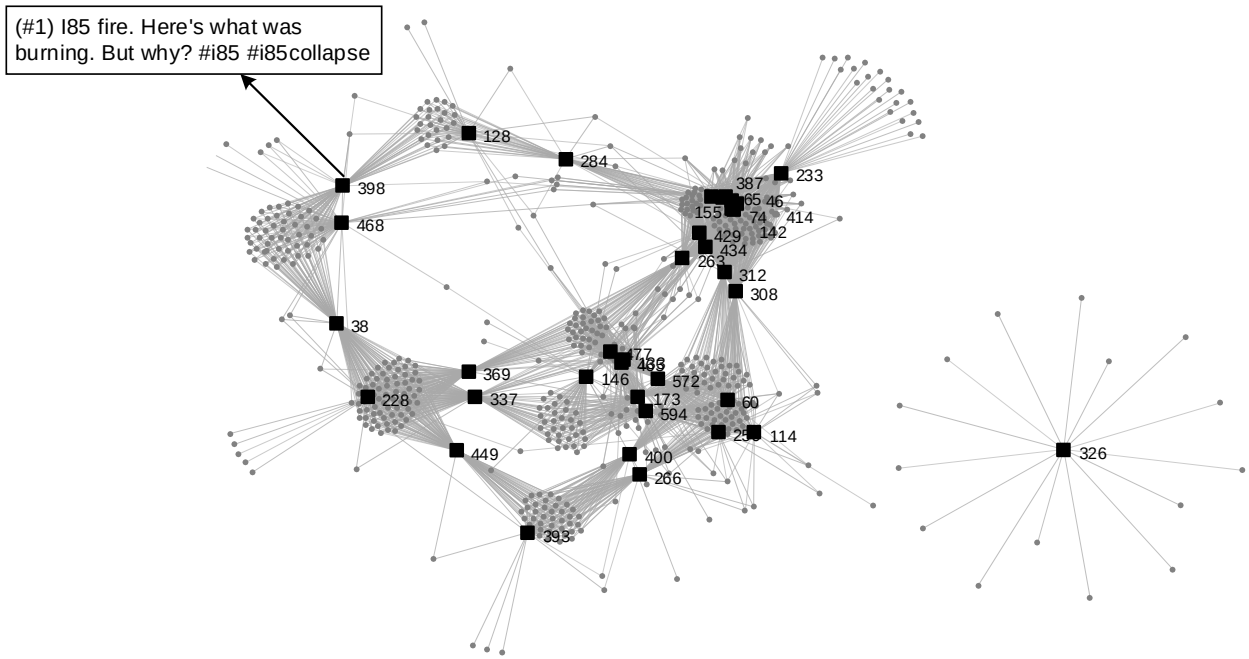

Figure 18: Network Visualization of Geo-Topics in Atlanta, Georgia

5.6 Discussion

DUET, our proposed detecting urban emergencies technique, built upon a Twitter Streaming API, comprises three modules: a data-preprocessing module, geo-topic detection module, and a sentiment-based geo-topic ranking module. We implemented the detection technique in distinct scenarios (e.g. different types of crises, geographical areas, spatial scales, and data volumes), and validated its capability in identifying general types of crises effectively. Comparing to former targeted-event detection techniques (Gu et al. 2016; Sakaki et al. 2010; Sun et al. 2016), DUET does not require pre-defined keywords regarding the emergency's type and characteristics, it detects emergencies based on rankings of intensity of negative sentiment over specific time windows. This can improve the situation awareness of emergency managers by providing a range of candidate crises to consider. Additionally, DUET is more targeted on detecting focal emergencies/crises when compared to current general-event detection systems (Abdelhaq et al. 2013; Schubert et al. 2014; Yu et al. 2017; Zhang et al. 2016). Specifically, we extended general-

event detection from large corpora of text into the field of disaster and emergency response. Our system can identify geo-topics that relate to general events, as well as detect candidate emergencies among all emergent geo-topics based on the degree of negative sentiment.

The identified emergent geo-topics can be reported to both the public and first responder organizations, to increase awareness of when and where an emergency is located, to share voluntarily provided details of an emergent crisis, and to provide an assessment of the sentiment level associated with the emergency. Extending functionality beyond current disaster information systems, DUET bridges the gap to detect emergencies from social media postings to supplement current emergency reporting during disasters. In doing so, it also addresses the paucity of research focused on the identification phase in disaster management systems in terms of agility, openness and effectiveness (Ghosh et al. 2013; Peña-Mora et al. 2010; Peña-Mora et al. 2012; Pradhan et al. 2007). By basing its emergency detection on crowdsourced data, DUET has extended beyond and integrated across former empirical studies on volunteered geolocation contents and sentiment from social media (Kryvasheyeu et al. 2016; Wang and Taylor 2018), extending them toward practical implementation.

To enable the application of DUET in more diverse scenarios with more agility, we still need to make some improvements in future studies. First, we assumed that emergencies are geographically proximal and semantically related; and that emergencies influence people's emotion and trigger a high intensity of negative sentiment over a certain time period. For this reason, it is difficult to detect crises that do not trigger a high intensity level of negative sentiment. To enable effective detection when a high intensity of sentiment may not exist, we plan to adjust the ranking module to rank the geo-topics based on the change in negative sentiment intensity, and adjust DUET to consider other dimensions, such as the geographic spreading speed.

Second, we exclusively focused on tweets in English, and this may lead to bias in identifying emergency events that may be incorporated in tweets in other languages. However, the English tweets that we examined represent nearly 90% of the collected geotagged tweets from our streaming API. Therefore, they are suitable for our analyses. Nevertheless, with the development of topic modeling and sentiment analysis in other languages (e.g. Chinese, French, and Spanish), we hope to enhance DUET in order to detect emergencies in multilingual corpora.

Additionally, our proposed detection technique has detected geo-topics related to the Interstate 85 bridge collapse, Grenfell tower fire, Oklahoma earthquake and Tubbs wildfires, and these geo-topics are ranked among the highest intensity of negative-sentiment clusters. We evaluated the geo-topics based the content of the hub tweets as well as all the connected tweets which mostly concern about the emergent events. Although in the earthquake case, one hub tweet does not directly show its relevance to the earthquake, other tweets under the same geo-topic are mostly about the earthquake. This can be caused by the centrality of its geographical location and the generality of the tweet's content. For this reason, it is necessary to check other tweets' content instead of focusing on the hub tweet.

Besides, we generally set the thresholds for semantic similarity and geographical closeness as 0.7 and zero in the four cases, but different selections of the thresholds can influence the number and scale of geo-topics. We hope to analyze the sensitivity of geo-topics to the thresholds in terms of their geographical scale and average intensity of negative sentiment in different urban areas with more available datasets. Also, since the number of LDA topics is place specific, we plan to examine the number of topics over different time periods (e.g. 30 minutes, hours, days) for distinct cities in order to select optimal settings in various detection scenarios.

Current implementations of the proposed detection system focus on several distinct areas over consecutive time windows (i.e. four to six hours) to identify the events currently happening during those periods. In the next step, we will employ an online mode to detect emergencies in real time. We plan to compare the efficiency of the final technique with existing detection systems, specifically, running time and scalability. After completing the real-time geosocial detection system, we hope to combine the human sensor, in this case, Twitter, and infrastructure sensor to enable more timely and accurate disaster reporting and warning.

5.7 Conclusion

In this paper, we developed and validated a novel technique for detecting urban crises using data collection from a geosocial networking platform (i.e. Twitter). The technique was capable of detecting different types of emergencies (e.g. infrastructure failure, building fire, city earthquake, and a wildfire near a city) in distinct urban environments over short time periods. This new technique for detecting urban emergencies leverages both semantic and geographical similarity in generating physical events, and evaluates the crisis level based on the intensity of negative sentiment. The next step of this study is to expand the technique for scalable geo-crisis detection in high-volume tweets. We will also incorporate an online module to identify emergencies in real time and add modules for disaster tracking, visualization and assessment. We will build an open platform to inform emergency management personnel regarding the type, content, location and sentiment level of an emergency.

The proposed detection system has the potential to provide first responders and emergency management agencies in affected areas with an updated understanding of the role geo-referenced social media can play in increasing the effectiveness of disaster response efforts. The designed approach contributes to improving disaster and emergency management, enhancing situation

awareness, and taking steps toward achieving urban resilience. The completed detection platform can also be incorporated into current disaster information systems in order to build an open, integrated, connected, and agile disaster management system.

CHAPTER 6: CONTRIBUTIONS

My doctoral research starts with empirical studies on examining disaster dynamics of the interactive human-spatial system from three related but evolutionary perspectives: human-mobility, spatial network, and coupled mobility and sentiment perspectives. After multiple empirical studies on diverse types of natural disaster (i.e. severe winter storm, flood, hurricane, and earthquake), the last part of the dissertation develops a detection technique for identifying and tracking urban emergencies of general types over a short period. Each of the four parts builds upon the previous part. However, each part also makes a distinct contribution to the academic literature. Additionally, the empirical and methodology research contributes to the practices of disaster management and building resilient cities. The findings presented in this dissertation provide a new lens to understand a disaster's impact on human-environment systems using crowdsourced data, and contributes to building an open and agile disaster response system in urban environments. The theoretical contributions of Chapter 2 through Chapter 5 can be found in Subsection 6.1, and the practical contributions can be found in Subsection 6.2.

6.1 Theoretical Contributions

6.1.1 Human Mobility Perspective

Previous research has found that natural disasters, e.g. hurricanes, floods and earthquakes, can cause significant impact on human mobility patterns (Bagrow et al., 2011; Gray & Mueller, 2012; Lu et al., 2012; Song et al., 2014; Wang & Taylor, 2014, 2016). My empirical study extends these studies to severe winter storms showing that human mobility patterns are impacted in this different context. With large-scale empirical geo-temporal data, this study also overcomes limitations caused by short-term or single-mode transportation data in traditional transportation research (Call, 2011; Datla & Sharma, 2008; de Montigny et al., 2011; Maze et al., 2006). The findings of the

study may provide a more general perspective on human mobility. Additionally, my research finding reveals that daily displacements can be best approximated with the lognormal distribution during severe winter storms, and the result is consistent with the findings on human mobility patterns under normal circumstance (Alessandretti et al., 2017; Zhao et al., 2015). Quantified by radii of gyration, human mobility patterns were significantly perturbed by the winter storm, however, individuals' recurrent mobility characterized by most frequented locations cannot better characterize individuals' mobility pattern during the severe winter storm than during the normal circumstances. The quantitative approaches adopted in this study form a framework to examine the impact of natural disasters on human mobility patterns using voluntarily reported geolocation data from social networking platforms. This framework can also be used to assess both spatial and temporal aspects of urban mobility during disasters, to supplement evaluations of evacuation performance, and to track urban resilience to natural disasters.

6.1.2 Spatial Network Perspective

The first study in this dissertation examined a disaster's impact and resilience process based on human mobility. It provides the stimulus to investigate the interaction of human movements and the underlying spatial structure pre, during, and post disasters. In the second perspective described in Chapter 3, I extend the first study by examining a disaster's impact and urban recovery process from a network perspective. The network was constructed based on human's movements between distinct spatial units (i.e. ZCTAs) at a daily basis in a disaster-affected urban area. I further used Fisher information (Fisher 1992) to evaluate system dynamics in the resilience process, inspired by the approach's application in ecology (Bodin & Norberg 2007; Fu et al., 2010; Jacoby & Freeman, 2016). The research findings uncover the dynamic relationship between human and spatial structure pre, during and post a flooding. For example, mass evacuation resulted in more

movements among distinct areas; and floodwater following the tropical storm inundated landscapes and prevented mobility, which caused a less connected spatial network. Additionally, analysis of FI over time suggested a loss of dynamic order during the disaster and a recovery to an alternative stable status post-disaster. This study is an important step towards determining the utility of descriptive network metrics and Fisher information in evaluating the dynamic process of urban resilience. It contributes to knowledge by providing a new and cross-disciplinary perspective for quantifying resilience of coupled human-spatial system in urban areas (Barrett & Constas, 2014; Quinlan et al., 2015). It also adds to the paucity of empirical literature on measuring urban resilience to disasters (Lam et al., 2015). The quantitative framework describes and tracks the dynamic process of resilience in terms of the population's movement and underlying spatial structure at both spatial and temporal scales.

6.1.3 Coupled Sentiment and Human Mobility Perspective

In the third part of my dissertation (Chapter 4), I expand the research questions from Chapter 2 and Chapter 3 to examine urban resilience process by coupling sentiment and mobility. I focused my investigation on a severe earthquake to understand the relationship between disaster magnitude and collective sentiment level, and the temporal relation between mobility and sentiment with the perturbation of disaster over time. The results suggest a significant negative correlation between sentiment levels and earthquake intensity levels, and demonstrate that sentiment tends to cluster in space in distinct earthquake intensity zones. Moreover, this study demonstrates the temporal dynamics of human mobility and sentiment with the interruption of the earthquake. This research extends prior studies (Bertrand et al. 2013; Lin 2014) on spatial characteristics of sentiment to the disaster context with numerical levels of sentiment. Findings from temporal analysis also extend former studies (Frank et al. 2013) regarding the relationship between mobility patterns and

sentiment to the field. This study provides the basis for simulating and predicting the influence of disasters on urban environments in terms of a population's collective sentiment and movement patterns from both spatial and temporal perspectives.

6.1.4 Urban Emergencies Detection – A Semantic and Spatial Approach

The former three perspectives contained in this dissertation contributes to a fuller understanding of urban resilience to disasters. However, the fourth part presented in Chapter 5 contributes in the most practical way to developing a disaster and emergency detection system to enable early detection and warning for urban resilience. The novel technique DUET was designed for detecting urban emergencies using a streaming data collection API from a geosocial-networking platform, Twitter. The technique is capable of detecting different types of emergencies (e.g. infrastructure failure, building fire, city earthquake, and a wildfire near a city) in distinct urban environments over a short time period. The proposed detection system addresses the paucity of research focused on the identification phase in disaster management systems in terms of agility, openness and effectiveness (Ghosh et al. 2013; Peña-Mora et al. 2010; Peña-Mora et al. 2012; Pradhan et al. 2007). Moreover, DUET bridges the gap to detect emergencies from social media postings to supplement current emergency reporting during disasters. This new technique for generating geo-topics (either emergent or not) leverages both semantic and geographical similarity in generating physical events, and evaluates the crisis level based on the intensity of negative sentiment. DUET does not require pre-defined keywords regarding the emergency's type and characteristics, which overcomes the limitation of former targeted-event detection techniques (Gu et al. 2016; Sakaki et al. 2010; Sun et al. 2016). In addition, DUET is more targeted on detecting focal emergencies when compared to current general-event detection systems (Abdelhaq et al. 2013; Schubert et al. 2014; Yu et al. 2017; Zhang et al. 2016). The detection system is built upon empirical studies

regarding spatiotemporal geographical and semantic characteristics of crowdsourced data (i.e. tweets), and extends them towards practical implementation for operationalizing urban resilience.

6.2 Practical Contributions

The research presented and discussed in this dissertation contributes to the practice of disaster and emergency management and constructing smart and resilient cities. The studies also address urban issues in the context of climate change.

6.2.1 Empirical Studies

Specifically, the three empirical studies on human mobility patterns, spatial network and a population's sentiment help bottom-to-top understanding of the influence of disasters from both spatial and temporal aspects. The research results may reveal the effect of early warning and other disaster preparation effort. For example, examining human mobility pattern at the city scale is helpful to observe residents' responses to disaster warning (e.g. evacuation). Quantifying displacements can also assess the quality of recovery (Sanderson & Sharma, 2016). Additionally, understanding the land structure change during disasters may inform urban planners and transportation managers to arrange the land use and urban mobility efficiently for disaster response. Moreover, understanding the spatiotemporal pattern of population's sentiment pre, during and post disaster can assist in decision making regarding disaster relief and humanitarian aid. By combining the "big" data with "small" data (e.g. weather data, geographic data) (Ford et al., 2016), both human mobility and sentiment may provide an approach to first responder organizations and the public that provides more detailed disaster warning, response, and recovery. With more empirical effort and more accurate disaster prediction, the research findings in this dissertation may pave the way for simulating human dynamics in different built environments in

order to arrange evacuation and resources more effectively and efficiently. This effort can further enable more timely and effective disaster preparation, response and recovery.

6.2.2 Methodology Studies

The proposed DUET technique has extended beyond and integrated across former empirical studies on voluntarily reported geolocation contents and sentiment from social media (Wang and Taylor 2017a; 2017b; 2018), extending them toward practical implementation. The technique has the potential to provide first responder organizations and emergency management agencies in affected areas with an updated understanding of the role geo-referenced social media can play in increasing the effectiveness of disaster response efforts. Specifically, the proposed detection system can inform resource-constrained disaster managers when and where a potential emergency is, the emergency details, and the collective sentiment level. The generated geo-topics and emergencies can raise situation awareness of the public, reduce their exposure to natural hazards, and may inform them the need and crises around them for timely help among communities. This system could also be incorporated into current disaster information systems in order to build an open, integrated, connected, and agile disaster management system.

CHAPTER 7. SUGGESTED AVENUES OF FUTURE RESEARCH

The primary focus of this study has been to understand the process of resilience in human-environment systems and to create agility in emergency and disaster detection. The research attempts to track the spatiotemporal changes of human dynamics across different types of disasters by characterizing human mobility pattern, spatial networks, and sentiment levels. Although the four-step studies are beneficial in moving toward the goal of building disaster-resilient cities in both proactive and reactive manners, it is not without its shortcomings. Effective and intelligent disaster preparation and response will require additional work. The following subsections outline three main avenues of future research that could build on the theoretical and methodological basis established in this dissertation.

7.1 Path Forward for Understanding Urban Resilience to Disasters

The empirical studies presented in this dissertation were primarily concerned with three types of the highly frequent natural disaster worldwide, including a severe winter storm, a major flooding, and an earthquake. Future initiatives should generalize the research findings further to other distinct types of natural disasters in diverse urban environments. Specifically, future work could expand these three empirical studies by conducting experiments on a type of disaster of different magnitudes in order to understand the correlation between disaster magnitude and human dynamics. Future research could also examine the spatial and temporal scale of a disaster's influence in distinct urban environments. Additionally, to quantify the impact of disasters and measure resilience for more practical purposes, researchers could analyze urban system with networked and multilayered methods by incorporating detailed geographical information, function and structure of the built environment, and nuanced weather data. Finally, with deeper and broader understanding of a disasters' influence on human-environment systems and the resilience process,

researchers could simulate human dynamics, estimate damage and take preventative measures for potential extreme events in distinct urban areas.

7.2 Emerging Opportunities for Creating Agility in Disaster and Emergency Management

In addition to enhancing the proactive adaptation of urban areas for future disasters, it is equally important to enable the timely and agile reactive adaptation of cities *during* emergencies and disasters. The fourth part of my dissertation has strived to develop an urban emergencies detection system based on a real-time streaming Twitter data. However, additional research is still needed for building place-specific detection systems based on social media to address the differences among areas in terms of population, semantic content, and urban spatial structure. In order to provide accurate and timely disaster reports, more attention could also be given to integrating diverse data-smart disaster response systems, combining human sensors (e.g., humans using smartphones) with infrastructure sensors, and creating openness among data platforms and disaster stakeholders. Furthermore, together with images from satellites and drones, more detailed disaster and emergency maps can be formed and allow first responder organizations to assess and constantly monitor the areas at risk. More available "big" and "small" data can offer possibilities to create an agile, open, and integrated disaster management system (Ford et al., 2016).

7.3 Toward Connected, Resilient and Smart Cities

The path forward for preparing cities for climate change and natural disasters depends on both technology development as well as social and political effort. Although development of information and communication technologies along with the increasingly available crowdsourced data (obtained from social media, smartphones, and wearables) may contribute to better understanding of human dynamics during disasters and effective response (Papa, et al., 2015), there still exists the "digital divide", which limits some people with access to the Internet and

smartphones. The different usage of technology can cause inequality in disseminating disaster information and indirectly incur issues when concluding from crowdsourced data without full digital inclusion. Therefore, future work should give enough attention to populations who are not in the digital network, and incorporate low-income areas that are vulnerable to disasters (Bolin & Kurtz, 2018). Additionally, "socio-political infrastructure" (i.e. social and political norms, values, rules, and relationships) is also influential in enhancing urban resilience (Eakin et al. 2017). Future research should also realize the significance of social and political processes to decision makers in the emergency and disaster context. By combining crowdsourced data with geographic information science and multicriteria decision analysis (Bojorquez-Tapia 2011), future studies can better consider social and political forces underlying human dynamics and urban resilience.

REFERENCES

Abdelhaq, H., Sengstock, C., and Gertz, M. (2013). "Eventweet: Online localized event detection from twitter." *Proceedings of the VLDB Endowment*, 6(12), 1326-1329.

Alstott, J., Bullmore, E., & Plenz, D. (2014). powerlaw: a Python package for analysis of heavy-tailed distributions. *PLoS ONE*, 9(1), e85777.

Ahmad, N., Derrible, S., Eason, T., & Cabezas, H. (2015). Using fisher information in big data. *arXiv preprint arXiv:1507.00389*.

Angeler, D. G., & Allen, C. R. (2016). EDITORIAL: Quantifying resilience. *Journal of Applied Ecology, 53*(3), 617-624.

Alessandretti, L., Sapiezynski, P., Lehmann, S., & Baronchelli, A. (2017). Multi-scale spatio-temporal analysis of human mobility. *PLoS ONE*, 12(2), e0171686.

Blei, D. M., Ng, A. Y., and Jordan, M. I. (2003). "Latent dirichlet allocation." *Journal of Machine Learning Research*, 3(Jan), 993-1022.

Brockmann, D., Hufnagel, L., & Geisel, T. (2006). The scaling laws of human travel. *Nature*, 439(7075), 462-465.

Bodin, Ö., & Norberg, J. (2007). A network approach for analyzing spatially structured populations in fragmented landscape. *Landscape Ecology, 22*(1), 31-44.

Bagrow, J. P., Wang, D., & Barabasi, A.-L. (2011). Collective response of human populations to large-scale emergencies. *PLoS ONE*, 6(3), e17680.

Bagrow, J. P., & Lin, Y.-R. (2012). Mesoscopic structure and social aspects of human mobility. *PLoS ONE*, 7(5), e37676.

Blei, D. M. (2012). "Probabilistic topic models." *Communications of the ACM*, 55(4), 77-84.

Bertrand KZ, Bialik M, Virdee K, Gros A, Bar-Yam Y (2013) Sentiment in new york city: A high resolution spatial and temporal view. *arXiv preprint arXiv*: 13085010.

Bergsten, A., & Zetterberg, A. (2013). To model the landscape as a network: A practitioner's perspective. *Landscape and Urban Planning, 119*, 35-43.

Barrett, C. B., & Constas, M. A. (2014). Toward a theory of resilience for international development applications. *Proceedings of the National Academy of Sciences, 111*(40), 14625-14630.

Bai, H. & Yu, G. (2016) A Weibo-based approach to disaster informatics: incidents monitor in post-disaster situation via Weibo text negative sentiment analysis. *Natural Hazards* 83:1177-1196.

Beigi G, Hu X, Maciejewski R, Liu H (2016) An overview of sentiment analysis in social media and its applications in disaster relief. In: *Sentiment Analysis and Ontology Engineering*. Springer, pp 313-340.

Bolin, B., & Kurtz, L. C. (2018). Race, class, ethnicity, and disaster vulnerability. In *Handbook of Disaster Research* (pp. 181-203). Springer, Cham.

Carpenter, S., Walker, B., Anderies, J. M., & Abel, N. (2001). From metaphor to measurement: resilience of what to what? *Ecosystems, 4*(8), 765-781.

Cools, M., Moons, E., Creemers, L., & Wets, G. (2010). Changes in travel behavior in response to weather conditions: Do type of weather and trip purpose matter? *Transportation Research Record: Journal of the Transportation Research Board* (2157), 22-28.

Call, D. A. (2011). The effect of snow on traffic counts in western New York State. *Weather, Climate, and Society*, 3(2), 71-75.

Cutter, S. L., Joseph A. Ahearn, Bernard Amadei, Patrick Crawford, Elizabeth A. Eide, Gerald E. Galloway, & Goodchild, M. F. (2012). *Disaster resilience: a National imperative*. Washington, D.C.: National Academy of Sciences.

Cutter, S. L., W. Solecki, N. Bragado, J. Carmin, M. Fragkias, M. Ruth, & Wilbanks, a. T. J. (2014). Ch. 11: Urban Systems, Infrastructure, and Vulnerability. *Climate Change Impacts in the United States: The Third National Climate Assessment*, 282-296. doi:10.7930/J0F769GR.

Chan, R., & Schofer, J. L. (2015). Measuring transportation system resilience: response of rail transit to weather disruptions. *Natural Hazards Review, 17*(1), 05015004.

Cimellaro, G. P., Tinebra, A., Renschler, C., & Fragiadakis, M. (2015). New resilience index for urban water distribution networks. *Journal of Structural Engineering, 142*(8), C4015014.

Cody EM, Reagan AJ, Mitchell L, Dodds PS, Danforth CM (2015) Climate change sentiment on twitter: an unsolicited public opinion poll. *PloS ONE* 10:e0136092

Cimellaro, G. P., Renschler, C., Reinhorn, A. M., & Arendt, L. (2016). PEOPLES: a framework for evaluating resilience. *Journal of Structural Engineering, 142*(10), 04016063.

Datla, S., & Sharma, S. (2008). Impact of cold and snow on temporal and spatial variations of highway traffic volumes. *Journal of Transport Geography*, 16(5), 358-372.

de Montigny, L., Ling, R., & Zacharias, J. (2011). The effects of weather on walking rates in nine cities. *Environment and Behavior*, 0013916511409033.

Davoudi, S., Shaw, K., Haider, L. J., Quinlan, A. E., Peterson, G. D., Wilkinson, C., . . . Davoudi, S. (2012). Resilience: A bridging concept or a dead end?"Reframing" resilience: challenges for planning Theory and practice interacting traps: Resilience assessment of a pasture management system in northern afghanistan urban resilience: What does it mean in planning practice? Resilience as a useful concept for climate change adaptation? The politics of resilience for planning: A cautionary note: Edited by Simin Davoudi and Libby Porter. *Planning Theory & Practice, 13*(2), 299-333.

De Montjoye, Y.-A., Hidalgo, C. A., Verleysen, M., & Blondel, V. D. (2013). Unique in the crowd: The privacy bounds of human mobility. *Scientific Reports*, 3.

Denny, M. J., and Spirling, A. (2017). "Text preprocessing for unsupervised learning: why it matters, when it misleads, and what to do about it." *Unpublished manuscript, Dep. Polit. Sci, Stanford Univ and Inst. Quant. Soc. Sci., Harvard Univ. https://ssrn. com/abstract*, 2849145.

Eakin, H., Bojórquez-Tapia, L.A., Janssen, M.A., Georgescu, M., Manuel-Navarrete, D., Vivoni, Bojorquez-Tapia LA, et al. (2011) Regional environmental assessment for multiagency policy making: implementing an environmental ontology through GIS-MCDA. *Environ Plann B Plann Des* 38(3):539–563.

Eason, T., & Cabezas, H. (2012). Evaluating the sustainability of a regional system using Fisher information in the San Luis Basin, Colorado. *Journal of Environmental Management, 94*(1), 41-49.

EERI (2014) EERI Special Earthquake Report: M 6.0 South Napa Earthquake of August 24, 2014. USA Earthquake Clearinghouse.

Eason, T., Garmestani, A. S., Stow, C. A., Rojo, C., Alvarez-Cobelas, M., & Cabezas, H. (2016). Managing for resilience: an information theory-based approach to assessing ecosystems. *Journal of Applied Ecology*.

E.R., Escalante, A.E., Baeza-Castro, A., Mazari-Hiriart, M. and Lerner, A.M., (2017). Opinion: Urban resilience efforts must consider social and political forces. *Proceedings of the National Academy of Sciences, 114*(2), pp.186-189.

Fisher, R. A. (1922). On the mathematical foundations of theoretical statistics. *Philosophical Transactions of the Royal Society of London. Series A, Containing Papers of a Mathematical or Physical Character, 222*, 309-368.

Fu, W., Liu, S., Degloria, S. D., Dong, S., & Beazley, R. (2010). Characterizing the "fragmentation–barrier" effect of road networks on landscape connectivity: A case study in Xishuangbanna, Southwest China. *Landscape and Urban Planning, 95*(3), 122-129.

Frank MR, Mitchell L, Dodds PS, Danforth CM (2013) Happiness and the Patterns of Life: A Study of Geolocated Tweets. *Scientific Reports*, 3:2625 doi:10.1038/srep02625

FEMA. (2015). 2015 Declared disasters. Retrieved from http://gis.fema.gov/DataFeeds.html

Ford, J. D., Tilleard, S. E., Berrang-Ford, L., Araos, M., Biesbroek, R., Lesnikowski, A. C., MacDonald, G. K., Hsu, A., Chen, C., and Bizikova, L. (2016). "Opinion: Big data has big potential for applications to climate change adaptation." *Proceedings of the National Academy of Sciences*, 113(39), 10729-10732.

Geary, R. C. (1954) The contiguity ratio and statistical mapping. The Incorporated Statistician 5:115-146

Granger, C. W. (1981) Some properties of time series data and their use in econometric model specification. *Journal of Econometrics*, 16:121-130

Godschalk, D. R. (2003). Urban hazard mitigation: creating resilient cities. *Natural Hazards Review, 4*(3), 136-143.

Gonzalez, M. C., Hidalgo, C. A., & Barabasi, A.-L. (2008). Understanding individual human mobility patterns. *Nature*, 453(7196), 779-782.

Gray, C. L., & Mueller, V. (2012). Natural disasters and population mobility in Bangladesh. *Proceedings of the National Academy of Sciences*, 109(16), 6000-6005.

Ghosh, J. K., Bhattacharya, D., Boccardo, P., and Samadhiya, N. K. (2013). "Automated geo-spatial hazard warning system GEOWARNS: Italian case study." *Journal of Computing in Civil Engineering*, 29(5), 04014065.

Garmestani, A. S., Allen, C. R., & Benson, M. H. (2013). Can law foster social-ecological resilience? *Ecology and Society, 18*, 37.

Guan X, Chen C (2014) Using social media data to understand and assess disasters. *Natural Hazards*, 74:837-850

Gu, Y., Qian, Z. S., and Chen, F. (2016). "From Twitter to detector: real-time traffic incident detection using social media data." *Transportation Research Part C: Emerging Technologies*, 67, 321-342.

Holling, C. S. (1973). Resilience and stability of ecological systems. *Annual Review of Ecology and Systematics*, 1-23.

Holling, C. S. (1986). The resilience of terrestrial ecosystems: local surprise and global change. *Sustainable Development of the Biosphere*, 292-317.

Holling, C. S. (1996). Engineering resilience versus ecological resilience. *Engineering within Ecological Constraints, 31*, 32.

Hufschmidt, G. (2011). A comparative analysis of several vulnerability concepts. *Natural Hazards, 58*(2), 621-643.

Sanderson, D., and A. Sharma. (2016). IFRC World Disasters Report Resilience: saving lives today, investing for tomorrow

Jacoby, D. M., & Freeman, R. (2016). Emerging network-based tools in movement ecology. *Trends in Ecology & Evolution, 31*(4), 301-314.

Johansen, C., Horney, J., & Tien, I. (2016). Metrics for evaluating and improving community resilience. *Journal of Infrastructure Systems, 23*(2), 04016032.

Karunanithi, A., Cabezas, H., Frieden, B. R., & Pawlowski, C. (2008). Detection and assessment of ecosystem regime shifts from Fisher information. *Ecology and Society, 13*(1).

Koetse, M. J., & Rietveld, P. (2009). The impact of climate change and weather on transport: An overview of empirical findings. *Transportation Research Part D: Transport and Environment*, 14(3), 205-221.

Kunkel, K. E., Karl, T. R., Brooks, H., Kossin, J., Lawrimore, J. H., Arndt, D., . . . Doesken, N. (2013). Monitoring and understanding trends in extreme storms: State of knowledge. *Bulletin of the American Meteorological Society*, 94(4), 499-514.

Kryvasheyeu Y, Chen H, Obradovich N, Moro E, Van Hentenryck P, Fowler J, Cebrian M (2016) Rapid assessment of disaster damage using social media activity. *Science Advances* 2:e1500779

Lu, X., Bengtsson, L., & Holme, P. (2012). Predictability of population displacement after the 2010 Haiti earthquake. Proceedings of the National Academy of Sciences, 109(29), 11576-11581.

Lu, X., Wetter, E., Bharti, N., Tatem, A. J., & Bengtsson, L. (2013). Approaching the limit of predictability in human mobility. Scientific Reports, 3.

Lee, A. V., Vargo, J., & Seville, E. (2013). Developing a tool to measure and compare organizations' resilience. *Natural Hazards Review, 14*(1), 29-41.

Lin Y-R. (2014) Assessing sentiment segregation in urban communities. In: Proceedings of the 2014 International Conference on Social Computing, ACM, p 9

Lam, N. S., Reams, M., Li, K., Li, C., & Mata, L. P. (2015). Measuring community resilience to coastal hazards along the Northern Gulf of Mexico. *Natural Hazards Review, 17*(1), 04015013.

Li, T., Xie, N., Zeng, C., Zhou, W., Zheng, L., Jiang, Y., Yang, Y., Ha, H.-Y., Xue, W., and Huang, Y. (2017). "Data-driven techniques in disaster information management." *ACM Computing Surveys (CSUR)*, 50(1), 1.

Moran PA (1950) Notes on continuous stochastic phenomena. *Biometrika* 37:17-23

Maze, T., Agarwai, M., & Burchett, G. (2006). Whether weather matters to traffic demand, traffic safety, and traffic operations and flow. *Transportation Research Record: Journal of the Transportation Research Board* (1948), 170-176.

Mayer, A. L., Pawlowski, C., Fath, B. D., & Cabezas, H. (2007). Applications of Fisher Information to the management of sustainable environmental systems *Exploratory Data Analysis Using Fisher Information* (pp. 217-244): Springer.

Metcalfe AV, Cowpertwait PS (2009) Introductory time series with R. Springer, New York. https://doi-org.ezproxy.lib.vt.edu/10.1007/978-0-387-88698-5.

Mitchell L, Frank MR, Harris KD, Dodds PS, Danforth CM (2013) The geography of happiness: Connecting twitter sentiment and expression, demographics, and objective characteristics of place. *PloS ONE* 8:e64417

Moore, C., Cumming, G. S., Slingsby, J., & Grewar, J. (2014). Tracking socioeconomic vulnerability using network analysis: insights from an avian influenza outbreak in an ostrich production network. *PloS ONE*, *9*(1), e86973.

Moore, C., Grewar, J., & Cumming, G. S. (2015). Quantifying network resilience: comparison before and after a major perturbation shows strengths and limitations of network metrics. *Journal of Applied Ecology*.

Maurya, A., Murray, K., Liu, Y., Dyer, C., Cohen, W. W., and Neill, D. B. (2016). "Semantic scan: detecting subtle, spatially localized events in text streams." *arXiv preprint arXiv:1602.04393*.

Meerow, S., Newell, J. P., & Stults, M. (2016). Defining urban resilience: A review. *Landscape and Urban Planning*, *147*, 38-49.

Munich RE (2017) NatCatSERVICE: Number of catastrophic natural loss events worldwide 2010-2016. http://natcatservice.munichre.com/. Accessed August 17, 2017

Newman, M. E. (2002). Assortative mixing in networks. *Physical Review Letters*, *89*(20), 208701.

Newman, M. E. (2003). Mixing patterns in networks. *Physical Review E*, *67*(2), 026126.

Newman, M. E., & Girvan, M. (2004). Finding and evaluating community structure in networks. *Physical Review E, 69*(2), 026113.

Nielsen, F. Å. (2011). "A new ANEW: Evaluation of a word list for sentiment analysis in microblogs." *arXiv preprint arXiv:1103.2903*.

Nagy, A., and Stamberger, J. (2012). "Crowd sentiment detection during disasters and crises." *Proc., Proceedings of the 9th International ISCRAM Conference*, 1-9.

NOAA. (2015a, March 7th, 2016). Regional snowfall index (RSI). Retrieved from http://www.ncdc.noaa.gov/cdo-web/#t=firstTabLink

NOAA. (2015b). Storm events database. Retrieved from https://www.ncdc.noaa.gov/stormevents/

NOAA. (2016). Climate Change and Extreme Snow in the U.S. Retrieved from https://www.ncdc.noaa.gov/news/climate-change-and-extreme-snow-us

National Hurricane Center. (2017). Hurricane HARVEY Advisory Archive. Retrieved from http://www.nhc.noaa.gov/archive/2017/HARVEY.shtml

NOAA. (2017). Hurricane Harvey & Its Impacts on Southeast Texas from August 25th to 29th, 2017. Retrieved from http://www.weather.gov/hgx/hurricaneharvey

National Academies of Sciences, E., and Medicine (2017). "Emergency Alert and Warning Systems: Current Knowledge and Future Research Directions." Washington, DC.

Neppalli VK, Caragea C, Squicciarini A, Tapia A, Stehle S (2017) Sentiment analysis during Hurricane Sandy in emergency response. *International Journal of Disaster Risk Reduction* 21:213-222.

OCIA. (2014). Critical infrastructure security and resilience note: winter storms and critical infrastructure.

Phillips P.C., Ouliaris S. (1990) Asymptotic properties of residual based tests for cointegration Econometrica: *Journal of the Econometric Society*: 165-193.

Pradhan, A. R., Laefer, D. F., and Rasdorf, W. J. (2007). "Infrastructure management information system framework requirements for disasters." *Journal of Computing in Civil Engineering*, 21(2), 90-101.

Peña-Mora, F., Chen, A. Y., Aziz, Z., Soibelman, L., Liu, L. Y., El-Rayes, K., Arboleda, C. A., Lantz Jr, T. S., Plans, A. P., and Lakhera, S. (2010). "Mobile ad hoc network-enabled collaboration framework supporting civil engineering emergency response operations." *Journal of Computing in Civil Engineering*, 24(3), 302-312.

Peña-Mora, F., Thomas, J. K., Golparvar-Fard, M., and Aziz, Z. (2012). "Supporting civil engineers during disaster response and recovery using a Segway mobile workstation Chariot." *Journal of Computing in Civil Engineering*, 26(3), 448-455.

Peng, C., Jin, X., Wong, K.-C., Shi, M., & Liò, P. (2012). Collective human mobility pattern from taxi trips in urban area. *PloS ONE*, 7(4), e34487.

Pappalardo, L., Simini, F., Rinzivillo, S., Pedreschi, D., Giannotti, F., & Barabási, A.-L. (2015). Returners and explorers dichotomy in human mobility. *Nature Communications*, 6.

Pavalanathan, U., & Eisenstein, J. (2015). Confounds and consequences in geotagged Twitter data. *arXiv preprint* arXiv: 1506.02275.

Pavalanathan U, Eisenstein J (2015) Confounds and consequences in geotagged Twitter data. *arXiv preprint* arXiv: 150602275.

Papa, R., Galderisi, A., Vigo Majello M.C., Saretta E. (2015). Smart and resilient cities. A systemic approach for developing cross-sectoral strategies in the face of climate change. Tema. *Journal of Land Use, Mobility and Environment*, 8 (1), 19-49. doi: http://dx.doi.org/10.6092/1970-9870/2883.

Pew Research Center (2017) Social Media Fact Sheet. http://www.pewinternet.org/fact-sheet/social-media/. Accessed April 11 2017.

Quinlan, A. E., Berbés-Blázquez, M., Haider, L. J., & Peterson, G. D. (2015). Measuring and assessing resilience: broadening understanding through multiple disciplinary perspectives. *Journal of Applied Ecology*.

Roth, C., Kang, S. M., Batty, M., & Barthélemy, M. (2011). Structure of urban movements: polycentric activity and entangled hierarchical flows. *PloS ONE*, *6*(1), e15923.

Röder, M., Both, A., and Hinneburg, A. (2015). "Exploring the space of topic coherence measures." *Proc., Proceedings of the Eighth ACM International Conference on Web Search and Data Mining*, ACM, 399-408.

Ribeiro, F. N., Araújo, M., Gonçalves, P., Benevenuto, F., and Gonçalves, M. A. (2015). "SentiBench-a benchmark comparison of state-of-the-practice sentiment analysis methods." *arXiv preprint arXiv:1512.01818*.

Ribeiro FN, Araújo M, Gonçalves P, Benevenuto F, Gonçalves MA (2015) SentiBench-a benchmark comparison of state-of-the-practice sentiment analysis methods. *arXiv preprint arXiv*:151201818.

Said SE, Dickey DA (1984) Testing for unit roots in autoregressive-moving average models of unknown order. *Biometrika* 71:599-607.

Song, C., Koren, T., Wang, P., & Barabási, A.-L. (2010). Modelling the scaling properties of human mobility. *Nature Physics*, 6(10), 818-823.

Song, C., Qu, Z., Blumm, N., & Barabási, A.-L. (2010). Limits of predictability in human mobility. *Science*, 327(5968), 1018-1021.

Sakaki, T., Okazaki, M., and Matsuo, Y. (2010). "Earthquake shakes Twitter users: real-time event detection by social sensors." *Proc., Proceedings of the 19th International Conference on World Wide Web*, ACM, 851-860.

Song, X., Zhang, Q., Sekimoto, Y., & Shibasaki, R. (2014). Prediction of human emergency behavior and their mobility following large-scale disaster. Paper presented at the Proceedings of the 20th ACM SIGKDD International Conference on Knowledge Discovery and Data Mining.

Squires, M. F., Lawrimore, J. H., Heim Jr, R. R., Robinson, D. A., Gerbush, M. R., & Estilow, T. W. (2014). The regional snowfall index. Bulletin of the American Meteorological Society, 95(12), 1835-1848.

Schubert, E., Weiler, M., and Kriegel, H.-P. (2014). "Signitrend: scalable detection of emerging topics in textual streams by hashed significance thresholds." *Proc., Proceedings of the 20th ACM SIGKDD International Conference on Knowledge Discovery and Data Mining*, ACM, 871-880.

Spanbauer, T. L., Allen, C. R., Angeler, D. G., Eason, T., Fritz, S. C., Garmestani, A. S., . . . Stone, J. R. (2014). Prolonged instability prior to a regime shift. *PloS ONE*, *9*(10), e108936.

Sapiezynski, P., Stopczynski, A., Gatej, R., & Lehmann, S. (2015). Tracking Human Mobility Using WiFi Signals. *PloS ONE*, 10(7), e0130824.

Shelton, T., Poorthuis, A., & Zook, M. (2015). Social media and the city: Rethinking urban socio-spatial inequality using user-generated geographic information. *Landscape and Urban Planning, 142*, 198-211.

Spears, B. M., Ives, S. C., Angeler, D. G., Allen, C. R., Birk, S., Carvalho, L., . . . Pocock, M. J. (2015). FORUM: Effective management of ecological resilience–are we there yet? *Journal of Applied Ecology, 52*(5), 1311-1315.

Swier, N., Komarniczky, B., & Clapperton B. (2015). Using geolocated Twitter traces to infer residence and mobility. (GSS Methodology Series No 41). UK Retrieved from www.ons.gov.uk.

Sun, H., Wang, Z., Wang, J., Huang, Z., Carrington, N., and Liao, J. (2016). "Data-driven power outage detection by social sensors." *IEEE Transactions on Smart Grid*, 7(5), 2516-2524.

Sundstrom, S. M., Eason, T., Nelson, R. J., Angeler, D. G., Barichievy, C., Garmestani, A. S., . . . Knutson, M. (2017). Detecting spatial regimes in ecosystems. *Ecology Letters, 20*(1), 19-32.

Seetharaman, D., & Wells, G. (2017). Hurricane Harvey Victims Turn to Social Media for Assistance. The Wall Street Journal. Retrieved from https://www.wsj.com/articles/hurricane-harvey-victims-turn-to-social-media-for-assistance-1503999001

Tang Z, Zhang L, Xu F, Vo H (2015) Examining the role of social media in California's drought risk management in 2014. *Natural Hazards*. 79:171-193

Towne, W. B., Rosé, C. P., and Herbsleb, J. D. (2016). "Measuring Similarity Similarly: LDA and Human Perception." *ACM TIST*, 8(1), 7:1-7:28.

UNISDR (2017) Disaster Statistics. https://www.unisdr.org/we/inform/disaster-statistics. Accessed May 2 2017.

USGS (2014) M 6.0 - 6km NW of American Canyon, California. https://earthquake.usgs.gov/earthquakes/eventpage/nc72282711#executive. Accessed April 11 2017.

USGS (2017) M 6.0 - 6km NW of American Canyon, California. https://earthquake.usgs.gov/earthquakes/eventpage/nc72282711#shakemap. Accessed April 9 2017.

Vo B-KH, Collier N (2013) Twitter emotion analysis in earthquake situations. International *Journal of Computational Linguistics and Applications* 4:159-173.

Wagner AK, Soumerai SB, Zhang F, Ross-Degnan D (2002) Segmented regression analysis of interrupted time series studies in medication use research. *Journal of Clinical Pharmacy and Therapeutics* 27:299-309.

Walther, M., and Kaisser, M. (2013). Geo-spatial event detection in the twitter stream. *Proc., European Conference on Information Retrieval*, Springer, 356-367.

Wang, B., Zhuang, J. (2017). Crisis information distribution on Twitter: a content analysis of tweets during Hurricane Sandy. *Natural Hazards*: 89(1), 161-181.

Wang, S. H., Huang, S. L., & Budd, W. W. (2012). Resilience analysis of the interaction of between typhoons and land use change. *Landscape and Urban Planning*, *106*(4), 303-315.

Wang, Q., & Taylor, J. E. (2014). Quantifying human mobility perturbation and resilience in Hurricane Sandy. *PloS ONE*, 9(11), e112608.

Wang, Q., & Taylor, J. E. (2015). Process map for urban-human mobility and civil infrastructure data collection using geosocial networking platforms. *Journal of Computing in Civil Engineering*, 30(2), 04015004.

Wang, Q., & Taylor, J. E. (2016). Patterns and limitations of urban human mobility resilience under the influence of multiple types of natural disaster. *PloS ONE*, 11(1), e0147299.

Wang Z, Ye X, Tsou M-H (2016) Spatial, temporal, and content analysis of Twitter for wildfire hazards. *Natural Hazards*, 83:523-540.

Wang, Y., Wang, Q., & Taylor, J. E. (2017). Aggregated responses of human mobility to severe winter storms: An empirical study. *PloS ONE, 12*(12), e0188734.

Wang, Y., and Taylor, J. E. (2017). "Tracking urban resilience to disasters: a mobility network-based approach." *Proceedings of the 14th International Conference on Information Systems for Crisis Response And Management* I. e. A. M. M. L. C. H. F. B. T. C. (Ed.), ed. Albi, France., pp. 97–109.

Wang, Y. & Taylor, J.E. (2018) Coupling sentiment and human mobility in natural disasters: a Twitter-based study of the 2014 South Napa Earthquake. *Natural Hazards*. https://doi.org/10.1007/s11069-018-3231-1.

Xie, W., Zhu, F., Jiang, J., Lim, E.-P., and Wang, K. (2016). "Topicsketch: Real-time bursty topic detection from twitter." *IEEE Transactions on Knowledge and Data Engineering*, 28(8), 2216-2229.

Yu, W., Li, J., Bhuiyan, M. Z. A., Zhang, R., and Huai, J. (2017). "Ring: Real-Time Emerging Anomaly Monitoring System over Text Streams." *IEEE Transactions on Big Data*.

Zhou, H., Wan, J., & Jia, H. (2010). Resilience to natural hazards: a geographic perspective. *Natural Hazards, 53*(1), 21-41.

Zobel, C. W. (2011). Representing perceived tradeoffs in defining disaster resilience. *Decision Support Systems, 50*(2), 394-403.

Zhong, C., Arisona, S. M., Huang, X., Batty, M., & Schmitt, G. (2014). Detecting the dynamics of urban structure through spatial network analysis. *International Journal of Geographical Information Science, 28*(11), 2178-2199.

Zhao, K., Musolesi, M., Hui, P., Rao, W., & Tarkoma, S. (2015). Explaining the power-law distribution of human mobility through transportation modality decomposition. *Scientific Reports*, 5.

APPENDIX A: SUPPORTING INFORMATION FOR CHAPTER 2

Supplementary Tables

Table A1: Daily Data Volume of Tweets in the Studied Area

Weeks	Days in weeks	Date (EST)	Number of Tweets	Number of Distinct Users
Pre-storm week 1	Monday	12/29/2014	59564	12753
	Tuesday	12/30/2014	60460	12755
	Wednesday	12/31/2014	62887	14562
	Thursday	1/1/2015	72706	15770
	Friday	1/2/2015	61067	13177
	Saturday	1/3/2015	72865	14540
	Sunday	1/4/2015	75799	14541
Pre-storm week 2	Monday	1/5/2015	52208	12697
	Tuesday	1/6/2015	64083	13235
	Wednesday	1/7/2015	66628	13932
	Thursday	1/8/2015	67121	14662
	Friday	1/9/2015	59727	13628
	Saturday	1/10/2015	74570	15519
	Sunday	1/11/2015	73988	14617
Pre-storm week 3	Monday	1/12/2015	70435	13875
	Tuesday	1/13/2015	62167	13564
	Wednesday	1/14/2015	60550	13399
	Thursday	1/15/2015	61696	14031
	Friday	1/16/2015	55977	13739
	Saturday	1/17/2015	59532	14305
	Sunday	1/18/2015	83717	16645

Pre-storm week 4	Monday	1/19/2015	67110	14262
	Tuesday	1/20/2015	66181	14428
	Wednesday	1/21/2015	63096	14277
	Thursday	1/22/2015	62077	29170
	Friday	1/23/2015	56261	14518
	Saturday	1/24/2015	65609	15488
	Sunday	1/25/2015	71178	15266
Storm week	Monday	1/26/2015	78878	16495
	Tuesday	1/27/2015	68706	16344
	Wednesday	1/28/2015	42541	11440
	Thursday	1/29/2015	53300	13375
	Friday	1/30/2015	61432	14726
	Saturday	1/31/2015	61652	14964
	Sunday	2/1/2015	124227	21421
Post-storm week	Monday	2/2/2015	88891	16398
	Tuesday	2/3/2015	72425	15031
	Wednesday	2/4/2015	68466	15615
	Thursday	2/5/2015	49624	13146
	Friday	2/6/2015	26745	9653
	Saturday	2/7/2015	28156	10017
	Sunday	2/8/2015	37044	11230

Table A2: Number of Displacements in Different Ranges

Weekday	**Date**	**8-100m**	**100-500m**	**500-1,000m**	**1km-5km**	**5km-10km**	**>=10km**	**Sum**
Monday	1/5/2015	18453	1664	1026	3585	1335	1901	27964

Tuesday	1/6/2015	24393	2235	1232	4228	1626	2434	36148
Wednesday	1/7/2015	26144	2091	1235	4178	1650	2325	37623
Thursday	1/8/2015	25635	2035	1225	4022	1549	2356	36822
Friday	1/9/2015	21156	2014	1202	4153	1590	2409	32524
Saturday	1/10/2015	29462	2296	1268	4009	1619	3082	41736
Sunday	1/11/2015	30471	1892	1191	3431	1289	2438	40712
Monday	1/12/2015	27329	2291	1358	4123	1416	2042	38559
Tuesday	1/13/2015	22265	2124	1261	4234	1387	2271	33542
Wednesday	1/14/2015	21992	2155	1163	4073	1453	2188	33024
Thursday	1/15/2015	21491	2329	1205	4174	1557	2302	33058
Friday	1/16/2015	18053	2100	1278	4104	1536	2725	29796
Saturday	1/17/2015	21048	1720	1056	3549	1538	2611	31522
Sunday	1/18/2015	33270	2485	1388	3931	1457	2736	45267
Monday	1/19/2015	25938	1799	5623	3233	1330	2511	35872
Tuesday	1/20/2015	23259	2690	1552	4230	1478	2356	35565
Wednesday	1/21/2015	22121	2672	1410	3968	1435	2332	33938
Thursday	1/22/2015	20973	2733	1481	4151	1380	2326	33044
Friday	1/23/2015	17228	2329	1318	3906	1426	2633	28840
Saturday	1/24/2015	24026	2055	1248	3202	1219	2064	33814
Sunday	1/25/2015	27844	2157	1205	3216	1421	2408	38251
Monday	1/26/2015	27534	2927	1580	4260	1315	2120	39736
Tuesday	1/27/2015	35824	2273	998	1583	439	917	42034
Wednesday	1/28/2015	16096	1207	704	1859	802	1020	21688
Thursday	1/29/2015	18565	2014	1086	3123	1237	1650	27675
Friday	1/30/2015	19351	2595	1484	4451	1722	2542	32145
Saturday	1/31/2015	20941	1915	1147	3531	1516	2848	31898
Sunday	2/1/2015	54238	3678	2034	5369	2097	3149	70565

Monday	2/2/2015	39725	2434	1255	2514	822	1393	48143
Tuesday	2/3/2015	26976	2951	1601	4336	1656	2084	39604
Wednesday	2/4/2015	22490	3152	1689	4954	1993	2744	37022
Thursday	2/5/2015	15259	2355	1255	3558	1352	1862	25641
Friday	2/6/2015	7276	920	577	1922	790	1091	12576
Saturday	2/7/2015	8265	744	471	1619	766	1194	13059
Sunday	2/8/2015	13869	901	475	1341	601	973	18160

Table A3: Binary Logistic Regression Results

Displacements	r_1	r_2	r_3	r_4	r_5	r_6
Coefficients	0.2095	-0.281	-1.4	-0.4933	-1.3461	-1.1236
$p-value$	0.0472 *	0.626	0.23	0.0495 *	0.0348 *	0.0257 *

* *p*-value <0.05, ** p-value <0.01, *** p-value <0.001

Table A4: Fitting Parameters of Lognormal Distribution for Daily Displacements and Comparison Results with Other Distributions

Date	μ	σ	**x-min**	**KS-test**	**Exponential Comparison**	$p-value$	**Power law Comparison**	$p-value$
1/5/2015	7.714074	1.8839467	100	0.0268917	8424.3149	7.48E-110	2718.9939	0
1/6/2015	7.633188	1.9864321	100	0.0271221	9451.5004	7.43E-123	3182.6568	0
1/7/2015	7.6415128	1.9697795	100	0.0268014	9905.9043	7.80E-123	3160.3226	0
1/8/2015	7.7009732	1.969914	100	0.026715	9437.3211	1.19E-115	3095.3377	0
1/9/2015	7.697949	1.977473	100	0.02578	9035.4759	2.95E-125	3204.3304	0
1/10/2015	7.7276292	2.0823367	100	0.021631	10225.788	5.40E-164	3273.7879	0

1/11/2015	7.6507344	2.1156943	100	0.0170946	10020.655	3.00E-149	2627.4689	0
1/12/2015	7.4736826	1.939222	100	0.0193051	11042.463	1.36E-117	2807.4205	0
1/13/2015	7.6693953	1.8912733	100	0.0217776	9858.674	4.73E-123	3099.5574	0
1/14/2015	7.5939045	1.9969652	100	0.0280066	10148.909	9.85E-123	2854.0504	0
1/15/2015	7.5654991	1.986476	100	0.0220747	10663.181	3.00E-123	2998.6752	0
1/16/2015	7.7598972	2.0050847	100	0.0198165	11420.769	1.11E-149	3222.2293	0
1/17/2015	7.8926021	1.974368	100	0.0185425	8150.6348	2.09E-135	3187.9657	0
1/18/2015	7.5029216	2.1834179	100	0.0159464	13965.906	6.79E-178	2732.1952	0
1/19/2015	7.7026855	2.1325026	100	0.0177264	10604.086	6.92E-155	2513.1236	0
1/20/2015	7.3805641	2.074052	100	0.0181226	13356.736	2.80E-138	2794.5249	0
1/21/2015	7.3624088	2.1126258	100	0.0181609	13754.039	8.81E-145	2564.8933	0
1/22/2015	7.3774537	2.039341	100	0.0135814	14028.924	1.30E-139	2699.9003	0
1/23/2015	7.5668989	2.0901793	100	0.0153008	11862.467	6.00E-155	2842.0584	0
1/24/2015	7.4675597	2.1152317	100	0.016239	12047.723	1.72E-136	2212.4427	0
1/25/2015	7.5634346	2.1752502	100	0.0160784	12723.146	6.61E-163	2386.8762	0
1/26/2015	7.1689987	2.1092831	100	0.0172147	14074.603	9.39E-128	2484.805	0
1/27/2015	4.6271196	3.2318684	100	0.0176299	24291.392	7.57E-104	364.05651	1.16E-78
1/28/2015	7.4620614	2.0056545	100	0.0254057	6919.1801	4.10E-66	1269.0605	1.56E-191
1/29/2015	7.4374064	1.9638626	100	0.0219782	9232.4775	1.90E-90	2166.5594	0
1/30/2015	7.5464953	1.9917914	100	0.0191083	14055.495	3.13E-154	3164.3035	0
1/31/2015	7.8242904	2.1045986	100	0.0184183	10747.275	1.82E-158	2996.9974	0
2/1/2015	7.3307505	2.0970269	100	0.0180372	17857.974	4.45E-191	3593.8176	0
2/2/2015	6.3714917	2.5656001	100	0.0141697	18711.605	1.09E-127	1048.058	1.04E-211
2/3/2015	7.3102283	1.9786274	100	0.0207702	13606.764	4.93E-128	2801.5288	0
2/4/2015	7.4882972	1.992182	100	0.0211203	16076.138	4.10E-155	3480.1326	0
2/5/2015	7.3837635	1.9893356	100	0.0177213	11942.932	7.69E-110	2367.748	0
2/6/2015	7.7729563	1.8456478	100	0.0223493	3757.4646	2.46E-53	1619.6998	2.09E-264

2/7/2015	7.9685543	1.8790777	100	0.0200402	3540.4139	2.84E-58	1574.2667	1.28E-273
2/8/2015	7.4656352	2.2436281	100	0.0241779	4709.3316	3.02E-63	951.9652	8.26E-168

Note: μ: location parameter; σ: shape parameter.

Table A5: Kolmogorov-Smirnov Test between the Distributions of MTW-based r_g of Distinct Weeks

D	MTW1	MTW2	MTW3	MTW4	MTW5
MTW1	--	0.09861***	0.11277***	0.061999***	0.23704***
MTW2	0.09861***	--	0.035275*	0.048103***	0.17397***
MTW3	0.11277***	0.035275***	--	0.055318***	0.15473***
MTW4	0.061999***	0.048103***	0.055318***	--	0.18573***
MTW5	0.23704***	0.17397***	0.15473***	0.18573***	--

* *p*-value <0.05, ** p-value <0.01, *** p-value <0.001

Table A6: Fitting Parameters of Truncated Power Law for Daily r_g

Date	α	**λ Value**	$x_{\min}$	**KS test**	**Exponential comparison**	$p-value$	**Lognormal comparison**	$p-value$
12/29/2014	1.677792	0.027186	1	0.003789	8792.695	7.27E-103	241.4795	1.24E-53
12/30/2014	1.64596	0.029858	1	0.004748	8698.552	2.51E-117	218.7952	1.37E-47
12/31/2014	1.682389	0.032819	1	0.0044	9245.274	4.20E-127	312.0221	2.27E-90
1/1/2015	1.617259	0.03285	1	0.004269	9711.858	9.60E-158	312.6552	1.65E-93

1/2/2015	1.639829	0.033407	1	0.005323	8903.266	5.35E-98	216.74	7.74E-26
1/3/2015	1.654193	0.024691	1	0.00334	10580	1.31E-115	274.0301	1.92E-62
1/4/2015	1.564084	0.029839	1	0.004329	9560.395	3.93E-141	297.7152	1.44E-70
1/5/2015	1.640834	0.034999	1	0.004595	7927.065	1.31E-121	210.2639	3.01E-43
1/6/2015	1.547737	0.044362	1	0.006098	7403.094	3.30E-121	282.7266	2.03E-42
1/7/2015	1.533663	0.039952	1	0.005688	8020.675	4.81E-128	291.7857	9.82E-46
1/8/2015	1.674923	0.029134	1	0.004265	9898.8	1.81E-106	295.7366	3.61E-56
1/9/2015	1.662929	0.033653	1	0.003962	8575.292	2.13E-103	287.6484	9.36E-55
1/10/2015	1.536642	0.039045	1	0.005073	9075.244	5.77E-80	316.9192	7.31E-17
1/11/2015	1.616772	0.027208	1	0.003814	10147.2	1.92E-91	272.8236	7.14E-29
1/12/2015	1.550665	0.035764	1	0.005885	9183.866	1.41E-97	263.7783	1.51E-23
1/13/2015	1.603237	0.037261	1	0.005898	8383.99	1.82E-111	286.6831	7.11E-46
1/14/2015	1.619396	0.036396	1	0.0048	8345.182	5.44E-110	258.482	5.15E-41
1/15/2015	1.624642	0.039199	1	0.005466	8603.699	1.73E-111	284.5446	7.81E-42
1/16/2015	1.672148	0.039928	1	0.005063	7998.887	1.88E-130	292.919	2.47E-75
1/17/2015	1.737222	0.032074	1	0.004111	9578.312	3.48E-109	267.3032	1.65E-56
1/18/2015	1.601419	0.029386	1	0.004105	11182.97	4.78E-141	342.8838	1.67E-69
1/19/2015	1.678987	0.026487	1	0.00354	10054.41	3.32E-127	232.9802	5.02E-61
1/20/2015	1.570153	0.04039	1	0.006769	8553.414	5.45E-122	303.9375	3.11E-47
1/21/2015	1.609329	0.038337	1	0.004666	8376.04	3.79E-130	315.1208	3.41E-71
1/22/2015	1.632637	0.038934	1	0.004505	8426.792	5.69E-134	319.238	1.80E-79
1/23/2015	1.715587	0.039831	1	0.004316	8452.071	2.14E-111	310.4018	7.42E-61
1/24/2015	1.645239	0.03889	1	0.004671	9125.734	2.41E-144	332.9112	4.80E-84
1/25/2015	1.658536	0.030503	1	0.005517	10392.84	5.33E-137	318.3105	9.82E-82
1/26/2015	1.624413	0.037256	1	0.005383	20542.45	3.75E-270	639.595	9.08E-99
1/27/2015	1.679003	0.03759	1	0.005582	10202.91	1.25E-137	347.8261	9.74E-73
1/28/2015	1.784641	0.037292	1	0.004356	6975.379	1.15E-85	221.6139	4.84E-43

1/29/2015	1.73854	0.03326	1	0.003584	8190.559	3.43E-94	275.3367	1.50E-53
1/30/2015	1.710285	0.035059	1	0.004757	9631.311	6.37E-68	263.7794	3.12E-17
1/31/2015	1.000015	0.016048	1	0.190696	1537.415	3.40E-08	1456.877	8.56E-18
2/1/2015	1.404604	0.035657	1	0.004393	11856.34	2.08E-206	533.3147	5.67E-88
2/2/2015	1.577818	0.027653	1	0.005359	11876.23535	1.30E-134	313.5181823	8.83E-50
2/3/2015	1.640446	0.029665	1	0.004402	10427.03535	6.57E-73	292.4733557	1.26E-20
2/4/2015	1.609433	0.040030	1	0.005186	9206.847724	9.72E-57	327.7400074	9.92E-13
2/5/2015	1.791092	0.032968	1	0.003510	8064.003338	7.14E-60	262.8304351	8.54E-27
2/6/2015	1.902266	0.057567	1	0.003153	4349.457135	7.46E-77	240.5248181	6.20E-69
2/7/2015	1.942033	0.050031	1	0.003159	4835.736536	6.50E-86	205.2845631	2.75E-61
2/8/2015	1.000012	0.322756	1	0.074552	3050.553846	1.71E-268	-2107.913365	2.74E-64